Flow Resistance in Simulated
Irrigation Borders and Furrows

CONTENTS

FLOW RESISTANCE IN SIMULATED IRRIGATION BORDERS AND FURROWS

By E. G. Kruse, *Soil and Water Conservation Research Division, Agricultural Research Service;* C. W. Huntley, *Agricultural Engineering Department, Colorado Agricultural Experiment Station;* and A. R. Robinson, *Soil and Water Conservation Research Division, Agricultural Research Service*

INTRODUCTION

The efficient application and distribution of water by irrigation furrows or borders is highly dependent on the rate of advance of water in these channels. The rate of advance is governed by the intake rate of the soil, the resistance offered by the channels to the flow of water, and the discharge rate into the channels. A knowledge of these factors is essential for the design of efficient irrigation systems. Intake rate has been the object of much study and methods are available for its measurement before the construction of irrigation systems. Previous flow resistance studies have dealt with either artificially roughened boundaries, conduits intended for uses other than irrigation, or discharges much greater than are likely to occur in small irrigation channels. Results of studies of flow resistance are not available for the types of roughness, sizes of channels, and discharges that are likely to be encountered in surface irrigation systems. Discharge can be regulated to correspond to other design conditions.

Channel boundaries and flow conditions in irrigation furrows and borders differ from conditions in most other open channels in several ways. Discharges carried by furrows and borders are small, possibly in the laminar flow range in some cases. Boundary roughness is relatively great; at the lowest rates of flow, height of roughness may be of the same order of magnitude as flow depth. Size, shape, and spacing of the roughness elements are not uniform. Under field conditions, irrigation flows are further complicated by changes in boundary roughness and channel cross section with time and distance because of erosion.

Resistance to flow in irrigation channels may be caused by several factors. In earth channels, the boundary roughness is the primary cause of flow resistance. In vegetated channels, plant stems and leaves may have a greater effect on flow retardance than the soil roughness. The cross-sectional shape and alinement of channels may also affect resistance.

Many previous flow resistance studies have involved measurements of energy losses in conduits intended for a specific use. Others have been attempts to determine the fundamental relationships between boundary roughness, channel shape, channel alinement, and resistance to flow. Results of the specific-use type of tests cannot be generalized to include conduits of other sizes or other boundary roughnesses. The fundamental studies have been conducted, for the most part, on artificially devised roughness, with roughness elements of uniform size, shape, and spacing. The effect of the roughness on resistance is often expressed in terms of the equivalent sand-grain size, by using the rough boundary equation of Nikuradse (*12*).[1] However, it has not yet been possible to find a general relation between the dimensions of the roughness (even uniform roughness) and the equivalent sand grain size.

It is currently necessary to make trial resistance measurements on every type of conduit before the resistance of that conduit to flow can be accurately known. In the installation of irrigation systems it is often impractical to base design on trial resistance measurements. A procedure is needed whereby resistance in irrigation channels can be estimated while the system is being designed in order that changes will not be necessary after the system is constructed.

The study reported in this bulletin was conducted to determine the resistance to flow in channels similar to irrigation furrows and borders. Channels having soil boundaries with different degrees of roughness were constructed in the laboratory. The relationships discovered between flow resistance and boundary roughness parameters, after field verification, will provide a method of estimating flow resistance for design of surface irrigation systems.

The specific objectives of the study were:

1. To determine if both laminar and turbulent flow are likely to occur in irrigation systems and, if so, under what conditions of discharge, temperature, slope, roughness, etc., each type of flow occurs.

2. To investigate the effects of boundary roughness on resistance to flow in channels with roughness elements formed of soil, and thus similar in roughness to irrigation furrows and borders.

3. To determine the effect of channel shape on flow resistance, within the range of shapes characteristic of irrigation furrows and borders.

[1] Italic numbers in parentheses refer to Literature Cited, p. 41.

The results of this study will provide the additional knowledge necessary for predicting the rate of advance of irrigation streams, which in turn will permit the design of systems with maximum water application efficiency. The specific contribution of the study is to develop the relations necessary for predicting resistance to flow in irrigation borders and furrows without trial resistance runs.

Methods are being developed concurrently (21) for determining the surface profile of an advancing water stream when resistance to flow is known. The volume of water in surface storage in the stream can be calculated if the water surface profile is known. Rate of advance is determined by equating the volume of water delivered to the channel to the volume infiltrated plus the volume in surface storage (4, 6, 19).

REVIEW OF LITERATURE

Flow Resistance Formulas

Numerous studies have been made of resistance to open channel flow. Both laminar and turbulent flow have been investigated. Most laboratory studies have considered only the effects of artificial roughness elements, uniform in size, shape, and spacing. The work most pertinent to the present study will be reviewed in this section.

Resistance equations have a different form for laminar and turbulent flow. In laminar flow over smooth boundaries the velocity is proportional to slope to the first power and to depth to the second power. Definitive equations have not been developed for laminar flows over rough boundaries. In turbulent flow, velocity is proportional to depth and slope to other powers.

A theoretical equation for uniform laminar flow in a wide, smooth, rectangular channel was derived by Cornish (3). It can be written:[2]

$$V=\frac{\gamma d^2 S}{3\mu} \qquad (1)$$

where:

V is the mean flow velocity,
γ is the unit weight of fluid,
d is the depth of flow,
S is the slope of the energy line, and
μ is the absolute viscosity of the fluid.

This relationship has been verified experimentally (1, 3, 13).

Resistance to uniform turbulent flow in open channels is often expressed in terms of the resistance coefficient from one of the following equations:

Manning:

$$V=1.486\frac{R^{2/3}S^{1/2}}{n} \qquad (2)$$

Chezy:

$$V=C\sqrt{RS} \qquad (3)$$

[2] A list of all symbols used in this bulletin can be found on p. 42.

or Darcy-Weisbach:

$$f-\frac{8gRS}{V^2} \qquad (4)$$

where:

R is the hydraulic radius,
g is the gravitational acceleration, and
n, C, and f are the resistance coefficients in the different equations.

The resistance coefficients can be related to each other and to the mean flow ratio as follows:

$$\frac{V}{V_*}=C/\sqrt{g}=\sqrt{\frac{8}{f}}=1.486\frac{R^{1/6}}{n\sqrt{g}} \qquad (5)$$

where: V_* is the shear velocity $\sqrt{gRS}$.

Laminar Flow

The relationship between the Darcy-Weisbach friction factor and the Reynolds number for smooth boundaries—$f=24/Re$—can be obtained by combining equations 1 and 4. Several investigators (15, 20, 23), have plotted f against Re for laminar flows over rough boundaries and found that the relationship is different from that over smooth boundaries. The f-versus-Re line for rough boundaries falls parallel to and above the line for flows over smooth boundaries, indicating greater flow resistance.

A criterion for pipe flow has been presented that specifies the height of roughness that will cause flow resistance greater than that caused by smooth boundaries (5). The criterion is based on the assumption that flow separation occurs when the Reynolds number at the tip of the roughness element (tip Reynolds number) reaches some critical value and that the eddies caused by separation increase the flow resistance but do not spread throughout the flow to cause general turbulence. The criterion also assumes that flow velocities have the same distribution as for smooth boundaries and are not affected by the presence of the roughness elements. The height of roughness

necessary for separation to occur in pipes, based on these assumptions, is:

$$\epsilon = \frac{r}{\sqrt{2}} \frac{Re_{kc}^{1/2}}{Re} \qquad (6)$$

where:

r is the pipe radius,

Re is the Reynolds number of the flow, and

Re_{kc} is a critical value of Reynolds number at the tip of the roughness element.

Transition From Laminar to Turbulent Flow

Several investigators have studied the transition from laminar to turbulent flow in open channels with smooth boundaries (1, 7, 9, 14). The range of critical Reynolds numbers varies from 300 to 1,400. The critical Reynolds number is apparently affected by the amount of initial disturbance in the flowing streams.

For rough boundaries, the critical Reynolds number may be defined as that for which the Darcy-Weisbach resistance coefficient ceases to be inversely proportional to the first power of the Reynolds number. This critical Reynolds number is generally lower than that for smooth boundaries and has been found by different investigators (15, 20, 23) to be a function of roughness height, channel slope, shape, etc. Parsons (15) presents the following criterion for critical Reynolds number for an earth channel with random roughness:

$$Re_c = \frac{7.5}{S^{2/3}} \qquad (7)$$

At a slope of 0.001 the critical Reynolds number has a value of 750. Woo and Brater (23) found critical Reynolds numbers of 400 for rough boundary conditions.

Turbulent Flow

The studies of Nikuradse (12, 13) show that the theoretical logarithmic resistance formulas of Prandtl and von Karman are applicable to turbulent flow. The studies also show that resistance to turbulent flow depends on boundary roughness and fluid viscosity. For smooth boundaries, flow resistance is a function of fluid viscosity. For rough boundaries, the relative roughness has the primary effect upon flow resistance. Intermediate cases exist where both roughness and viscosity affect resistance. The boundary condition is determined by the thickness of the laminar sublayer, δ', relative to the roughness height. Nikuradse (13) found:

$k_s > 6\delta'$, for a rough boundary,

$k_s < \frac{\delta'}{4}$, for a smooth boundary, and

$6\delta' > k_s > \frac{\delta'}{4}$, for a transitional boundary, (8)

where k_s is the diameter of the equivalent sand grain roughness.

Keulegan (10) integrated the Prandtl-von Karman universal velocity distribution law over the cross sections of open channels of several shapes. He considered the effects of channel shape and free surface, as well as the boundary conditions, on flow resistance. The following are Keulegan's equations:

For rough boundaries—

$$(1+\bar{\epsilon}) \frac{V}{V_*} = a_r - \frac{1}{\kappa} + \frac{2.30}{\kappa} \log \frac{R}{k} + \frac{\beta}{\kappa} \qquad (9)$$

For wavy boundaries—

$$(1+\bar{\epsilon}) \frac{V}{V_*} = a_w - \frac{1}{\kappa} + \frac{2.30}{\kappa} \log \frac{RV_*}{\nu} + \frac{\beta}{K} \qquad (10)$$

And for smooth boundaries—

$$(1+\epsilon) \frac{V}{V_*} = a_s - \frac{1}{\kappa} + \frac{2.30}{\kappa} \log \frac{RV_*}{\nu} + \frac{\beta}{\kappa} \qquad (11)$$

where $\bar{\epsilon}$ represents the effect of channel shape on distribution of boundary shear, β represents the effect of channel shape on the flow-area-to-velocity-distribution relationship, ν represents kinematic viscosity, and κ is the universal turbulence constant. The symbols a_r, a_w, and a_s, are hydraulic characteristics of the boundaries; a_w depends on the ratio of height to spacing of the boundary roughness elements; a_s is a constant; a_r is probably a function of roughness spacing.

Keulegan suggested that the boundary conditions can be determined by a plotting of $\frac{V}{V_*} - \frac{2.30}{\kappa}$ log R against log $\frac{V_*}{\nu}$. For smooth and wavy boundaries, such a plotting of data would describe an inclined straight line having the equation:

$$\frac{V}{V_*} = \frac{2.30}{\kappa} \log \frac{RV_*}{\nu} + A \qquad (12)$$

The theoretical value of A for very wide, smooth channels is 3.0. Using the experimental data of Bazin (2), Keulegan found values of A equal to −1.3 and −3.0 for different degrees of waviness. For rough boundaries, resistance is independent

of viscosity. An equation of the following form results:

$$\frac{V}{V_*} = \frac{2.30}{\kappa} \log R + B \qquad (13)$$

where, for Bazin's data, B is a function of the height of the roughness.

Using Bazin's data, Keulegan was also able to derive the following criterion for distinguishing between wavy and rough boundaries:

$$\frac{k_s V_*}{\nu} > 42.2 \text{ for a rough boundary, and}$$

$$\frac{k_s V_*}{\nu} < 42.2 \text{ for a wavy boundary,} \qquad (14)$$

where k_s is the diameter of the equivalent sand grain roughness.

Sayre and Albertson (17) studied the effects of spacing of baffle plate roughness on flow resistance. Their resistance measurements can be represented by the formula:

$$\frac{C}{\sqrt{g}} = 6.06 \log \frac{d}{\chi} \qquad (15)$$

where:

  d is the normal flow depth in a wide rectangular channel,

  χ is a resistance parameter with a different value for each boundary, and

  C is the resistance coefficient from Chezy's formula.

The significance of χ can be better understood by comparing equation 15 with equation 9 of Keulegan. If a_r is equal to $\frac{2.30}{\kappa} \log A$, and $\beta - 1$ is equal to $2.30 \log B$, and if $\bar{\epsilon}$ is assumed negligible (as Keulegan found), equation 9 becomes:

$$\frac{V}{V_*} = \frac{2.30}{\kappa} \log \frac{R}{k/AB}$$

or, say:

$$\frac{C}{\sqrt{g}} = \frac{2.30}{\kappa} \log \frac{R}{\chi} \qquad (16)$$

This equation is identical to equation 19 if κ is given the value 0.38 and it is assumed that d can be replaced by R for channels that are not infinitely wide. Therefore, χ represents effects of roughness height and spacing and also the effects of channel shape.

Many other studies have resulted in similar logarithmic-type formulas. Investigators have not agreed on the proper value of κ for these logarithmic formulas. From Nikuradse's studies it was assumed that κ is a universal constant with the value 0.40. However, later studies have indicated values in the range of 0.36 and 0.38. The apparent value of κ determined from experimental data can vary with the shape of the channel and according to the way that the depth of flow is measured.

Bed Elevation

Previous investigators have measured depth of flow to different datums relative to the mean bed elevation. In studies of artificial roughness, the roughness elements are usually fastened to a plane wall that becomes the natural datum for depth measurements. However, for some studies (18, 22), other datums have been chosen. A datum nearer the tops of the roughness elements is often used when the elements occupy a large volume (i.e., are densely spaced). Sayre and Albertson (17) found no depth correction necessary and attributed this to the small spacing density of the roughness elements used in their studies. They concluded that the roughness elements did not greatly inhibit flow turbulence near the bed. Schlichting (18) used a datum such that the volume occupied by roughness above the datum was equal to the volume open to flow below the datum.

Channel Geometry

Several studies (2, 10, 11, 16, 20) have been made to determine the effect of channel cross section on resistance. Most of these studies (2, 10, 11, 16) have found that the use of hydraulic radius to represent the dimensions of irregularly shaped channels is sufficient to allow for the effect of shape on resistance.

The studies of Keulegan, already discussed, indicated that the effect of nonuniform boundary shear on flow resistance was negligible and that the shape effect represented by B (equation 9) could be accounted for by use of a small, constant value for this term. Powell (16) found that the error involved in neglecting channel shape effect did not exceed 5 percent. Straub and coworkers (20) found that channel shape had some effect on resistance in rough channels, but a lesser effect in smooth channels.

REQUIREMENTS IF FLOW RESISTANCE STUDIES ARE TO BE APPLICABLE TO SURFACE IRRIGATION DESIGN

The boundaries of irrigation channels are rougher than those of most commercial conduits. Hence, the results of previous research on smooth boundaries are not generally applicable to the study presented in this bulletin. For the laminar flow range, boundary roughness affects both the resistance to flow and the transition to turbulence. Both of these effects need to be studied over a boundary roughness similar to that of irrigation channels.

Most fundamental studies of turbulent flow have considered artificially roughened conduits where all roughness elements on a given boundary have identical size and spacing. Even when considering uniform boundary roughness, investigators have not agreed on the roughness dimension, i.e., height or spacing, that exerts the primary influence on flow resistance, although most investigators consider roughness height to have the greater effect. Variations in spacing of roughness elements, for roughness of a constant height, will cause variations in flow resistance. In studies of flow resistance, the roughness height and longitudinal spacing should both be measured as the variables most likely to affect flow resistance. Transverse spacing and shape of the roughness elements should have a lesser effect on resistance.

Previous studies of flow resistance have shown that it is difficult to relate the effective dimensions of natural or artificial roughness elements to a roughness standard without the use of trial resistance runs. The relationship between the dimensions of the roughness elements and the resistance to flow can be applied directly to field conditions with the least difficulty if the roughness constructed in the laboratory is as similar as possible to natural soil roughness.

It is apparent from past investigations that the resistance coefficients of uniform flow formulas such as Manning's or Chezy's are not constant for a given channel, but vary with the depth of flow. Therefore, study of these coefficients should involve the full range of flow conditions likely to be encountered in practical applications, especially low depths of flow such as occur in irrigation channels.

The effects of channel shape on flow resistance are less important than the effects of boundary roughness. However, the magnitude of channel shape effects seems to vary with flow and boundary conditions. Shape effects should be studied under conditions of low flow rates and very rough boundaries.

EQUIPMENT AND PROCEDURES

It would be difficult to control and measure the variables necessary to evaluate flow resistance in small irrigation channels with sufficient precision in the field. For the experiments described and evaluated in this bulletin, flow resistance in small channels was studied in the hydraulics laboratory. Flow boundaries created in the laboratory were similar to those of irrigation borders and furrows; hence, the relation of resistance to roughness dimensions found in this study should find direct application in the field.

Channel Construction

A wooden flume, 4 feet wide, 60 feet long, and with an adjustable slope, was used to support the flow channels used in this study. A supporting structure constructed inside the flume contained the soil-like material used for the experimental channels. This structure extended the full 60-foot length of the flume. The flume channels emptied into a weir box where discharge could be measured by a calibrated, 90°, V-notch weir; to measure small flows, the discharge over a timed interval was caught and weighed. The headbox of the flume was supplied with water by pump from a large sump. Rails on the flume walls provided a datum from which channels could be constructed and experimental measurements taken. Figure 1 is a sketch of the flume and two types of channel used.

Three pumps—3 inches, 4 inches, and 8 inches in size—were used to supply water to the soil channels at steady rates, ranging from 0.01 to 1.1 c.f.s. Higher rates of discharge sometimes caused erosion of the channel boundaries and, for this reason, were not used.

For the first group of tests, channels were built with a rectangular cross section, to correspond to the cross section of irrigation borders. The width of the channels was limited to 1.88 feet. Parallel sheets of masonite formed the side walls of the rectangular channels. The floor of the channel, hereafter called the bed, was composed of a soil-like material from which different roughnesses could be formed. A polyethylene sheet inserted beneath this soil-like material prevented seepage from the channel. For most of the soil roughnesses formed, the side walls were much smoother than the channel bed. Figures 25 to 35 in the appendix show the rectangular channels constructed; the identifying letters in the legends for these figures
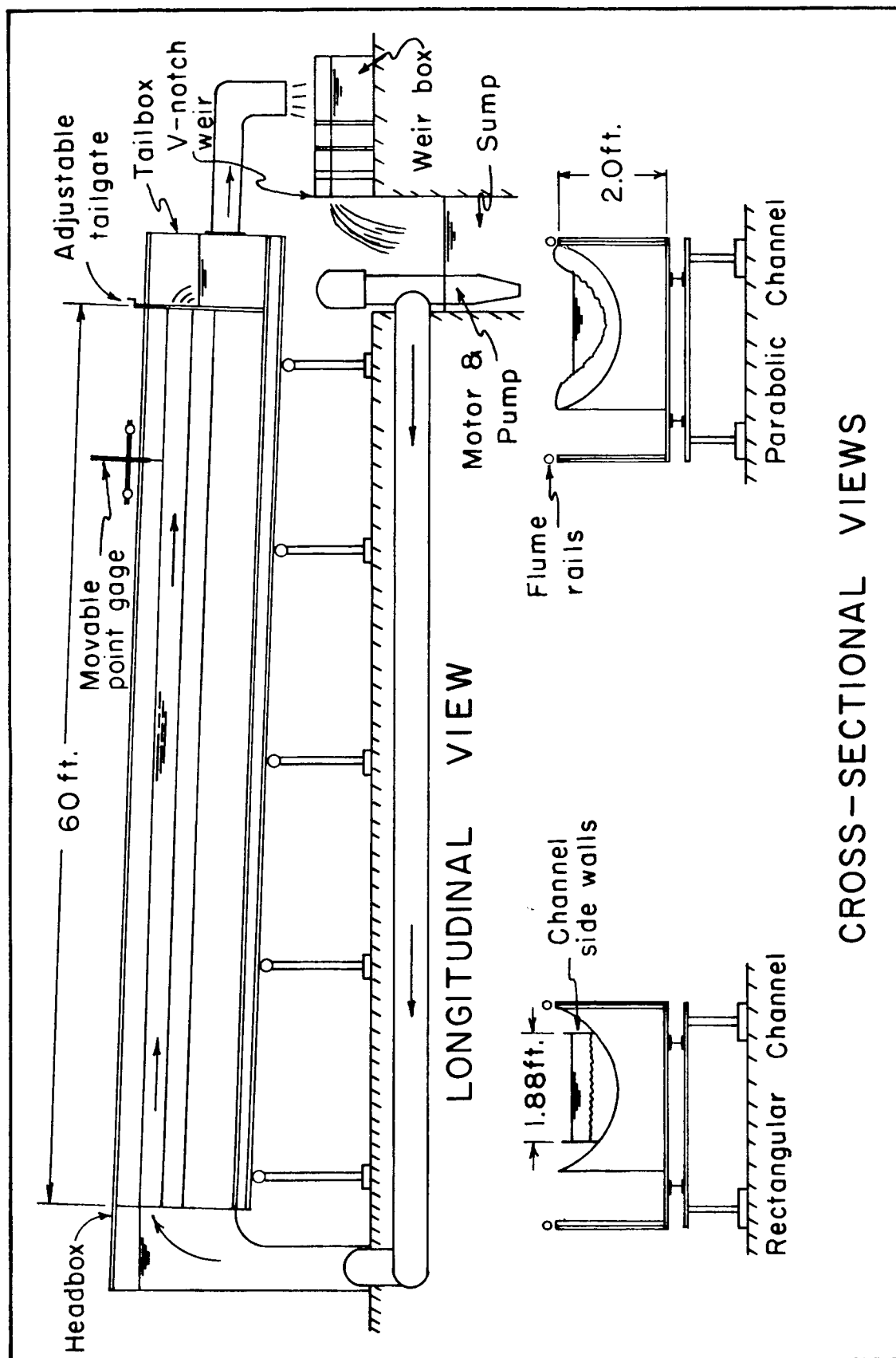
FIGURE 1.—Flume and two types of channels used for flow resistance experiments.

correspond to the identifying letters used in the tables.[3]

For the second group of tests, channels were constructed with parabolic cross sections approximating the range of common shapes of irrigation furrows. The shape of each parabolic channel was described by the formula:

$$y = ax^2 \qquad (17)$$

Channels were constructed having values of a equal to 0.40, 0.65, and 0.90. Figures 36 to 42 in the appendix show the parabolic channels constructed; the identifying letters in the legends for these figures correspond to the identifying letters used in the tables.

The material used in the channels was not a natural soil but a sandy material washed from the gravel at a local gravel pit. It originally contained lumps of clay. Before the sandy material was used in the channel, the largest of these clay lumps were removed by sieving all the material through a ¼-inch screen. The material, after removal of the clay lumps, is shown by mechanical analysis to be a very fine sand (see fig. 2).

All channels were formed by a plywood screed fastened to a cart that ran on the flume rails. For rectangular channels (borders) the screed had a straight edge; for furrows the screed had the desired parabolic shape. Channel elevation was constant relative to the rails, which had been preset at the desired slope.

After the channels were screeded, they were modified in different ways to produce the range of roughness necessary for the study. The range of roughness exceeded that likely to be found in actual irrigation channels. The smoothest boundaries were formed by hand troweling the screeded channel. The roughest boundaries were formed by using a tillage tool that provided an irregular, cloddy surface. Some boundaries were modified by ponding water on the surface for a short length of time. To form others, flows of water just large enough to cause small amounts of soil movement were run over the surface until the desired boundary was produced.

So that the change of resistance with discharge for a given bed form could be investigated, the different boundaries were stabilized with a chemical treatment of the type developed by Vanoni and Brooks (22). Spray applications of sodium silicate, sodium aluminate, and calcium chloride solutions prevented any alteration of the boundary roughness for the slopes and discharges used in this study.

___

[3] Descriptive tabulations of many of the boundary roughnesses used in this study are included in E. G. Kruse's Ph. D. dissertation—EFFECTS OF BOUNDARY ROUGHNESS AND CHANNEL SHAPE ON RESISTANCE TO FLOW OF WATER IN VERY SMALL OPEN CHANNELS. On file, Library, Colo. State University, Fort Collins. 1962.

After the roughness was stabilized, elevations of the rectangular channels were determined with point gage readings at 0.05-foot intervals transverse to the direction of flow at each 5-foot station. The average of these readings was assumed to be the mean bed elevation at the station where taken.

The cross-sectional profiles of each parabolic channel were measured in a similar manner. The coefficient a of a least-squares parabola through the set of points was determined, the coordinates of the vertex being fixed at the same depth for all stations for a given channel. By integrating the least-squares parabolic equation, it was possible to obtain the area and wetted perimeter of the channel as functions of the flow depth.

Experimental Procedures

Experimental runs were taken for two to four channel slopes for each boundary. The group of runs for a given channel at a given slope constitutes a series. The first run of each series was made at the lowest depth of discharge that would submerge almost all of the roughness on the channel boundary. Discharge was approximately doubled for each subsequent run. Before the elevation of the water surface was measured, weir readings were checked every 5 minutes for 15 minutes, to make sure that all variation had ceased. During this time, water temperature was measured at the headbox of the channel.

When discharge became steady, the tailgate was adjusted to give uniform flow in the channel. This adjustment was the one requiring the most judgment and the one most subject to error during the tests. As has been mentioned, screeding left the channel soil surface parallel to the flume rails. However, roughening the soil left its average elevation slightly above the overall mean at some stations and slightly below it at others. This condition was especially evident in the rippled beds. For this reason, flow was judged to be uniform when the water surface elevation was most nearly constant relative to the flume rails. Both bed and water surface elevations were read with a point gage mounted on the movable carriage used for screeding the boundaries. Thus, all elevations were measured from the same datum parallel to the channel slope and could be compared directly. The slope of the flume rails, set before each series of runs, was assumed equal to the energy line slope for computational purposes. The measured depth of flow sometimes varied considerably (as much as 25 percent) from station to station. When resistance coefficients were calculated, the error due to this variability was reduced by averaging results for at least four stations between station 20 and station 50 (of the 61 stations located at 1-foot intervals along the 60-foot flume). (Readings of water surface
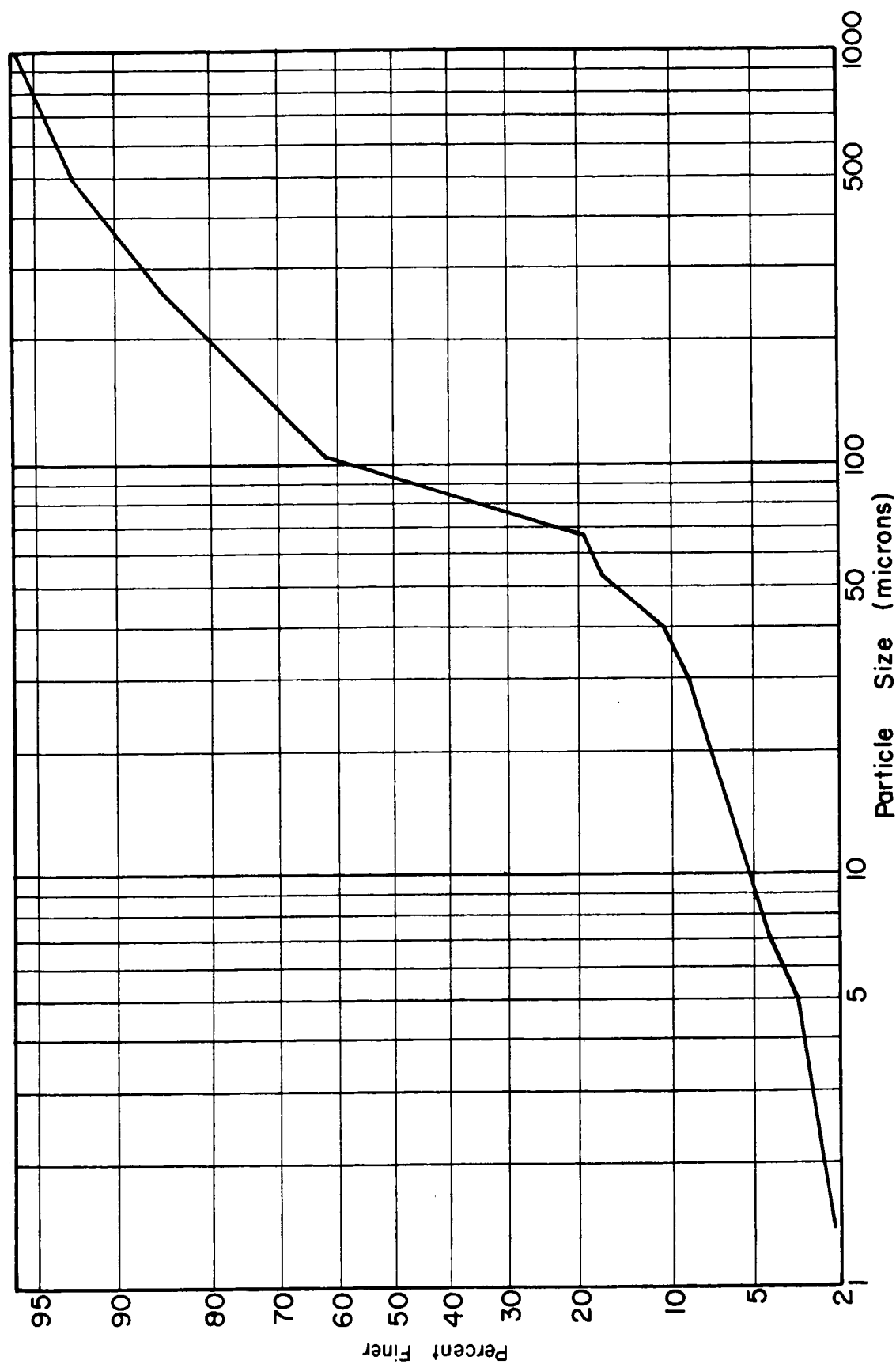
FIGURE 2.—Particle size distribution of soil-like material used for forming channel boundary roughness.

elevation were taken every 5 feet between station 10 and station 55.)

Slight variations in the roughness of some sections caused unavoidable nonuniformities in flow depth for some channels. For instance, the water depths in one channel were slightly lower in the middle of the test section than at stations further upstream or downstream. In such cases the mean water surface was adjusted to the same elevation at the two ends of the channel by changing the tailgate setting.

The water surface elevation was measured to the nearest 0.001 foot at every 5-foot station along the channel. When the water surface was rough, three readings of water surface elevation were taken across the channel and averaged for each station.

After a series of runs at one slope, the flume was set at a different slope by means of the adjustable screw jacks that supported it. For most channels, runs were made at slopes of 0.005, 0.001 and 0.0005. Slopes of 0.0001 and 0.0003 were included for some channels. At slopes of 0.0005 or less, rail elevations were estimated to the nearest 0.0001 foot in order to set the slope as precisely as possible. At a slope of 0.0001 there was only a 0.006-foot drop in elevation between the upstream and downstream ends of the channel, making it extremely difficult to be sure when flow was uniform.

After the last run for each boundary, six plaster casts, each 1 foot long and about 0.2 foot wide, were made in order to be able to make additional roughness measurements, if necessary, after the boundary was changed. The location of each cast was chosen at random along the test reach of the channel. The long dimensions of the casts were aligned with the direction of flow so that both height and longitudinal spacing of the roughness could be obtained from them.

Because of the random nature of the roughness, a statistical representation of roughness dimensions was necessary. The measure used for roughness height was the standard deviation of evenly spaced surface elevation measurements about the mean elevation. This was computed for the rectangular channels by use of the following formula:

$$\sigma = \sqrt{\frac{\Sigma(y_i - \overline{y})^2}{n-1}} \quad (18)$$

where:

σ is the standard deviation,
y_i is the individual bed elevation measurement,
$\overline{y}$ is the mean bed elevation,
n is the number of elevation measurements.

The values of σ could be calculated directly from measurements of the casts for rectangular channels because the cast measurements were referenced to the true bed elevations.

A different procedure was used to calculate standard deviation from casts of the parabolic channels. Because readings were not referenced to bed elevations, a regression line was first computed through the elevations read from the casts. This regression line was assumed to be parallel to the slope of the channel. The standard deviation of elevation measurements about this regression line was then calculated by the formula:

$$\sigma = \sqrt{\frac{\Sigma(y_i - a + bx_i)^2}{n-2}} \quad (19)$$

where:

$$b = \frac{\Sigma xy - \Sigma x \Sigma y/n}{\Sigma x^2 - (\Sigma x)^2/n}$$

$$a = \overline{y} - b\overline{x}$$

x_i is the distance from some datum at which the elevation y_i is measured.

Standard deviations were computed for casts from both the sides and bottom of the channels and the results averaged. The significance of σ is indicated diagrammatically in figure 3.

Considerable variation existed in values of σ from different casts for the same channel boundary. In extreme cases the value of σ for a given cast was as much as twice as great as the mean value for the channel. No consistent variation was evident in values of σ measured on the sides or in the bottoms of parabolic channels.

Measurements of the longitudinal roughness spacing were made only on the rectangular channels. Spacing was defined and measured in two ways. Both measurements were taken along a line parallel to the direction of flow. To obtain the first spacing measure, λ_σ, the number of roughness elements that projected more than 1σ above the mean bed elevation was counted and the average spacing computed. The second spacing measure, λ_p, was obtained by counting all the roughness element crests along a length of boundary and determining the average spacing. Results obtained from this procedure depend to some extent on the judgment of the person making the measurement. Both spacing values were obtained from measurements along 6 linear feet of each boundary. The significance of the two measurements of longitudinal spacing can be seen in figure 3.

No procedure was available for evaluating the rugosity of the individual roughness elements. Rugosity did vary over a wide range, being represented at one extreme by a cloddy-type roughness that was stabilized in the same condition in which it was formed by a tillage tool. At the other extreme were the roughnesses that had been smoothed and rounded by low-velocity flows of water.
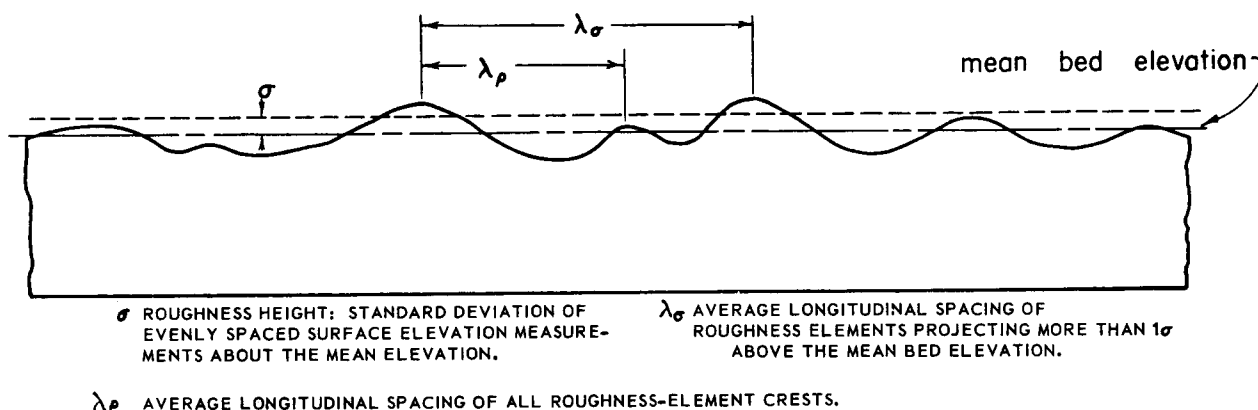
σ ROUGHNESS HEIGHT: STANDARD DEVIATION OF
EVENLY SPACED SURFACE ELEVATION MEASURE-
MENTS ABOUT THE MEAN ELEVATION.

λ_σ AVERAGE LONGITUDINAL SPACING OF
ROUGHNESS ELEMENTS PROJECTING MORE THAN 1σ
ABOVE THE MEAN BED ELEVATION.

λ_ρ AVERAGE LONGITUDINAL SPACING OF ALL ROUGHNESS-ELEMENT CRESTS.

FIGURE 3.—Diagrammatic representation of measured roughness dimensions.

RESULTS

The experimental data obtained are given in tables 8, 9, 10, and 11 in the appendix. For channels where the mean bed elevations were different at different stations, it was difficult to determine when flow was uniform. To determine whether any runs were nonuniform, mean depth of flow was plotted against discharge for all turbulent runs in the rectangular channels. For furrows the hydraulic radius was plotted against discharge. A well defined relationship existed between Q (total discharge) and d or R. The relationship was represented by a different line for each channel slope. The lines for all slopes were parallel. If it was assumed that the lines relating discharge to depth represented data for uniform flows, deviations of individual points from the lines could be attributed to nonuniform flow or other errors in taking the data. Data that varied by more than 5 percent from the lines were considered to be of questionable value and are not included in the following analysis.

Laminar Flow

A plotting of the Darcy-Weisbach resistance coefficient, f, against Reynolds number is often used to illustrate resistance characteristics of the various regimes of pipe flow. The same type of data can be plotted for open channel flows. If the Reynolds number (Re) for open channels is defined as being equal to RV/ν (where ν represents kinematic viscosity) and d is assumed equal to R for wide channels, equations 1 and 4 can be combined to yield:

$$f=\frac{24}{Re} \qquad (20)$$

A line corresponding to this equation is plotted on each of figures 4 to 9 and represents the theoretical resistance relation for laminar flows over smooth boundaries.

In figures 4 to 9, coefficient of friction is plotted against Reynolds number, for six rectangular channels with some runs at Reynolds numbers in the 30 to 1,000 range (channels D, E, I, K, L, M). The curves for the data for five of these channels (D, E, I, K, M) lie above the theoretical straight line for laminar flows over smooth boundaries. Data for each channel slope is represented by a different straight line for Reynolds numbers less than 500. For these five channels the resistance to flow was apparently increased by the boundary roughness. The data for bed L (fig. 8) and for the lowest slope of bed K (fig. 7) indicate that resistance for these runs was the same as for theoretically smooth channels. Although bed L functioned as a smooth bed, it was not a true plane. The boundary had a very-fine-sand-grain roughness and a slight waviness.

The lines defined by the data for low Reynolds numbers have a slope of 45° and are parallel to the theoretical line (solid line) for smooth boundaries, indicating that the flows were similar to true laminar flows.

Critical Roughness Height

On the basis of the assumptions used by Goldstein (5) a criterion can be developed for the height of roughness necessary for separation to occur in laminar flow in wide, open channels. The velocity distribution for two-dimensional laminar flow is given by:

$$v=\frac{3V}{d^2}\left(yd-\frac{y^2}{2}\right) \qquad (21)$$

where:

v is the velocity at a distance y from the boundary, and
d is the depth of flow.
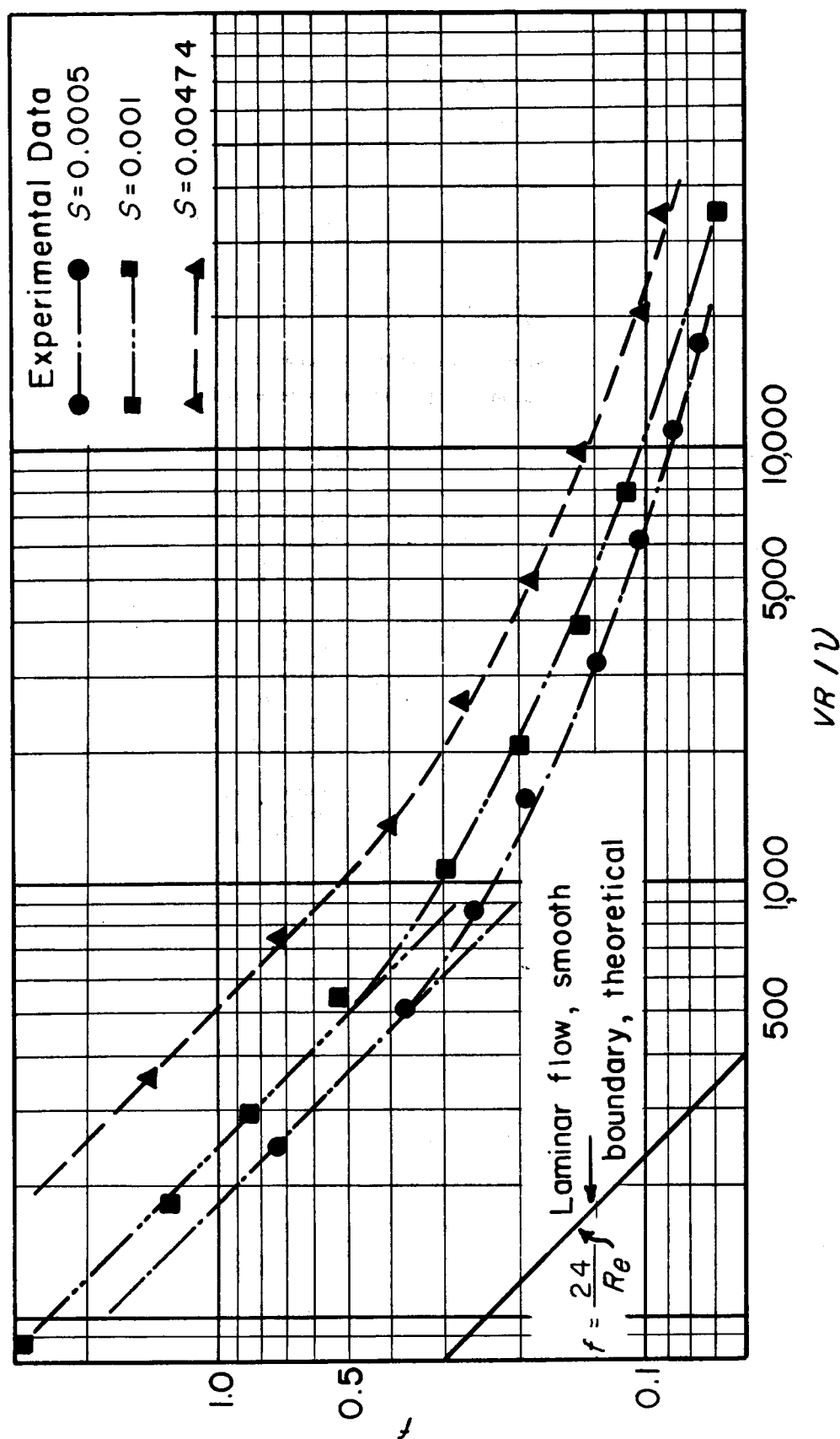
FIGURE 4.—Resistance coefficient f as a function of Reynolds number, VR/v, for rectangular channel D.
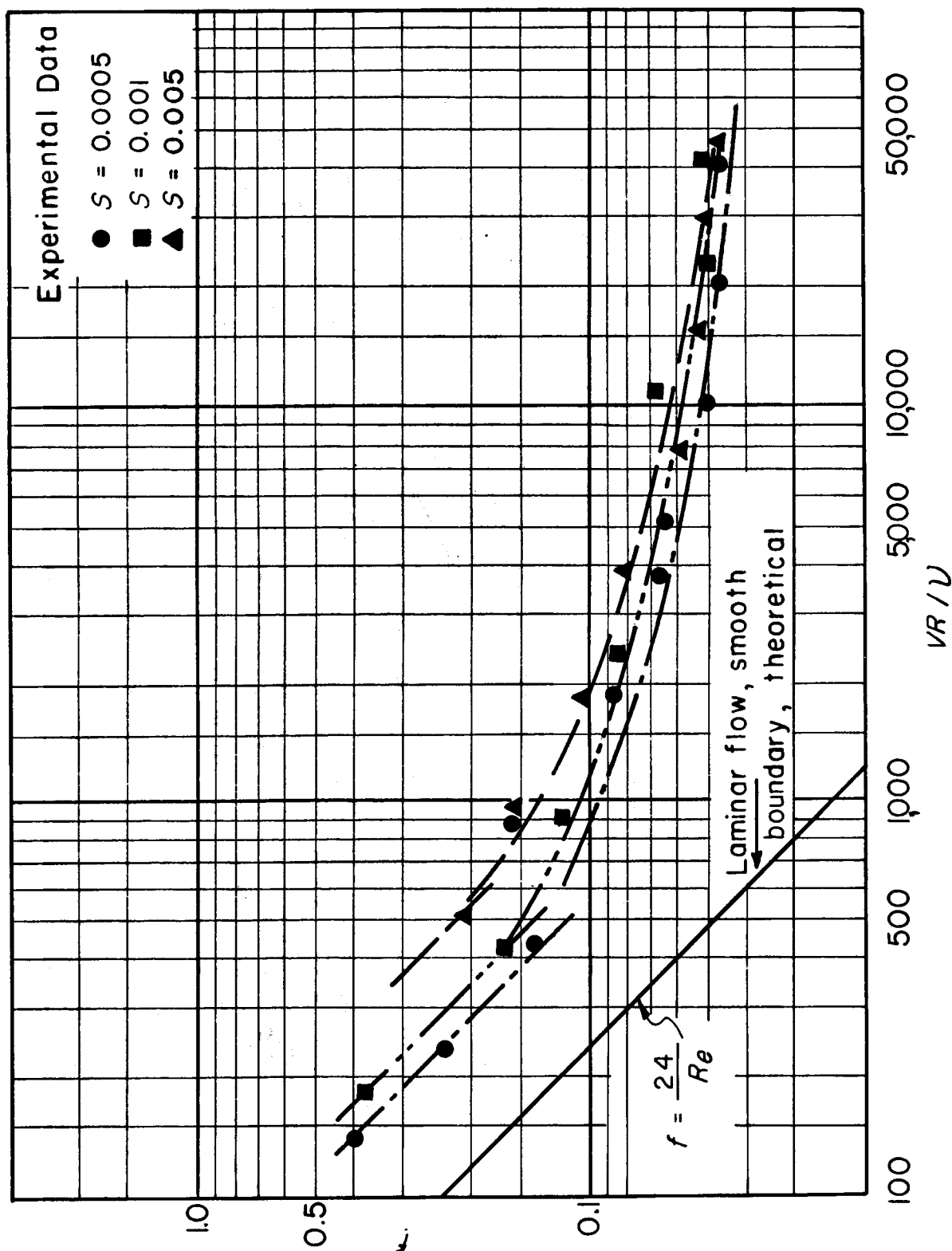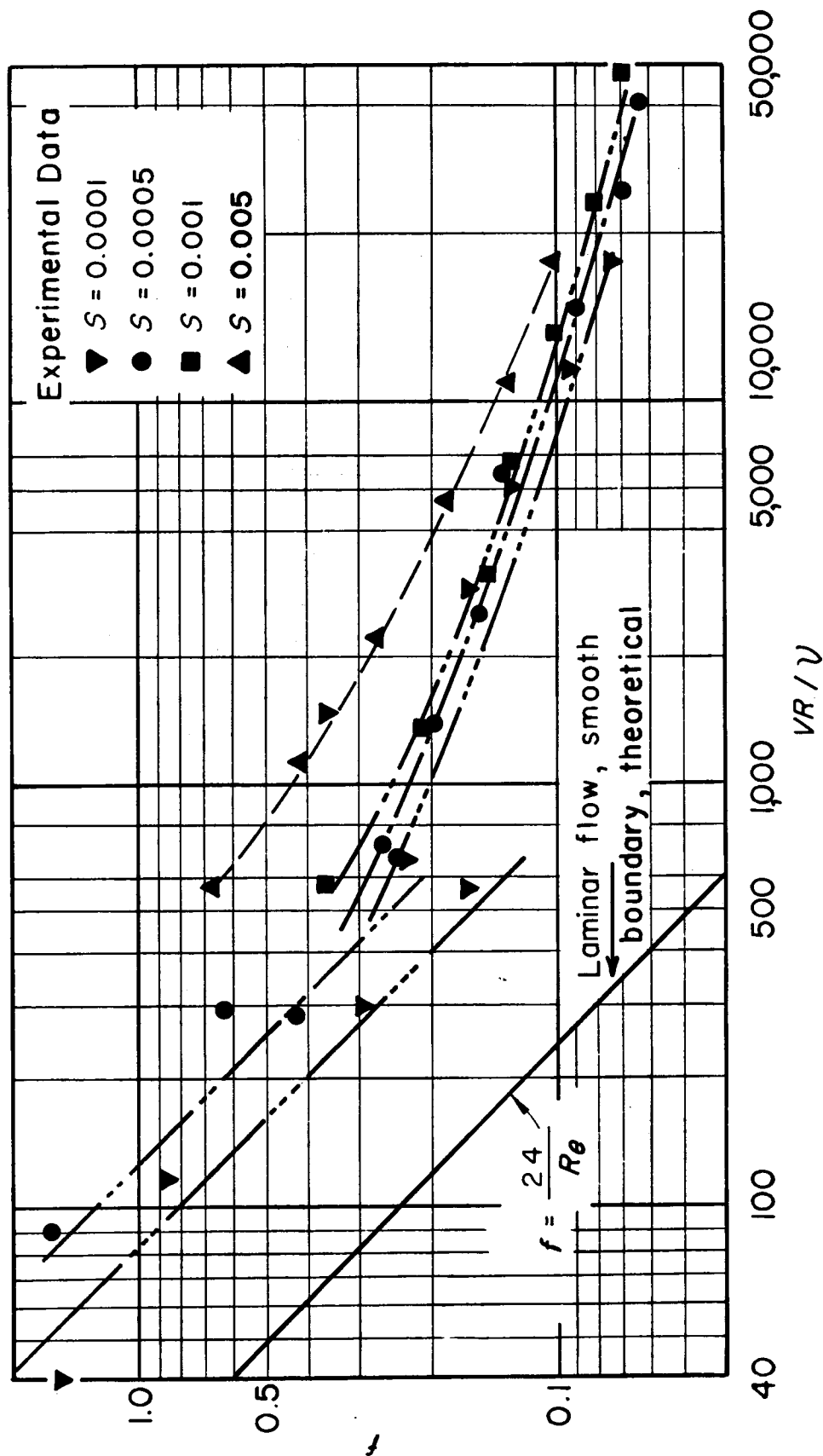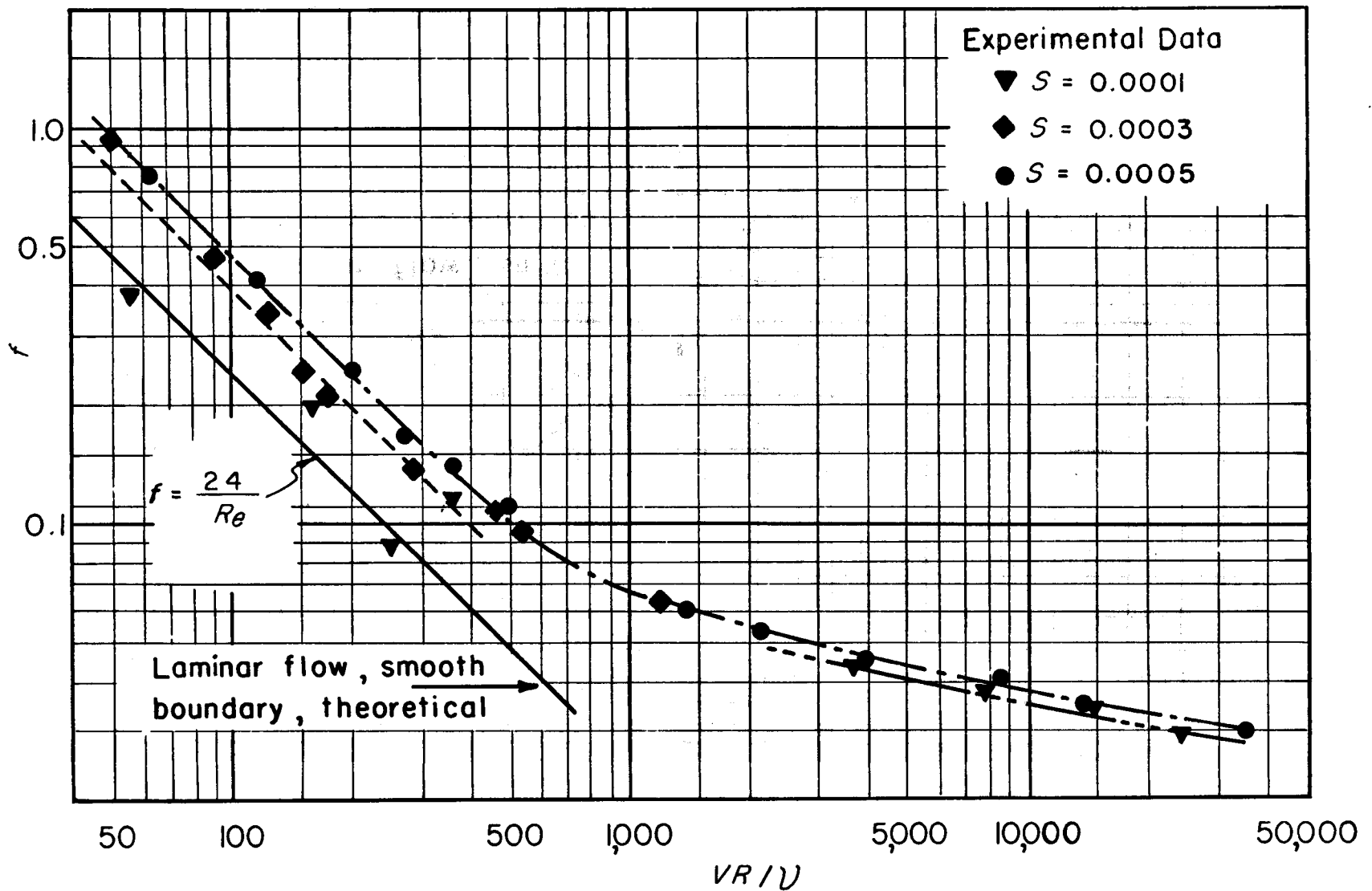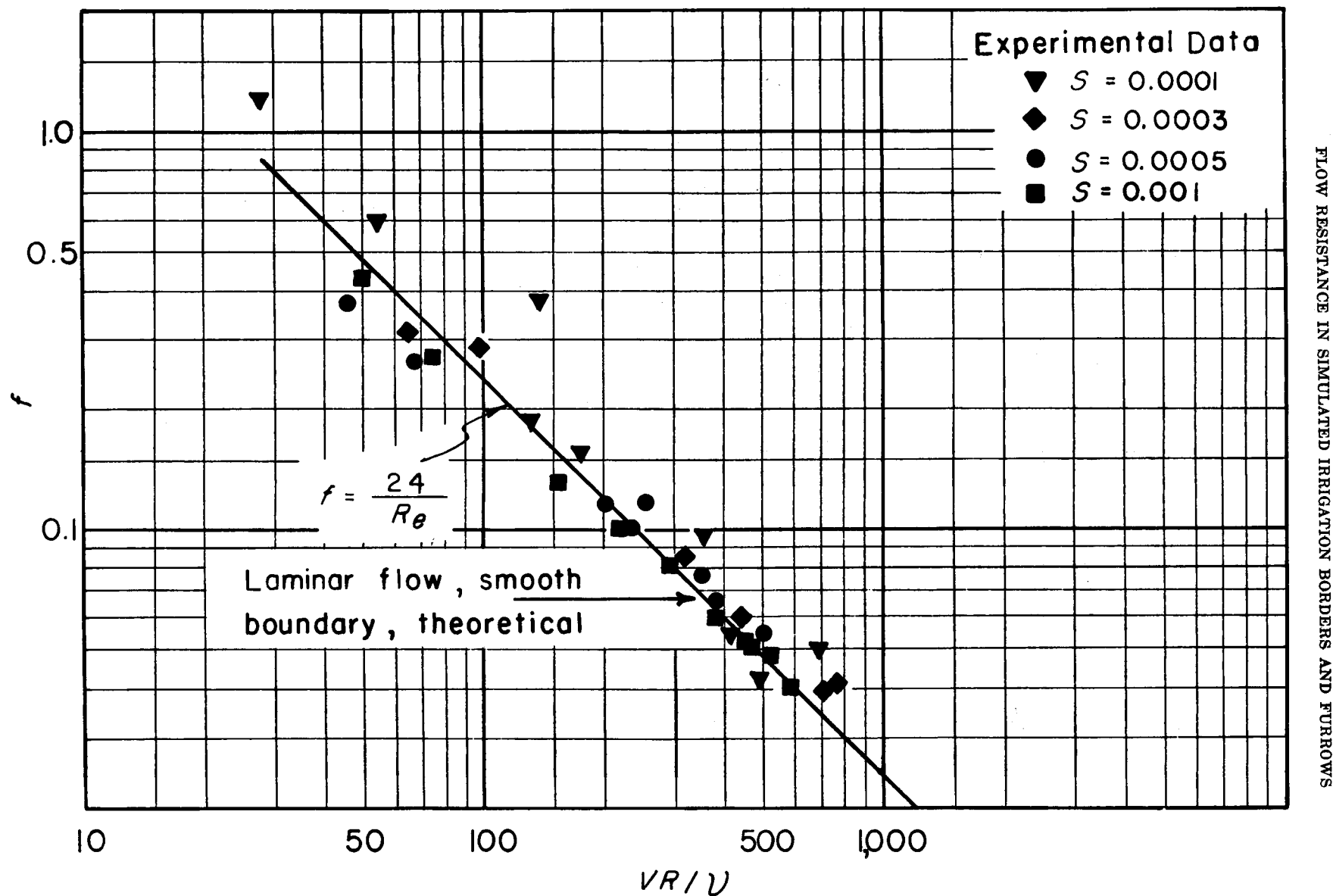
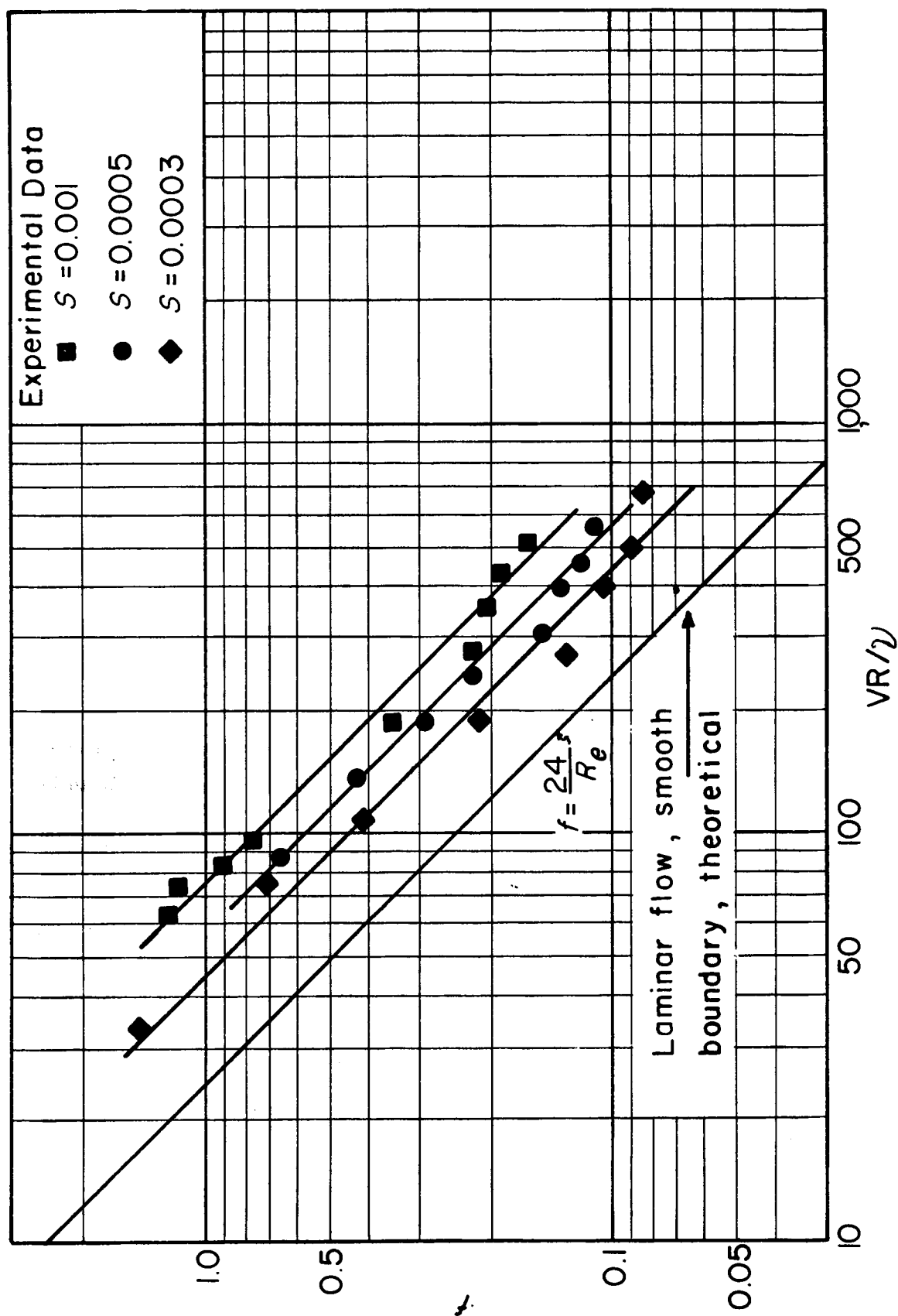FIGURE 5.— Resistance coefficient f as a function of Reynolds number, VR/ν, for rectangular channel E.

FIGURE 6.—Resistance coefficient f as a function of Reynolds number, VR/ν, for rectangular channel I.

FIGURE 7.—Resistance coefficient f as a function of Reynolds number, VR/ν, for rectangular channel K.

FIGURE 8.—Resistance coefficient f as a function of Reynolds number, VR/ν, for rectangular channel L.

FIGURE 9.—Resistance coefficient f as a function of Reynolds number, VR/ν, for rectangular channel M.

The velocity at a level equal to the roughness height k is:

$$V_k = 3V\left(k\frac{d}{d^2} - \frac{k^2}{2d^2}\right)$$

or, if $\frac{k}{d}$ is small:

$$V_k = 3V\frac{k}{d}$$

Now, the tip Reynolds number is defined as:

$$Re_k = V_k\frac{k}{\nu}$$

$$= 3V\frac{k^2}{d\nu}$$

$$= 3V\frac{d}{\nu}\frac{k^2}{d^2}$$

$$= 3Re\left(\frac{k}{d}\right)^2 \qquad (22)$$

Let Re_{kc} be the value of tip Reynolds number at which separation occurs at the tops of the roughness elements (critical value). Then the height of roughness necessary for separation to occur in open channel flow is:

$$k = \frac{d}{\sqrt{3}}\left(\frac{Re_{kc}}{Re}\right)^{1/2} \qquad (23)$$

The data collected and the concept of a critical tip Reynolds number were used to derive an expression for the height of roughness necessary to affect the flow (to cause head losses greater than the theoretical for laminar flow). Rectangular channel L was not rough enough to cause head losses greater than the theoretical. The highest value of tip Reynolds number observed for this channel was 16. Likewise, bed K behaved as a smooth bed at a slope of 0.0001. Only one tip Reynolds number at this slope was greater than 20. With steeper slopes, resistances were greater than predicted by the theoretical equation for smooth boundaries. All but one of the tip Reynolds numbers for these slopes were greater than 20. Critical values, therefore, were assumed equal to 20 and were substituted into equation 23 to find the critical roughness height, expressed in terms of the standard deviation of bed elevation measurements:

$$\sigma = \left(\frac{20}{Re}\right)^{1/2}\frac{d}{\sqrt{3}}$$

$$= \frac{2.58d}{\sqrt{Re}} \qquad (24)$$

Therefore, the height of roughness necessary to cause head losses greater than the theoretical

for laminar flow is:

$$\sigma \geq \frac{2.58d}{\sqrt{Re}} \qquad (25)$$

One set of data does not agree with criterion 25. For a slope of 0.0001, the data indicated bed I to be rough. However, tip Reynolds numbers at this slope were all less than 20. Bed I was composed of sharp-edged angular roughness elements. Apparently, separation occurred over these elements, although the tip Reynolds number was low.

Resistance Equation

It has been shown that the resistance equation for smooth boundaries is not applicable to laminar flows over most of the soil roughnesses studied. However, the data presented in figures 4 to 9 were used to develop an empirical equation. First, the data for each channel were combined into a single equation by expressing the intercept of each parallel straight line in terms of the channel slope. The resulting equation was:

$$f = AS^{0.5}Re^{-1}$$

where A has a different value for each channel.

The channels differed only in degree of channel roughness. Therefore, A was apparently a function of the roughness dimensions. By repeated trials, A was related to the measured roughness height, longitudinal spacing, roughness density, and various combinations of these terms. The relation that best describes the experimental data is $A = 6.0\times10^4\left(\frac{\sigma}{\lambda_p}\right)$. Therefore, the value of the resistance coefficient can be predicted by the following equation:

$$f = \frac{6.0\times10^4 S^{0.5}}{Re}\left(\frac{\sigma}{\lambda_p}\right) \qquad (26)$$

where σ represents the roughness height, measured as shown on page 9, and λ_p is the average longitudinal spacing between roughness crests. A comparison between measured values of f and values computed from equation 26 is shown in figure 10.

Equation 26 is a purely empirical relationship expressing the resistance coefficient in terms of the slope of the energy line, a roughness parameter, and the Reynolds number for flows in the laminar range. The equation indicates that as the height of roughness is increased, both the disturbance to flow and the resistance coefficient increase. An increase in roughness spacing decreases both the number of disturbances and the resistance coefficient. The effect of slope can be illustrated by considering a constant discharge. At small slopes
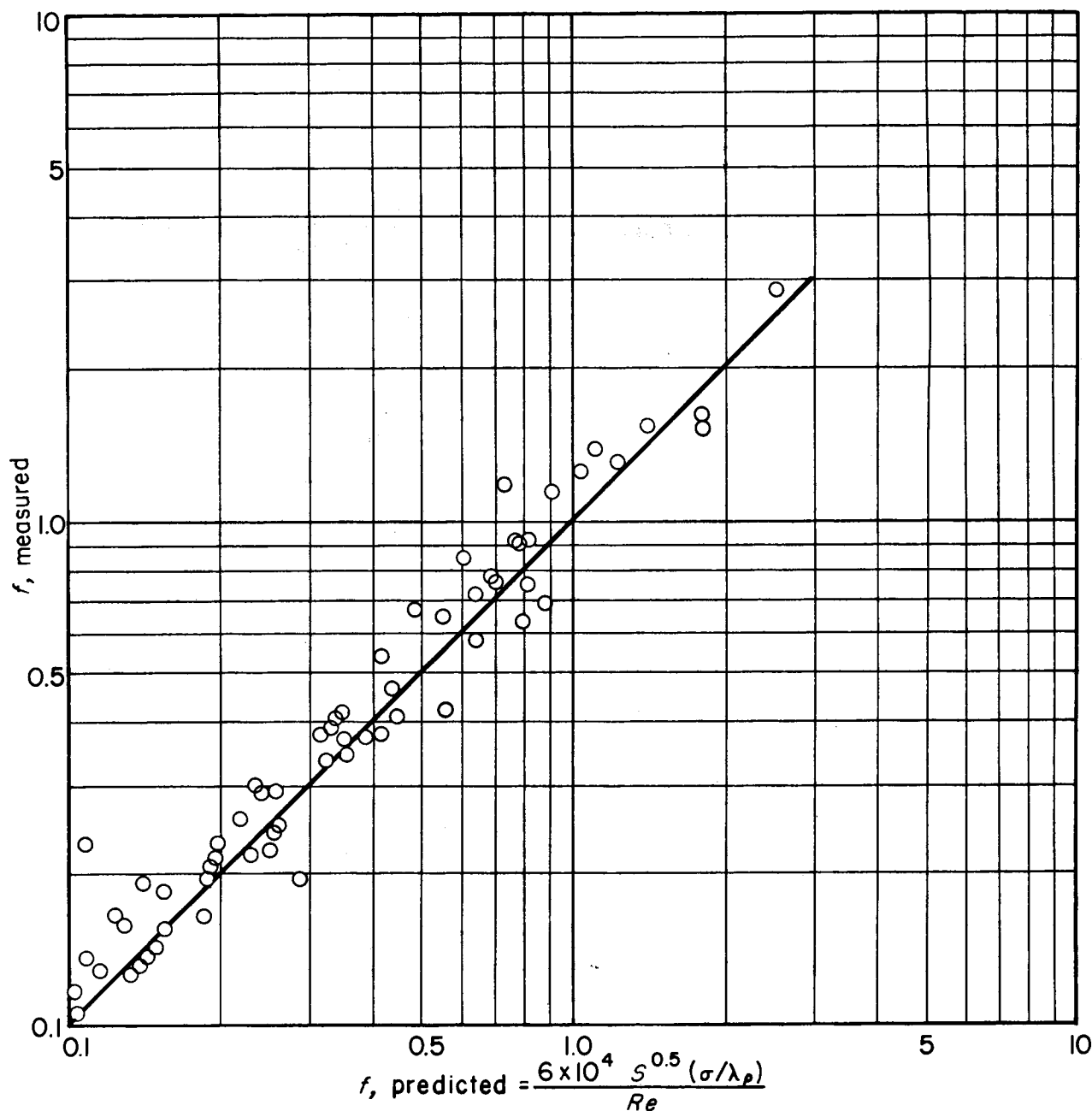
FIGURE 10.—Comparison between predicted and measured values of f for low Reynolds number flows in wide, rectangular channels.

the flow will be deep and low in velocity; the eddies formed at the roughness crests will be weak and will cause turbulence only throughout a small portion of the flow depth. At higher slopes flow depth will be smaller and velocities greater. The turbulent wakes will occupy a relatively large portion of flow depth and resistance will be accordingly greater.

Equation 26 is a desirable one for the computation of resistance coefficient because all variables can be determined. The slope is generally predetermined or can be measured, the roughness parameter can be computed from measurements taken of the boundary, and the Reynolds number is merely the unit discharge divided by the viscosity of the water. The computed resistance

coefficient can then be combined with the Darcy-Weisbach equation, equation 4, and the continuity equation $(q=Vd)$ to find the mean velocity of flow or depth of flow. The following equation is obtained for depth of flow:

$$d=\sqrt[3]{\frac{7.5\times10^3 q\nu}{g\sqrt{S}}\left(\frac{\sigma}{\lambda_p}\right)} \qquad (27)$$

Transition From Laminar to Turbulent Flow

The transition from laminar to turbulent flow was studied by observing streams of dye injected into the flow. At the very lowest Reynolds numbers, no turbulence could be detected. At higher Reynolds numbers, wakes and general instability of laminar flow over the rough boundaries began in a region close to the roughness elements. Dye streams were straight near the surface but undulating and beginning to break up near the bottom. At still higher Reynolds numbers, turbulence was observed throughout the entire flow depth. The critical Reynolds number for laminar flow over rough boundaries was between 400 and 500 for the range of slopes and roughnesses studied. The critical Reynolds number for laminar flow over a smooth boundary was greater than 500 and as high as 766.

The value of the critical Reynolds number was also determined from the point at which the plot of the experimental data diverged from the theoretical 45° line in figures 4 to 9. For channels with rough boundaries (channels D, E, I, K, and M) the transition from laminar to turbulent flow as indicated by these plots occurred at Reynolds numbers of 400 to 500. For a smoother boundary (channel L, the troweled soil surface), the transition occurred at a Reynolds number of 700. These results are in agreement with the dye stream observations.

Observations of critical Reynolds number in this study are in general agreement with the values reported for rough boundaries by previous investigators: Jeffreys (9), 310; Hopf (7), 300 to 330; and Allen (1), 300. For the smooth boundary used in this study, the critical Reynolds number was above 700. Horton and coworkers (8) observed laminar flow conditions up to a Reynolds number of 548 and Owen (14) observed the same up to a Reynolds number of 1,000.

Turbulent Flow

The analysis of critical Reynolds number has shown that flows in the type of boundaries likely to be encountered in irrigation channels are in a transitional or turbulent state at Reynolds numbers greater than 500. Previous studies have shown that resistance formulas of the logarithmic type are applicable to turbulent flows. In this study, all flows with Reynolds numbers greater than 500 were analyzed by assuming that logarithmic resistance formulas were appropriate. Figures 4 to 9 show coefficient of friction plotted against Reynolds number for six of these channels.

Turbulence Constant

Different investigators have found different values for the universal turbulence constant, κ. Values of 0.40 and 0.38 are most commonly proposed. These values correspond to values for the coefficient of the logarithmic term of equation 20 equal to 5.75 and 6.06, respectively.

Values of κ can be determined experimentally from either velocity distribution data or mean flow data. In this study, since no valid velocity profiles could be obtained, it was necessary to estimate κ values from the mean flow data. Values of κ determined in this way varied from one channel to the next. All but one value were smaller than 0.40, the constant found by Nikuradse. Apparent values of κ as determined from mean flow data can differ for two reasons— nonuniform boundary shear or inconsistent measurement of flow depth. If boundary shear is not uniformly distributed, the value of $\bar{\epsilon}$ in equation 9 will differ from zero and the apparent value of κ will differ from the true value by the factor $1+\bar{\epsilon}$. Keulegan (10), from examinations of Bazin's data, found the effects represented by $\bar{\epsilon}$ to be negligible. Powell (16), however, found $\bar{\epsilon}$ values varying from -0.137 to -0.221, for different channel shapes. If the assumption made for rectangular channels in this study is valid, i.e., flow is unaffected by the side walls, the value of $\bar{\epsilon}$ should be zero.

Values of κ were determined in this study by plotting $C/\sqrt{g}$, resistance coefficient, against σ/R, a measure of the relative roughness (figs. 11 to 20). The data for nine of the rectangular channels and all of the parabolic channels plot as straight lines on the semilog graph paper. They can therefore be represented by an equation of the form:

$$\frac{C}{\sqrt{g}}=A-\frac{2.30}{\kappa}\log\frac{\sigma}{R} \qquad (28)$$

This equation has the same form as equation 9, the theoretical equation for rough-boundaried open channels.

The value of $2.30/\kappa$, the coefficient of the logarithmic term in equation 28, ranges from 5.13 to 11.95 for the different channels. Values for all but one boundary are larger than the most commonly accepted value of 5.75. The boundary with the small value of $2.30/\kappa$ (channel H) is one with a relatively small value of σ.
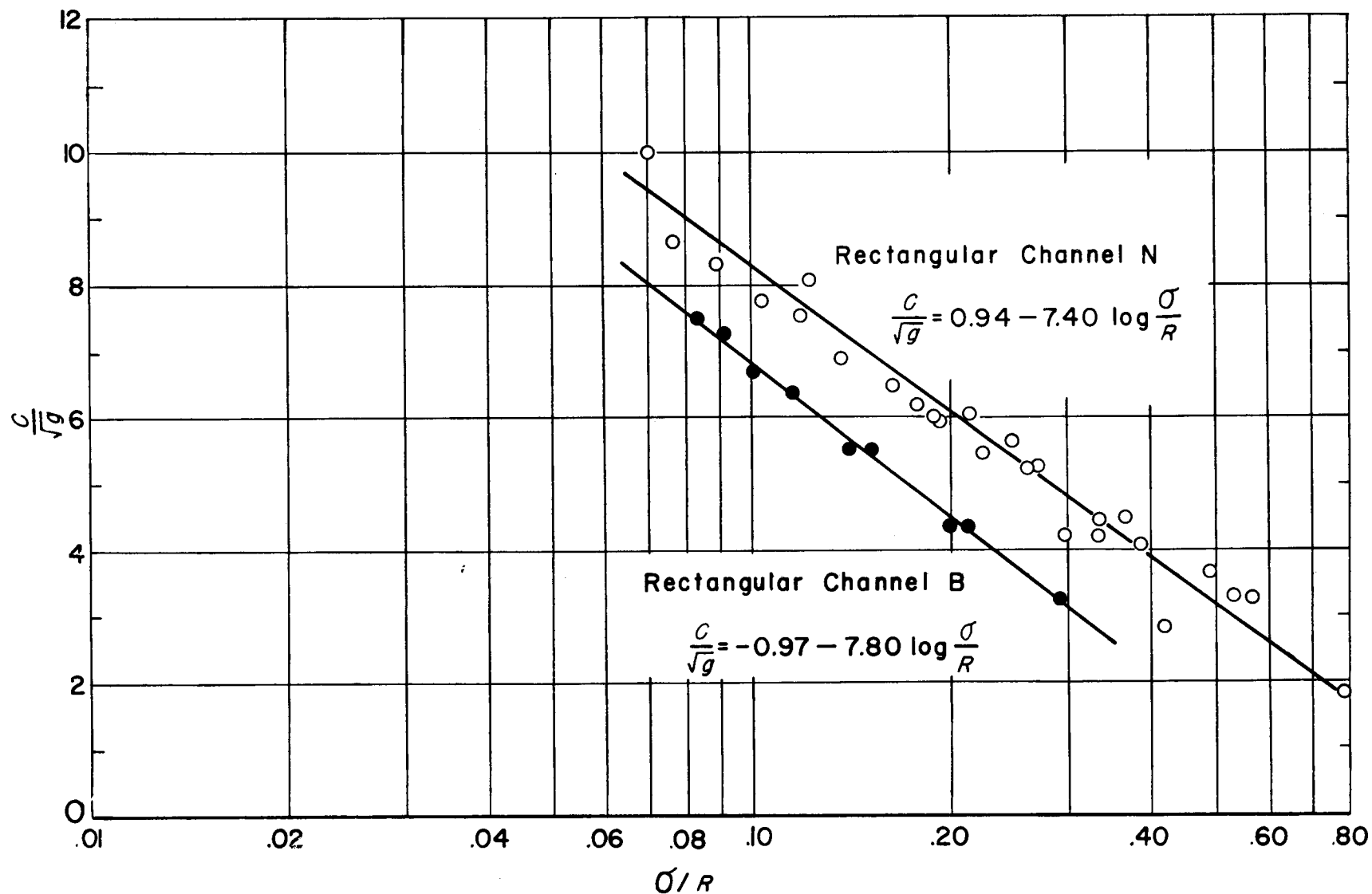
Rectangular Channel N

$$\frac{C}{\sqrt{g}} = 0.94 - 7.40 \log \frac{\sigma}{R}$$

Rectangular Channel B

$$\frac{C}{\sqrt{g}} = -0.97 - 7.80 \log \frac{\sigma}{R}$$

FIGURE 11.—Relation of resistance coefficient $(C/\sqrt{g})$ to relative roughness (σ/R) for rectangular channels N and B.
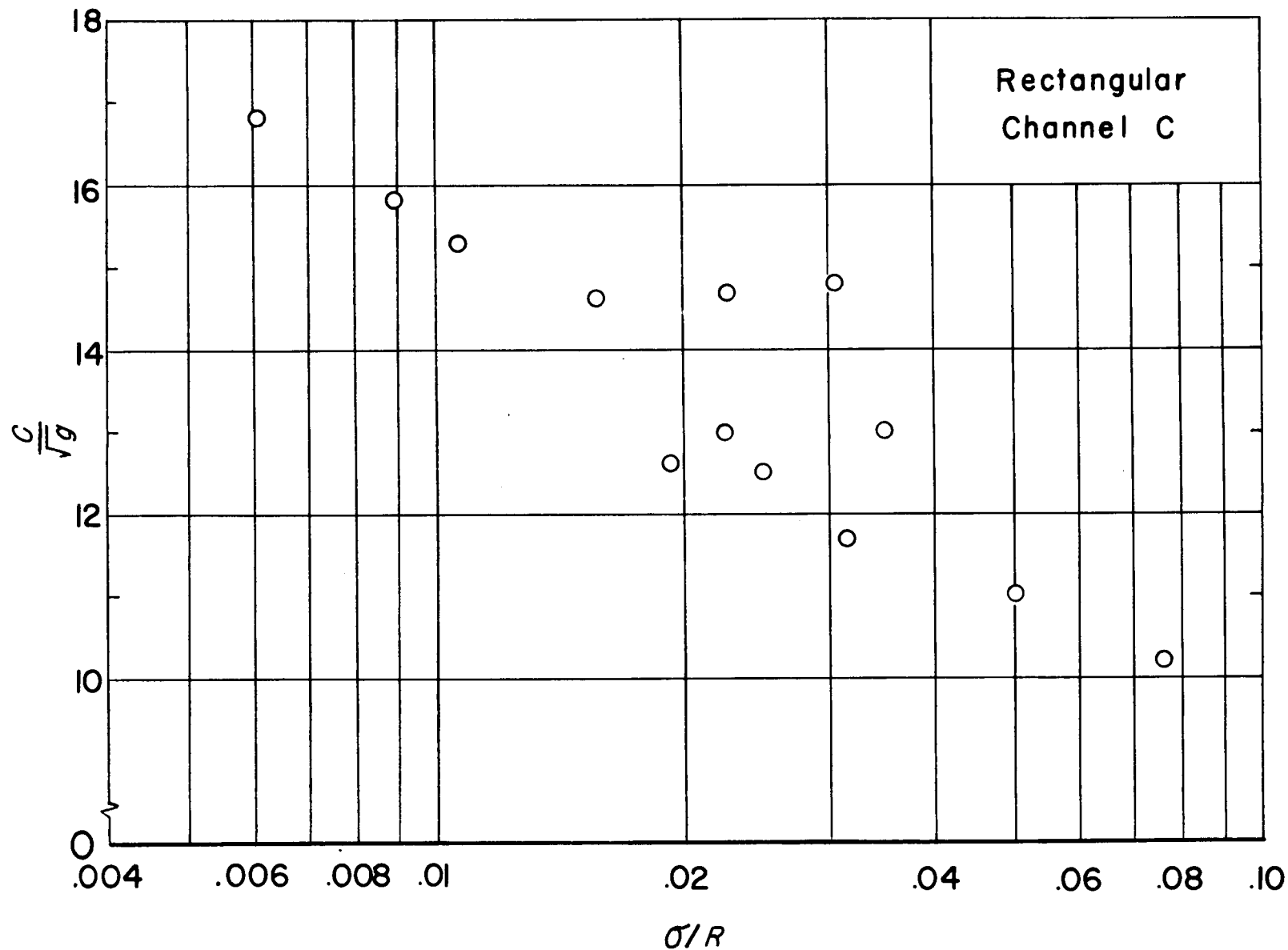
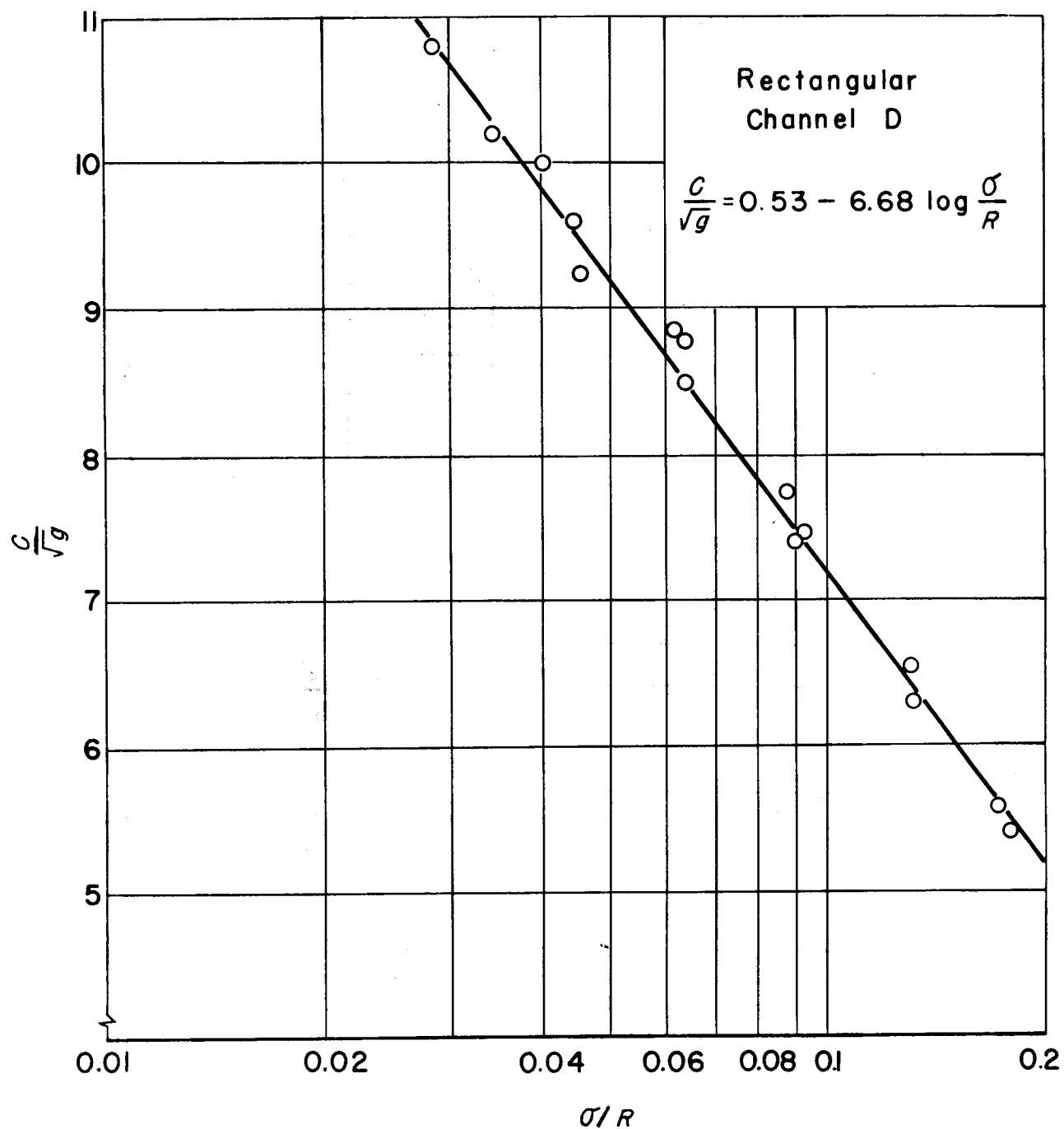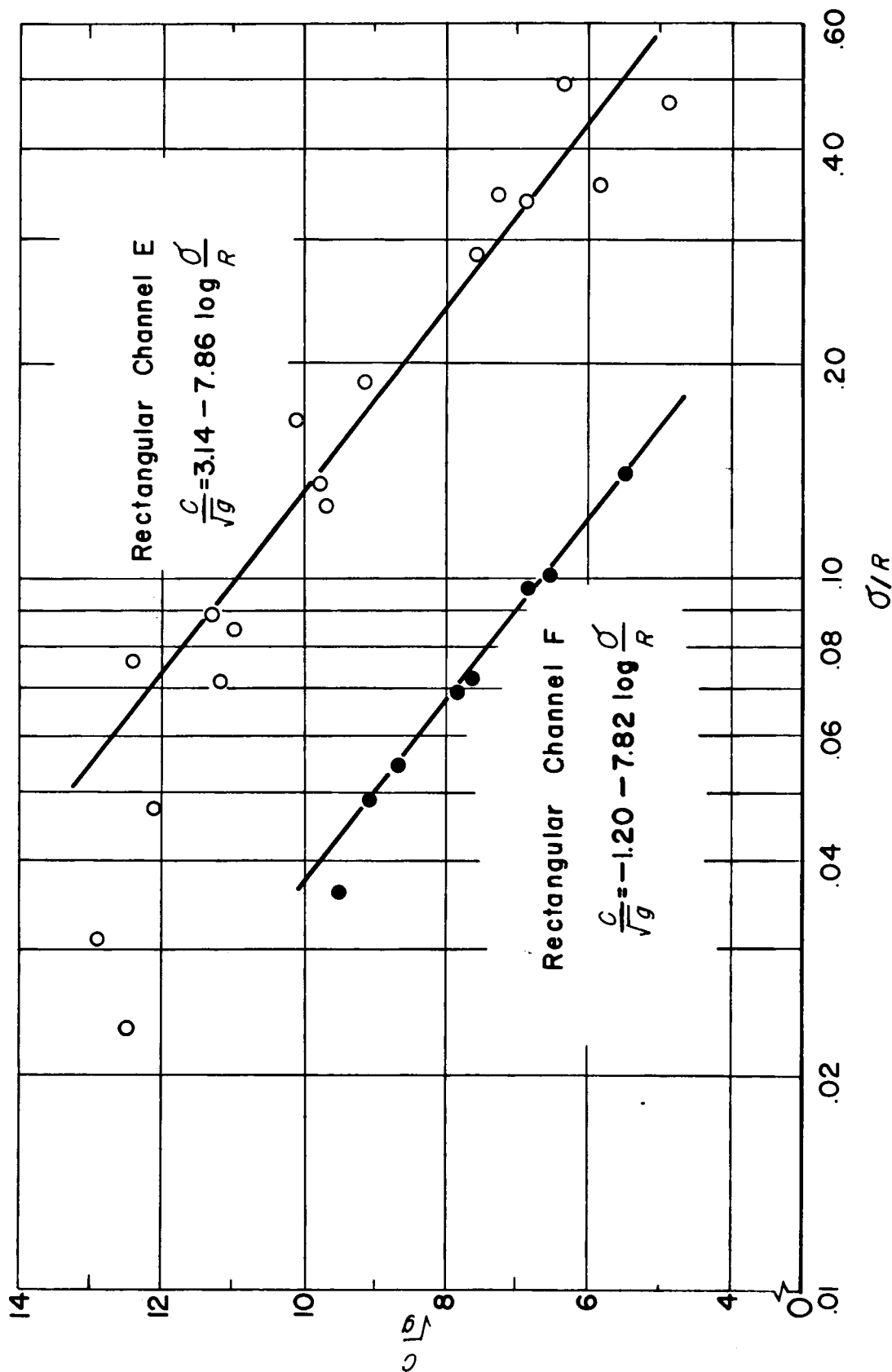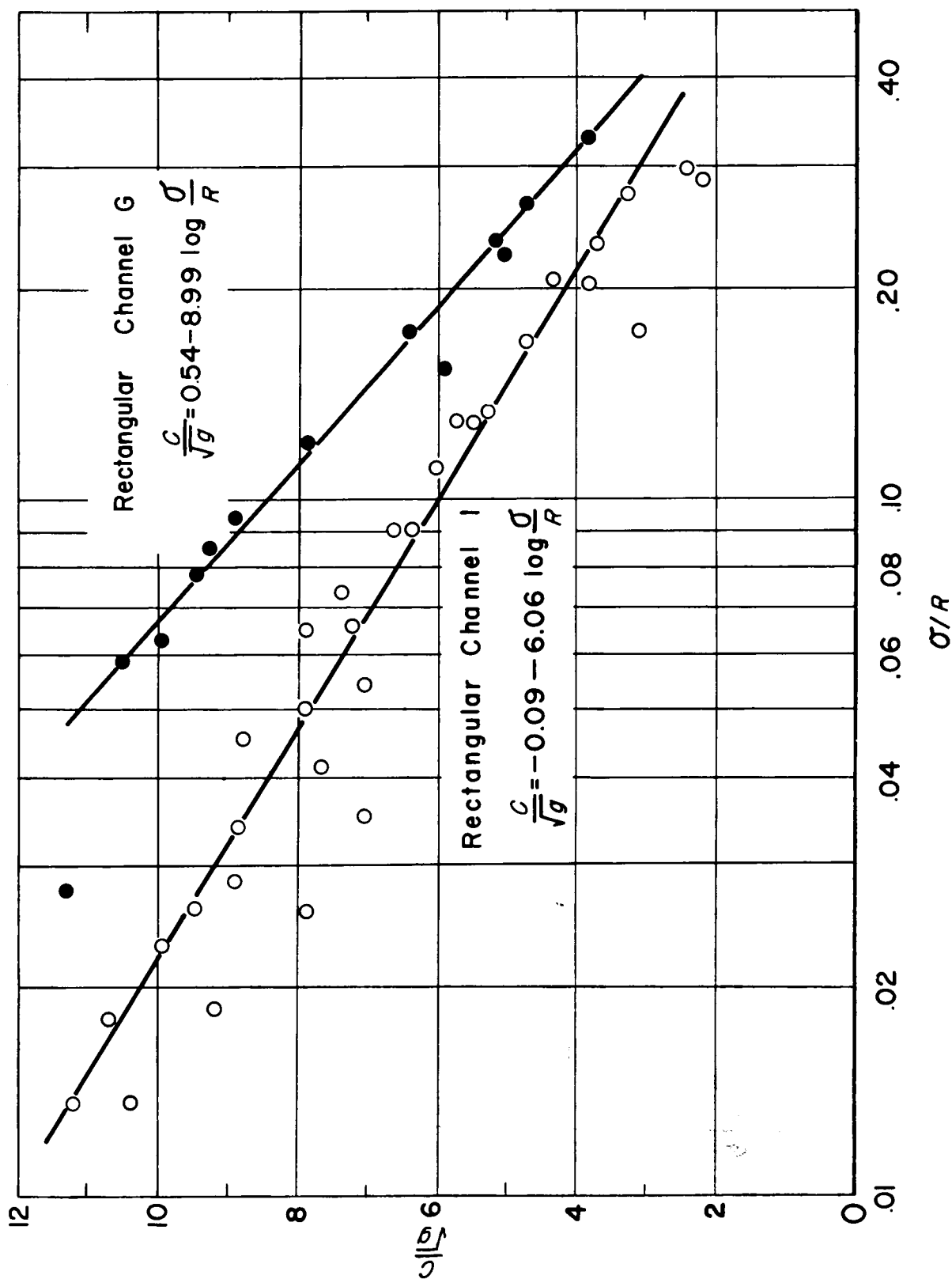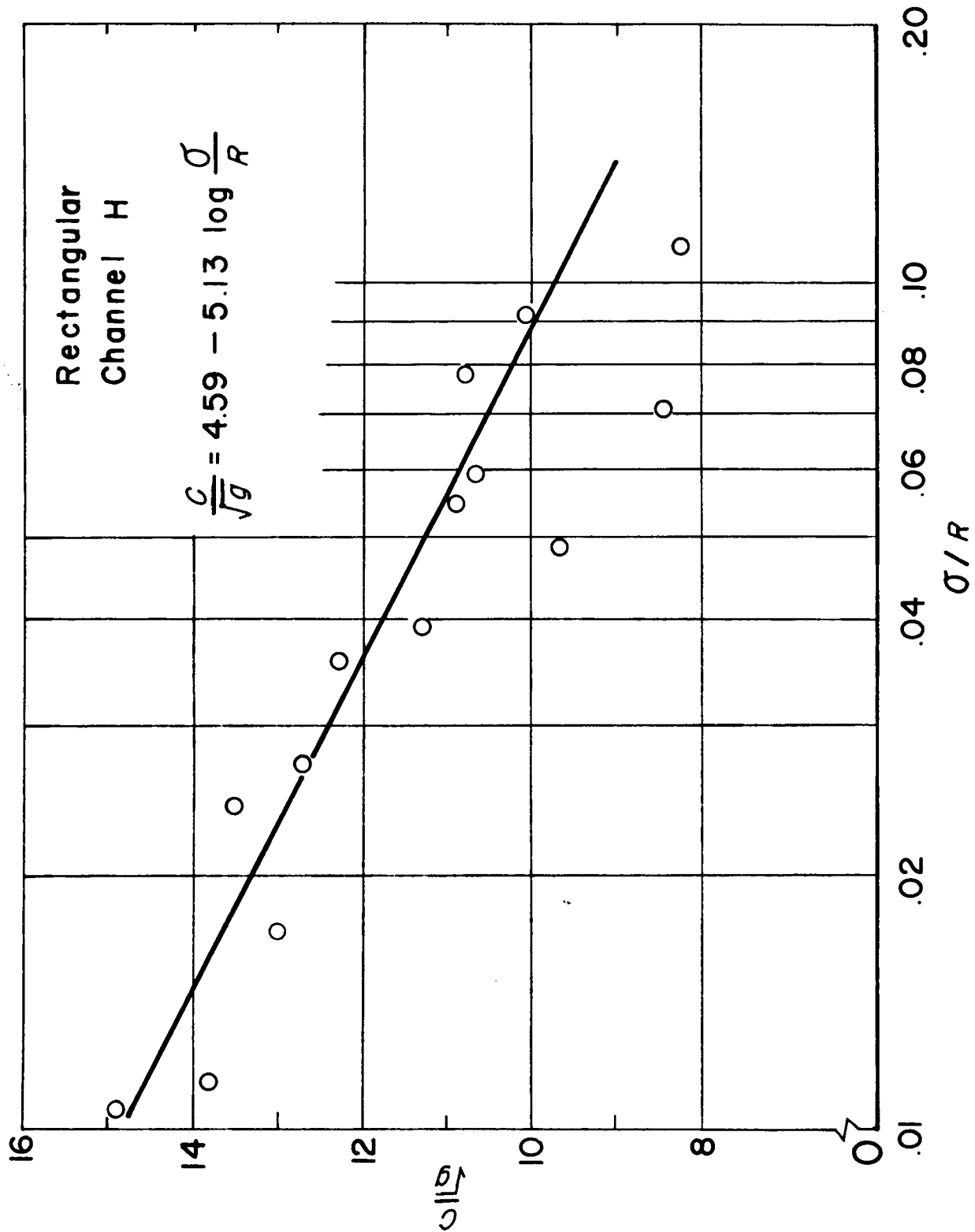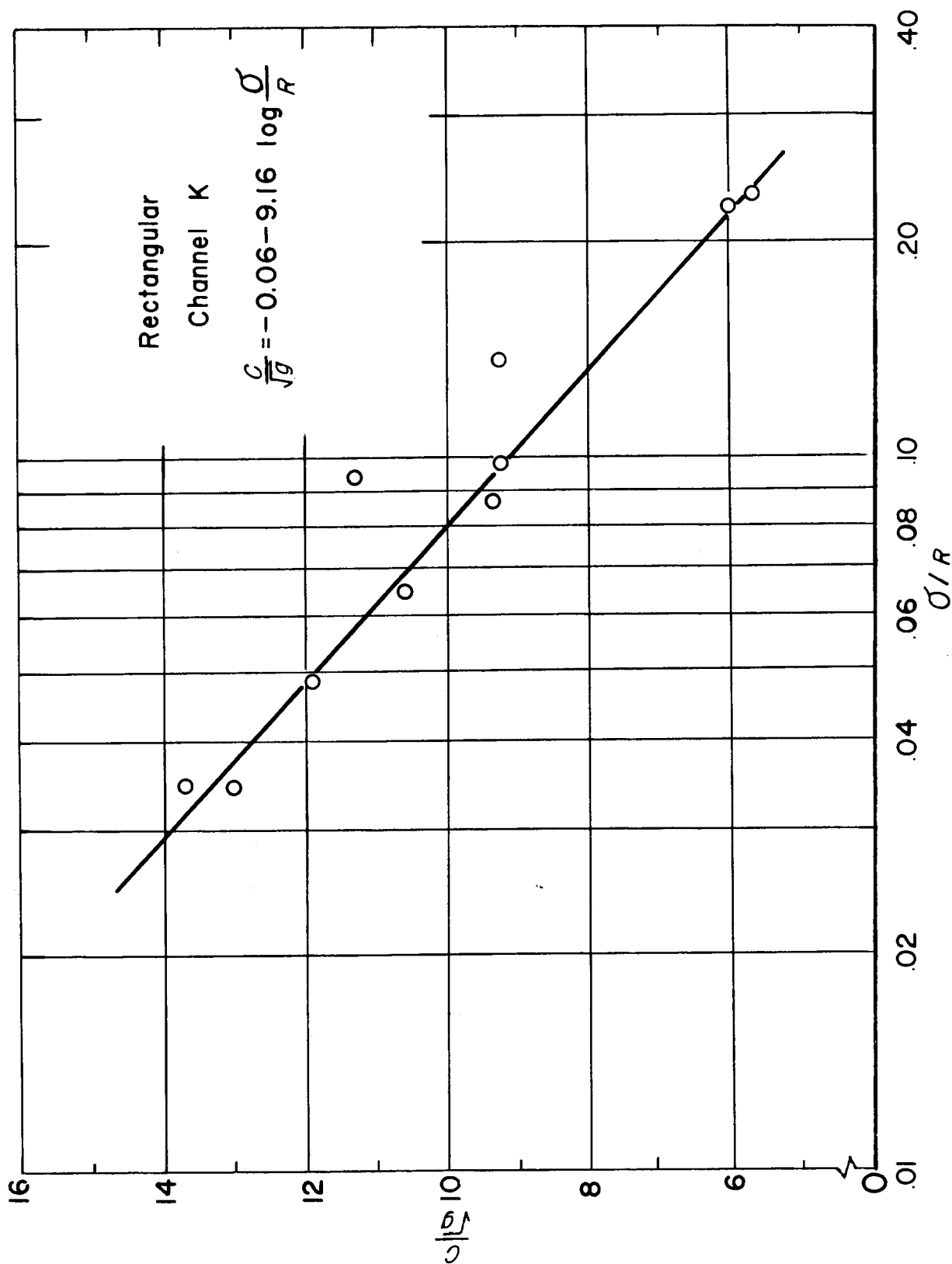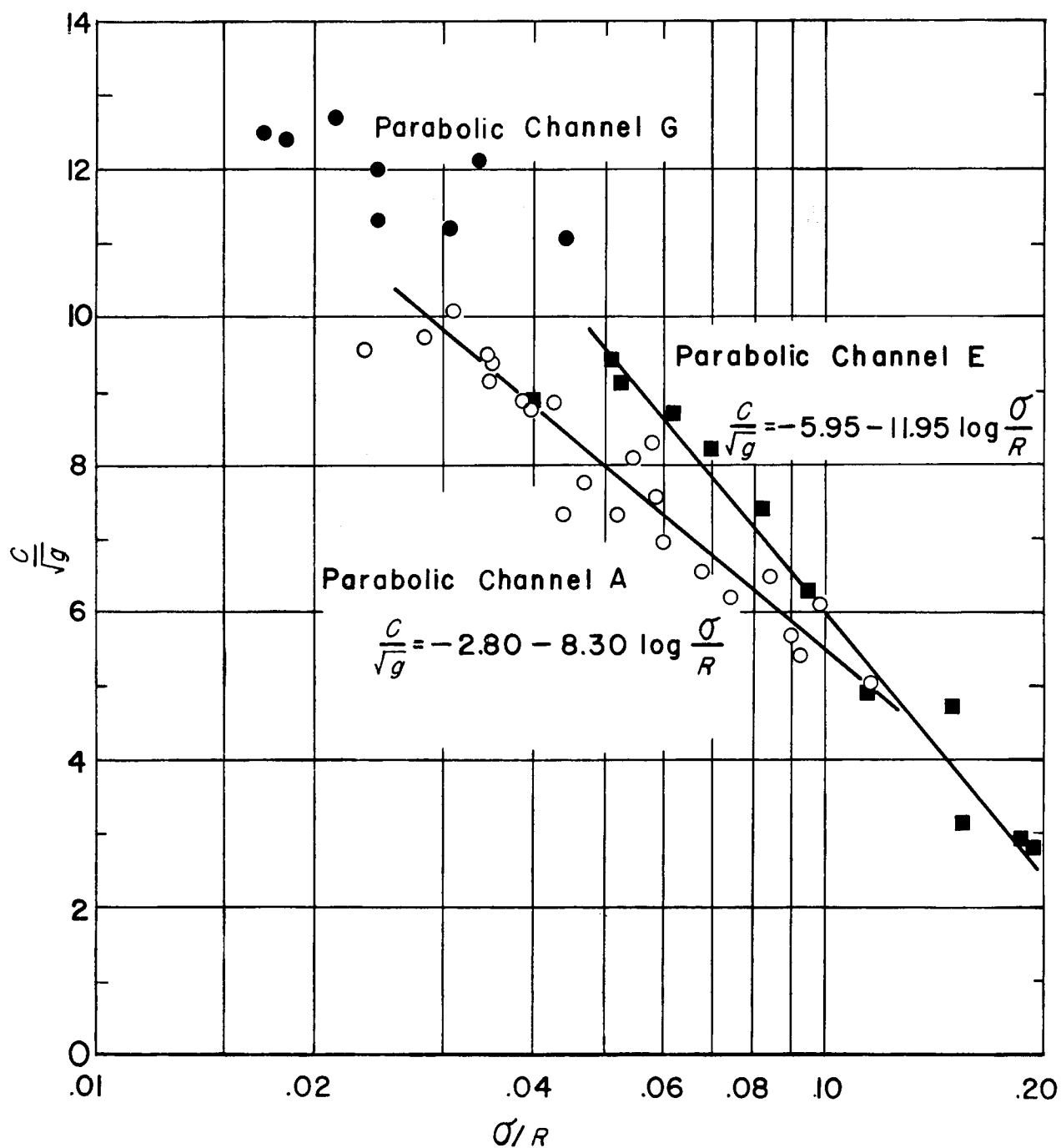FIGURE 12.—Relation of resistance coefficient ($C/\sqrt{g}$) to relative roughness (σ/R) for rectangular channel C.

FIGURE 13.—Relation of resistance coefficient $(C/\sqrt{g})$ to relative roughness (σ/R) for rectangular channel D.
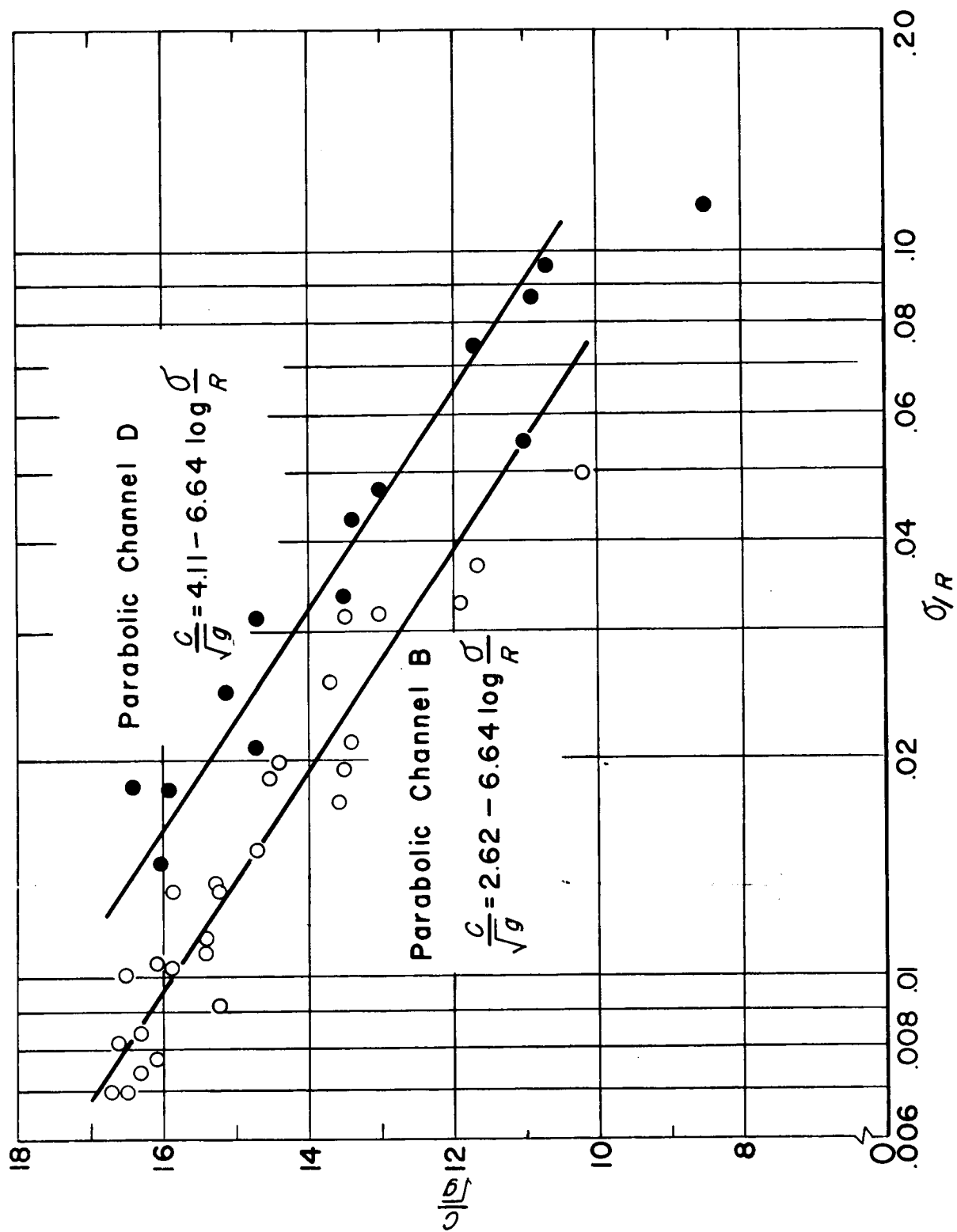
FIGURE 14.—Relation of resistance coefficient ($C/\sqrt{g}$) to relative roughness (σ/R) for rectangular channels E and F.

FIGURE 15.—Relation of resistance coefficient $(C/\sqrt{g})$ to relative roughness (σ/R) for rectangular channels G and I.

Rectangular
Channel H

$$\frac{C}{\sqrt{g}} = 4.59 - 5.13 \log \frac{\sigma}{R}$$

FIGURE 16.—Relation of resistance coefficient ($C/\sqrt{g}$) to relative roughness (σ/R) for rectangular channel H.

Figure 17.—Relation of resistance coefficient ($C/\sqrt{g}$) to relative roughness (σ/R) for rectangular channel K.

FIGURE 18.—Relation of resistance coefficient $(C/\sqrt{g})$ to relative roughness (σ/R) for parabolic channels G, E, and A.

FIGURE 19.— Relation of resistance coefficient $(C/\sqrt{g})$ to relative roughness (σ/R) for parabolic channels B and D.
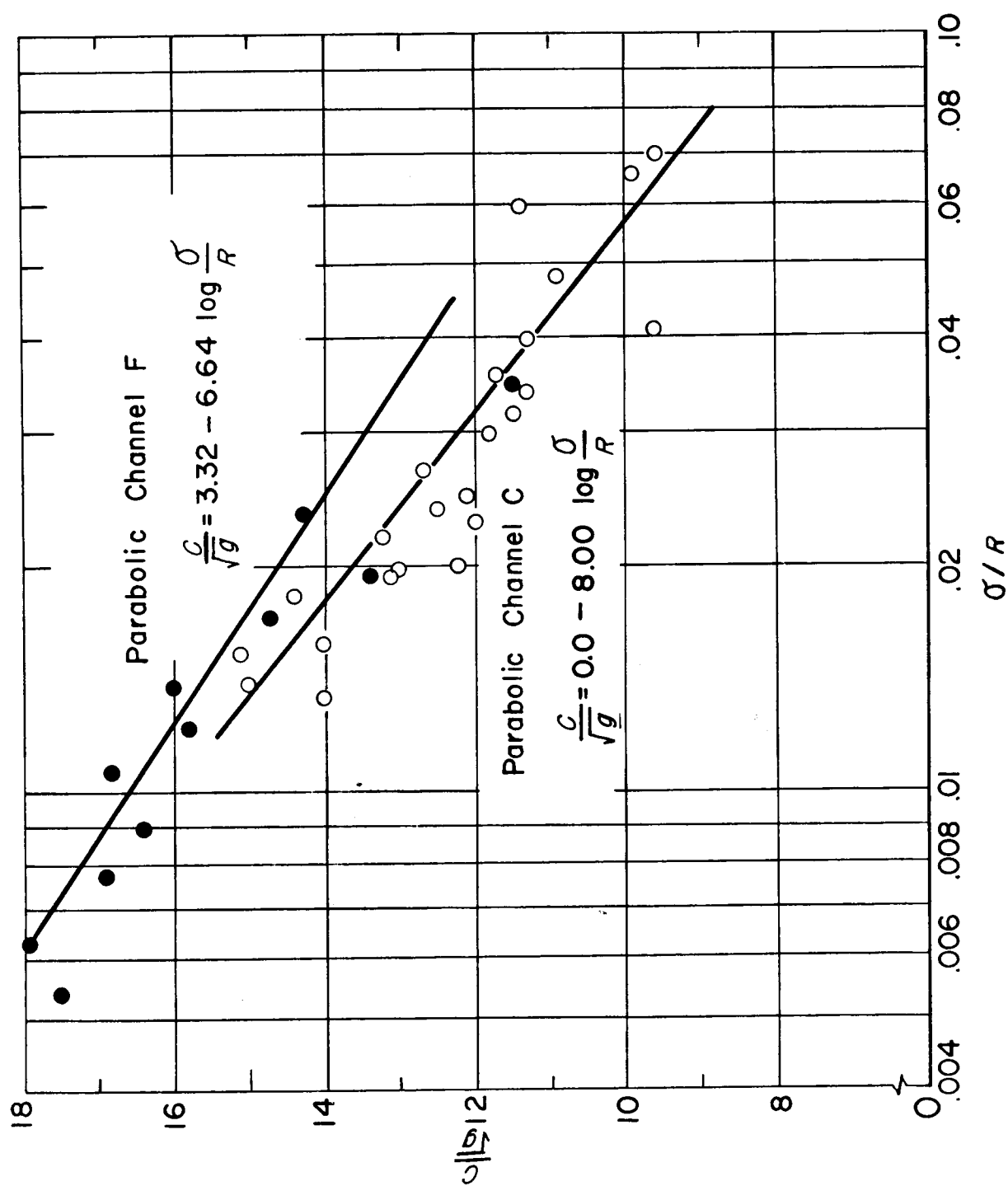
FIGURE 20.—Relation of resistance coefficient ($C/\sqrt{g}$) to relative roughness (σ/R) for parabolic channels F and C.

If it is assumed that the value of κ is constant and that the corresponding proper value of $\dfrac{2.30}{\kappa}$ is either 5.75 or 6.06, a depth correction can be found for each channel such that the plot of $\dfrac{C}{\sqrt{g}}$ against $\dfrac{\sigma}{R}$ will have the chosen slope. Values of the correction for $\dfrac{2.30}{\kappa}$ equal to 5.75 are given in table 1 both in absolute amounts and as fractions of the roughness height. There is no simple relationship between the depth correction and the height of roughness.

Viscosity and Roughness Effects

Figures 11 to 20 indicate that since the resistance of most channels is represented adequately as a function of relative roughness, the boundaries are hydraulically rough. However, for any one channel, depth increases and relative roughness decreases as discharge increases. As discharge increases, Reynolds number also increases. A relationship between resistance coefficient and Reynolds number could therefore be confused with a relationship between resistance coefficient and relative roughness. A more positive method of determining the type of flow resistance occurring is necessary.

Keulegan (10) plotted $\dfrac{V}{V_*}-\dfrac{2.30}{\kappa}\log R$ against $\log \dfrac{V_*}{\nu}$. For channels with rough boundaries, flow resistance was independent of viscosity and $\dfrac{V}{V_*}-\dfrac{2.30}{\kappa}\log R$ was a constant. Viscosity effects were evident for hydraulically smooth channels and the line formed by plotting data from such channels was inclined. This line can be represented by the equation:

$$\frac{V}{V_*}-\frac{2.30}{\kappa}\log R=A+\frac{2.30}{\kappa}\log \frac{V_*}{\nu}$$

or

$$\frac{V}{V_*}=A+\frac{2.30}{\kappa}\log \frac{RV_*}{\nu} \qquad (29)$$

as would be expected from theory. Keulegan also found some boundaries which he termed "wavy." Data for wavy boundaries described lines parallel to and below the smooth boundary lines, indicating a higher resistance for a given value of $\dfrac{RV_*}{\nu}$.

The data for the channels studied were plotted in the form suggested by Keulegan (figs. 21, 22, and

TABLE 1.—*Depth corrections*

Channel type and identifying letter	Roughness height, σ	Depth correction, c [1]	Relative depth correction c/σ
	Feet	*Feet*	
Rectangular:			
B	0. 0187	0. 0083	0. 445
D	. 0118	. 00923	. 782
E	. 0090	. 0024	. 267
F	. 0141	. 0120	. 852
G	. 0117	. 0096	. 820
H	. 0024	([2])	
I	. 0064	. 0010	. 156
K	. 0054	. 0050	. 926
N	. 0198	. 0080	. 404
Parabolic:			
A	. 0080	. 0130	1. 62
B	. 0013	. 0007	. 539
C	. 0029	. 0045	1. 55
D	. 0030	. 0015	. 500
E	. 0092	. 0236	2. 57
F	. 0015	. 0008	. 533

[1] c is the depth correction necessary to make $C/\sqrt{g}$ proportional to $5.75\log \sigma/R$, where R is the hydraulic radius based on the corrected depth.
[2] Negative value.

23). A value of $\dfrac{2.30}{\kappa}$ equal to 6.06 was used because this value approached more nearly the values found for the experimental channels in figures 11 to 20 than the more commonly accepted 5.75. The boundaries are rough for all but one of the channels, as indicated by the independence of $\dfrac{V}{V_*}-6.06\log R$ and the $\log \dfrac{V_*}{\nu}$ term. Much of the scatter of the experimental points about the mean value of the ordinate for each of these channels is due to the difference between 6.06 and the best-fit value of $\dfrac{2.30}{\kappa}$ for the channel.

The data for rectangular channel C show a functional relationship between $\dfrac{C}{\sqrt{g}}-6.06\log R$ and $\dfrac{V_*}{\nu}$. This relationship is represented in figure 21 by a straight line with slope of 6.06. The intercept of the straight line with the y axis is lower than would occur for hydraulically smooth boundaries. The relationship is therefore typical of that for wavy boundaries as presented by Keulegan. Data were taken for only one channel with wavy boundaries; therefore, an expression relating the constant to the degree of waviness could not be derived. However, the boundary for channel C was smoother than any likely to be encountered in natural irrigation channels and, in this respect, has no practical importance.
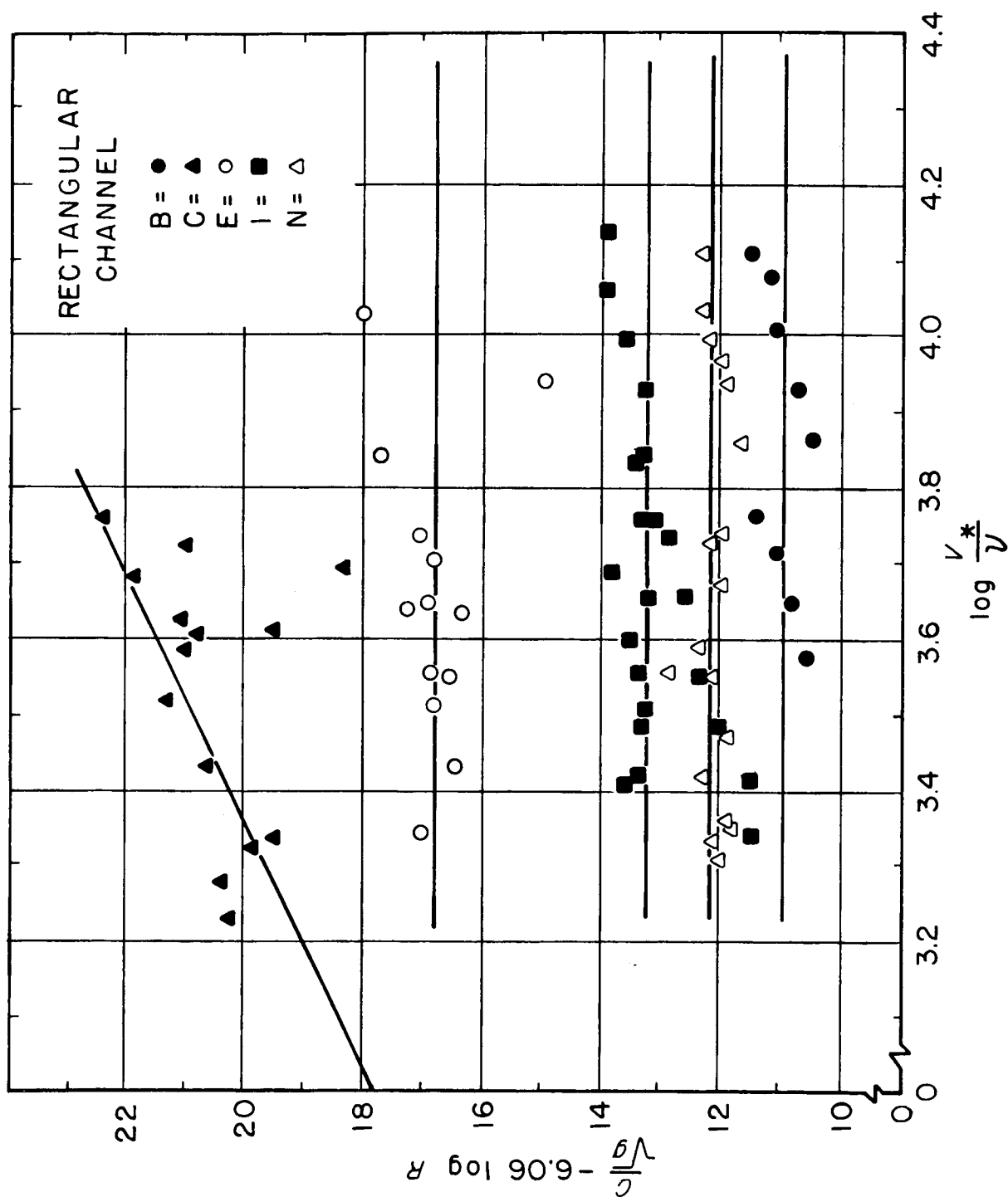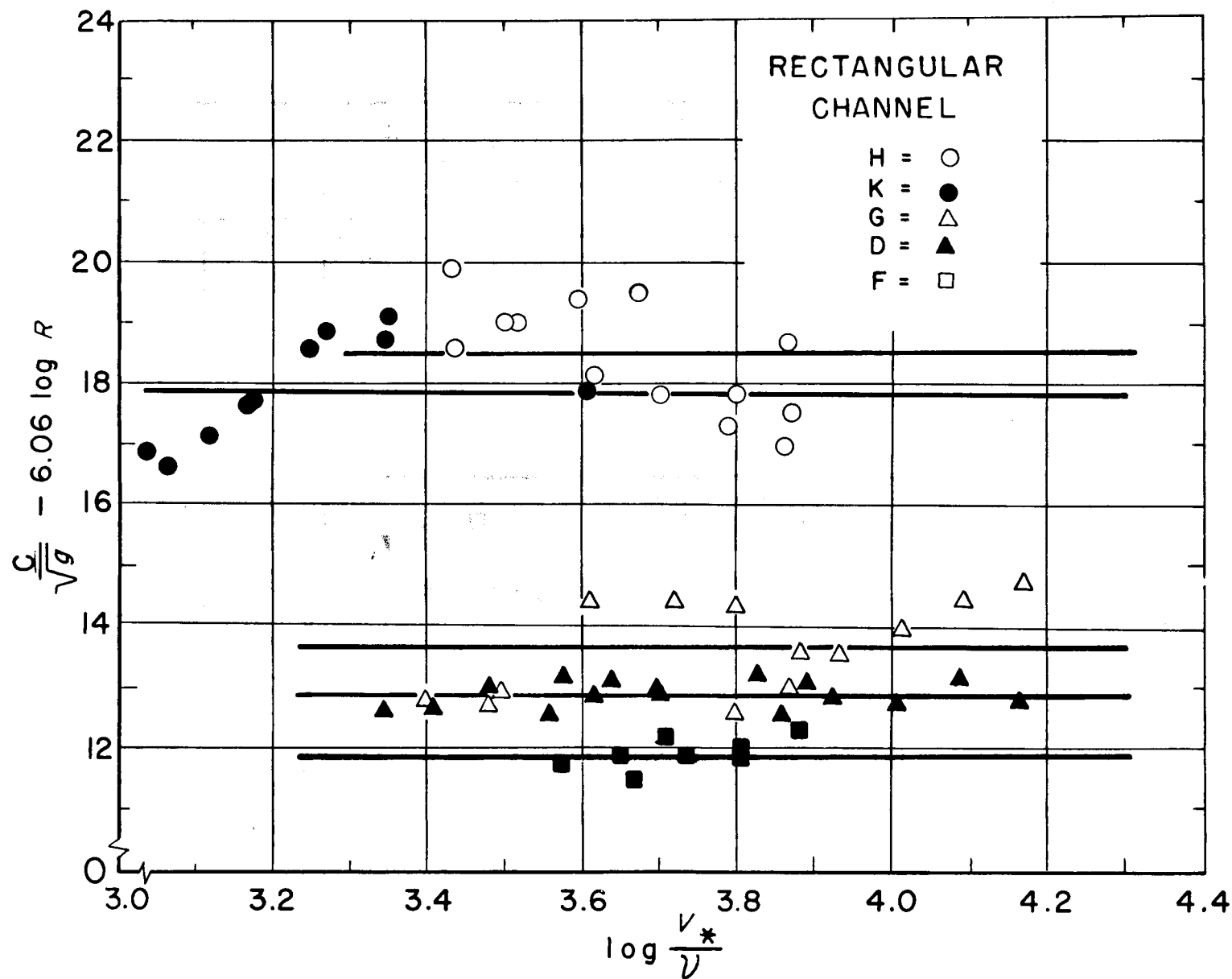
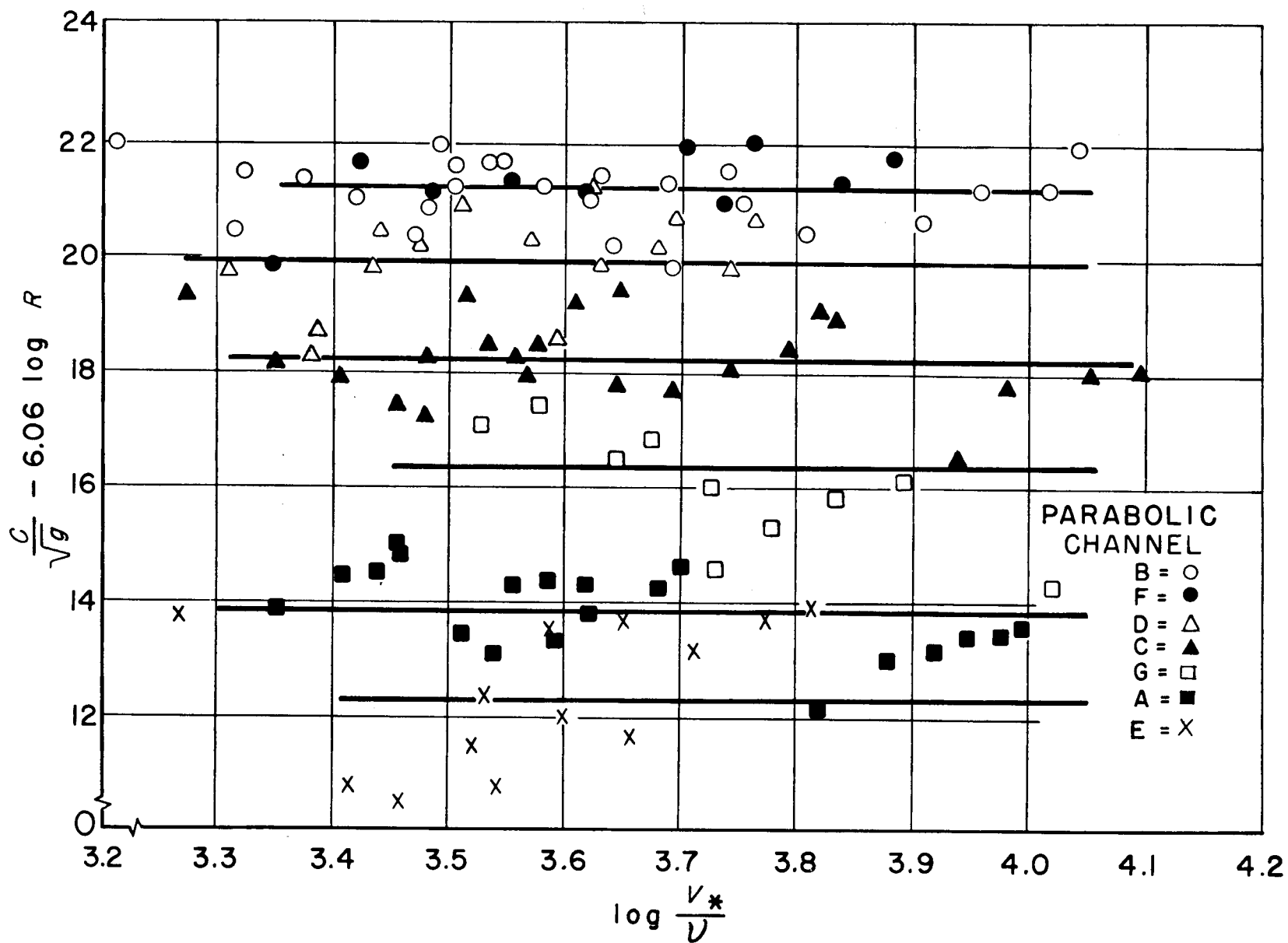FIGURE 21.—$C \sqrt{g} - 6.06 \log R$ as a function of $\log V_*/\nu$ for rectangular channels. Horizontal lines represent hydraulically rough boundaries. The inclined line represents a wavy boundary.

FIGURE 22.—$C/\sqrt{g} - 6.06 \log R$ as a function of $\log V_*/\nu$ for rectangular channels. Horizontal lines represent hydraulically rough boundaries.

FIGURE 23.—$C/\sqrt{g} - 6.06 \log R$ as a function of $\log V_*/\nu$ for parabolic channels. Horizontal lines represent hydraulically rough boundaries.

On the basis of figures 21 to 23, a criterion can be established for distinguishing between rough and wavy boundaries, using standard deviation of bed elevation measurements as an estimate of roughness height. It is assumed that the thickness of the laminar sublayer, δ', can be defined by the same formula as is used for pipe flows:

$$\delta' = 11.6 \frac{\nu}{V_*} \qquad (30)$$

In table 2, values of the ratio of σ to δ' are shown for the one wavy boundary and for the two rough boundaries having the smallest value of σ. Only two values of $\frac{\sigma}{\delta'}$ exceed 0.520 for the wavy boundary, channel C. There are two values of $\frac{\sigma}{\delta'}$ smaller than 0.520 for the rough boundaries, channels H and K, which would be expected to most nearly approach the wavy condition. For these data, the distinguishing criterion for the transition from wavy to rough boundaries would then be:

$$\frac{\sigma}{\delta'} = 0.520$$

or, combining this equation with equation 30:

$$\frac{V_* \sigma}{\nu} = 6.03 \qquad (31)$$

Resistance Parameter

The use of an equivalent resistance term (χ) to take account of all factors affecting resistance was discussed in the Review of Literature section. Such a term can be calculated most easily from equation 16. The equivalent resistance term, χ, in this equation was shown to represent effects of both roughness and channel shape on flow resistance. By using equation 16, values of χ can be calculated for the channels with rough boundaries from data contained in figures 21 to 23. The average value of the ordinate for each channel, $\frac{C}{\sqrt{g}} - 6.06 \log R$, is equal to $-6.06 \log \chi$. Values of χ were calculated in this way for each rough channel. A tabulation of χ values is shown in table 3.

The values of χ may now be related to the physical characteristics of the channel that affect resistance. Results of previous research have indicated that channel roughness will exert the primary effect on flow resistance. The methods used to measure channel roughness have been described in the section on Experimental Procedures. Values of the following roughness measures are listed in table 3: σ, the standard deviation

TABLE 2.—*Ratio of roughness height (σ) to laminar sublayer thickness (δ') for three rectangular channels with small roughness height* [1]

Channel C		Channel H		Channel K	
Run	σ/δ'	Run	σ/δ'	Run	σ/δ'
2–C	0.422	2–H	1.29	4–K	0.530
3–C	.500	3–H	1.55	6–K	.500
4–C	.545	6–H	.565	7–K	.601
9–C	.279	7–H	.660	8–K	.674
10–C	.336	8–H	.820	9–K	.805
11–C	.403	9–H	.983	10–K	1.01
12–C	.441	11–H	1.53	16–K	1.85
13–C	.553	14–H	.468	31–K	.690
18–C	.178	15–H	.570	33–K	.855
19–C	.197	16–H	.688		
20–C	.221	17–H	.856		
23–C	.429	18–H	1.05		
24–C	.517	19–H	1.32		
		20–H	1.51		

[1] The boundary of channel C was wavy. Channels H and K had hydraulically rough boundaries.

TABLE 3.—*Calculated values of resistance parameter and measured roughness dimensions for rough channels*

Channel type and identifying letter	χ [1]	σ [2]	λ_c [3]	λ_p [4]
	Feet	*Feet*	*Feet*	*Feet*
Rectangular:				
B	0.0155	0.0187	0.197	0.141
D	.00740	.0118	.375	.099
E	.00166	.0090	.860	.257
F	.0107	.0141	.625	.358
G	.00561	.0117	.667	.275
H	.00089	.0024	.215	------
I	.00691	.0064	.240	.054
K	.00115	.0054	.400	.139
N	.0100	.0198	.286	.133
Parabolic: [5]				
A	.00525	.0084	------	-----
B	.000323	.0013	------	-----
C	.00100	.0029	------	-----
D	.000512	.0030	------	-----
E	.00933	.0092	------	-----
F	.000316	.0015	------	-----
G	.00204	.0044	------	-----

[1] Resistance parameter.
[2] Roughness height: standard deviation of evenly spaced surface elevation measurements about the mean elevation.
[3] Average longitudinal spacing of roughness elements projecting more than 1 σ above the mean bed elevation.
[4] Average longitudinal spacing of all roughness element crests.
[5] No measurements of longitudinal roughness spacing made.

TABLE 4.—*Differences between measured and predicted values of the resistance parameter, and related measured roughness-spacing indexes*

Rectangular channel	χ, measured	χ, predicted	Absolute difference	Relative difference	λ_r	λ_p
	Feet	*Feet*	*Feet*	*Percent*		
B	0. 0155	0. 0174	+0. 0019	+12. 3	0. 197	0. 141
D	. 00740	. 00813	+. 00073	+9. 9	. 375	. 099
E	. 00166	. 00516	+. 00350	+210. 0	. 860	. 257
F	. 0107	. 0112	+. 0005	+4. 7	. 625	. 358
G	. 00561	. 00812	+. 00253	+45. 7	. 667	. 275
H	. 00089	. 00058	−. 00031	−34. 8	. 215	----------
I	. 00691	. 00297	−. 00394	−57. 0	. 240	. 054
K	. 00115	. 00219	+. 00104	+99. 0	. 400	. 139
N	. 0100	. 0194	+. 0094	+94. 0	. 286	. 133

of equally spaced measurements of bed elevations; λ_r, the average longitudinal spacing of roughnesses that projected more than one standard deviation (1σ) above the mean bed elevation; and λ_p, the average longitudinal spacing of all roughness crests.

Attempts were made to correlate values of χ with measured dimensions of roughness. A correlation existed only between χ and σ; the calculated value of the correlation coefficient is 0.93. The relationship of the resistance parameter, χ, to roughness height, σ, is plotted in figure 24. The regression line representing the relationship of χ to σ was determined by least-squares methods. The equation of this line is:

$$\chi = 12.9\sigma^{1.66} \qquad (32)$$

The spacing of the roughness elements cannot be related directly to the flow resistance parameter, χ. However, previous studies (*17, 18*) have shown that the flow resistance of conduits with the same roughness height but different spacing differs. Therefore, it would be expected that the scatter of the data about the line relating χ and σ, figure 24, might be correlated with the roughness spacing. Table 4 includes both absolute and percentage deviations of measured χ values from those predicted by equation 27, and values of the two measured roughness-spacing indexes. The relations are not well enough defined so that these measures of spacing can be used to improve the estimate of χ.

Channel Shape Effects

The value of χ theoretically expresses the effects of both roughness dimensions and channel shape on flow resistance (see equation 16). Values of χ for parabolic channels with three different shapes are plotted against σ in figure 24. In this plot, the shape of the channels is represented by use of the hydraulic radius as a length parameter. There is

no relationship between the deviation of the individual points from the best-fit line in this plot and the shape of the channels.

Supporting Data

Parsons (*15*) measured the resistance to turbulent flow over a short section of rough channel. The channel roughness was formed by directing a water spray on a soil-cement mixture, which formed small, closely spaced craters. The resulting surface was similar to that of soil roughened by falling raindrops.

Data are available for the computation of χ and σ for two series of Parsons' runs. For series IV the computed value of χ is 0.00138 foot. The value of σ, computed from the bed roughness measurements, is 0.00490 foot. For series V runs the corresponding values are: $\chi = 0.00160$ foot, $\sigma = 0.00590$ foot. These values of χ and σ are plotted on figure 24. Parsons' data are represented by equation 32 equally as well as the data from the present study.

Prediction Errors

Equations 16, 26, and 32 may now be used to predict flow conditions for natural channels if measurements of σ and λ for these channels can be made.

When an irrigation system is being designed, slope is determined by topographic and land forming limitations, channel shape depends on the crop to be grown, and discharge rate may be assumed. The problem is then to predict the depth of flow. The magnitude of error likely to be encountered in predicting depth of laminar flow over rough boundaries can be determined by reference to figure 10. Examination of this figure indicates that for 66 of the 73 values, the error in predicting f (the Darcy-Weisbach resistance coefficient) by equation 26 was less than 30 percent.
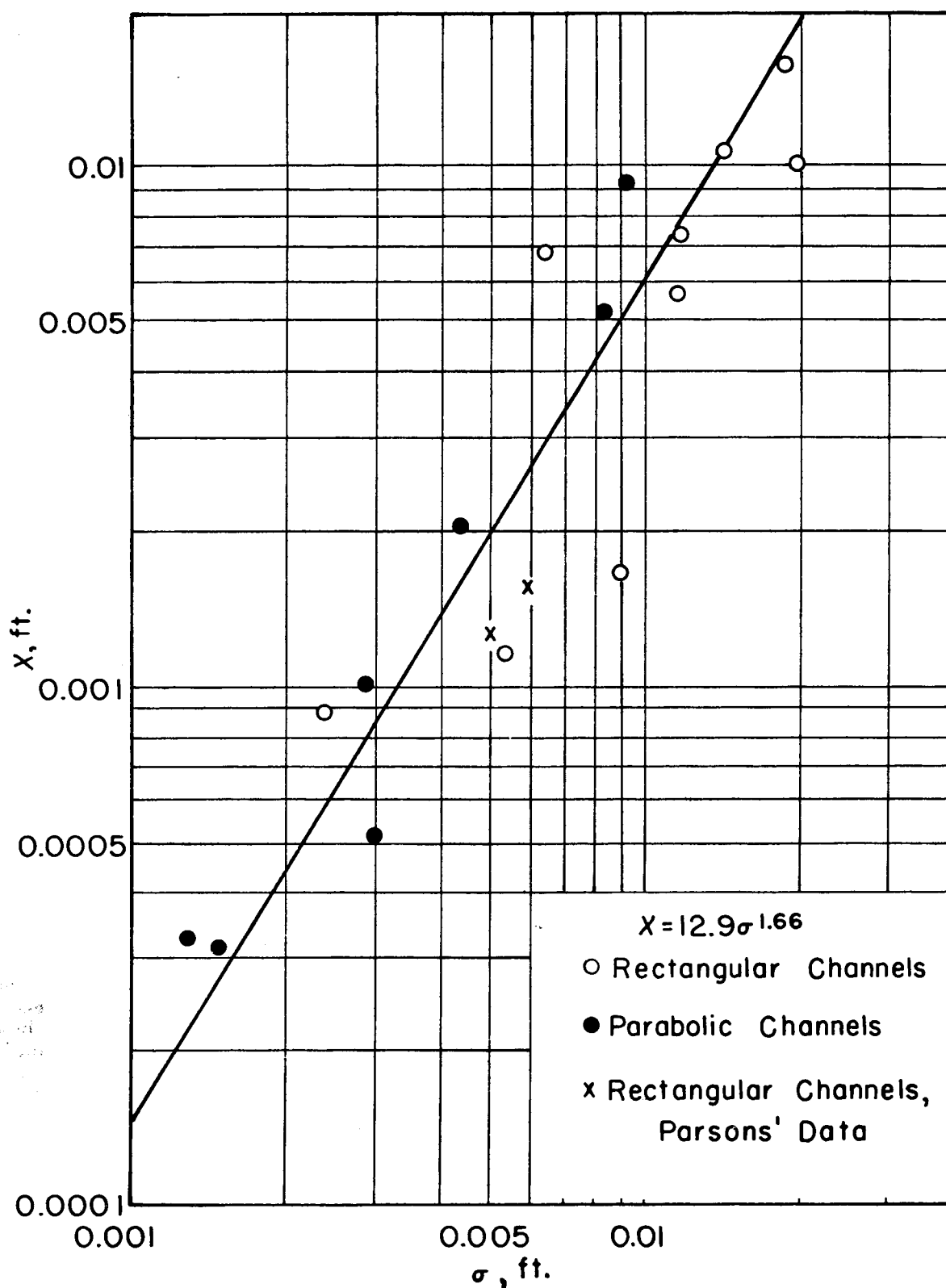
FIGURE 24.—Relationship of resistance parameter, χ, to roughness height, σ.

The defining equation for f can be written:

$$f=\frac{8gdS}{V^2}=\frac{8gd^3S}{q^2}$$

Taking logarithms of both sides and differentiating:

$$\frac{df}{f}=\frac{3dd}{d}+\frac{dS}{S}-\frac{2dq}{q}$$

Each of the terms in this equation represents the relative error in one of the variables. If q and S are accurately known, dS/S and dq/q are negligible and:

$$\frac{dd}{d}=\frac{1}{3}\frac{df}{f}$$

Thus, a 30-percent error in f results in only a 10-percent error in d.

The best method found for estimating x was to relate it to a measure of the roughness height, σ, by means of equation 32. The correlation coefficient determined for x and σ was 0.93, indicating a highly significant relationship. Although other dimensions of roughness affect resistance, they could not be measured accurately enough to be of practical value. The error in using equation 32 to estimate x is indicated in figure 24, where the plotted points represent measured values and the straight line represents estimated values. The error is quite large for some channels—as much as 210 percent for rectangular channel E. However, because x appears only in a logarithmic term in the flow resistance formula, equation 16, the errors involved in practical applications of the formula are smaller.

Normal flow depth for very wide channels can be calculated from equation 16 written in the form:

$$\frac{q}{\sqrt{gSd^{3/2}}}-6.06\log d=-6.06\log x \qquad (16a)$$

Some trial calculations of d were made, using both measured and estimated values of x, so that the error in d could be determined. An intermediate value of slope, 0.001, was assumed for all the calculations. Two values of q were assumed—one the lowest for which turbulent flow would occur, and the other near the upper limit of the range of discharges used in this study.

Table 5 lists the errors found in predicted normal depth of turbulent flow for two rates of discharge, when using the equations developed from this study. The maximum error for any channel is 27.5 percent at the lower turbulent unit discharge. At the higher rate of discharge, errors in determining depth are about half those at the lower rate.

The error in using equations 16 and 32 for calculating the hydraulic radii of parabolic channels was also investigated. The computation for

TABLE 5.—*Error in calculating normal flow depth in rectangular channels*

Assuming $q=0.0060$ c.f.s./ft. and $S=0.001$

Channel	d, measured	d, predicted	Error
	Feet	*Feet*	*Percent*
B	0.0508	0.0533	+4.9
D	.0402	.0413	+2.7
E	.0283	.0361	+27.5
F	.0452	.0457	+1.1
G	.0369	.0412	+11.6
H	.0254	.0238	−6.3
I	.0392	.0318	−18.9
K	.0266	.0299	+12.4
N	.0443	.0556	+25.2

Assuming $q=0.500$ c.f.s./ft. and $S=0.001$

Channel	d, measured	d, predicted	Error
B	.462	.470	+1.7
D	.412	.417	+1.2
E	.341	.391	+14.7
F	.434	.436	+0.5
G	.396	.416	+5.5
H	.318	.306	−3.8
I	.407	.365	−10.3
K	.328	.352	+7.3
N	.429	.478	+11.4

parabolic channels is more difficult than for rectangular channels. The relation between area and hydraulic radius must be known so that the velocity can be calculated from the Q/A relationship and the equation can be solved by trial and error. Values of R were determined by this procedure for both small and large discharges. Values of hydraulic radius based on both predicted and measured X values are shown in table 6. The maximum error for these channels was 12.4 percent, at the low rate of discharge. At the higher rate of discharge, the error was reduced, just as it was in calculating normal flow depth for rectangular channels.

The common method of determining the resistance of an irrigation channel in the field is to estimate Manning's resistance coefficient, n, from visual observation of the roughness, alinement, vegetation, etc.; the estimate is based on the designer's experience. The resistance coefficient is usually given a single value for each channel and its variation with depth of flow is not considered. The range of values of Manning's n measured for turbulent flows in each of the rectangular channels studied is shown in table 7. A large range of values of n existed for the channels with the larger values of σ. Thus, any one value of n assumed for these channels would be considerably in error at depths of flow other than that to which it applies. These data illustrate the inadequacy of a single n value to characterize the resistance in a small, rough channel.

TABLE 6.—*Error in calculating hydraulic radius of parabolic channels from predicted* x *values*

ASSUMING Q=0.0030 c.f.s. AND S=0.001

Channel	R, measured	R, predicted	Error
	Feet	*Feet*	*Percent*
A	0.0349	0.0343	−1.7
B	.0225	.0220	−2.2
C	.0261	.0254	−2.7
D	.0209	.0220	+5.3
E	.0348	.0305	−12.4
F	.0216	.0214	−0.9
G	.0276	.0266	−3.6

ASSUMING Q=0.350 c.f.s. AND S=0.001

Channel	R, measured	R, predicted	Error
A	.239	.236	−1.3
B	.188	.185	−1.6
C	.204	.201	−1.5
D	.172	.178	+3.5
E	.230	.215	−6.5
F	.180	.179	−0.6
G	.208	.204	−1.9

The error involved in assuming a constant value of n for a channel can be compared with the error of the prediction equations. Assuming q and S known, taking logarithms of both sides of the Manning equation (equation 2), and differentiating:

$$\frac{dq}{q}=\frac{5}{3}\frac{dd}{d}+\frac{1}{2}\frac{dS}{S}-\frac{dn}{n}$$

If q and S are constant:

$$\frac{dd}{d}=\frac{3}{5}\frac{dn}{n}$$

TABLE 7.—*Range of measured Manning's* n *for turbulent flows*

Channel type and identifying letter	n
Rectangular:	
B	0.022–0.049
C	.010– .013
D	.016– .029
E	.014– .021
F	.019– .031
G	.016– .039
H	.012– .017
I	.016– .032
K	.012– .017
N	.018– .045
Parabolic:	
A	.019– .030
B	.011– .014
C	.013– .018
D	.012– .014
E	.011– .052
F	.011– .013
G	.015– .017

The maximum relative error in estimating flow depth for the rectangular channels was 27.5 percent, using equations 16 and 32. This is equivalent to an error in n of 46 percent. Now consider the range of observed n values. For some of the rough channels one would have errors as high as 70 percent in n at low flow depths even if, through extreme good fortune, the average value for the range of discharges encountered had been originally estimated correctly. Therefore, use of measured roughness heights in conjunction with equations 16 and 32 should produce resistance estimates having less error than the procedure currently in common use.

APPLICATIONS TO FIELD CONDITIONS

The equations for uniform flow over small earth channels in both the laminar and turbulent regimes that were developed from the laboratory studies reported in this bulletin might be applied to the calculation of flow parameters in irrigation borders and furrows. It should be remembered, however, that the equations have not yet been verified under field conditions.

Where channels have no vegetation, boundaries will be hydraulically rough for almost all laminar and turbulent flows. Therefore, the first step in analyzing such flow is to measure roughness height and spacing. The following procedure is suggested.

For the measurement of roughness height, six to ten 1-foot sections of the bed parallel to the direction of flow may be selected at random. Bed elevations should be measured, with a precision of 0.001 foot, at 0.05-foot intervals relative to some arbitrary datum. The value of σ can be calculated by using equation 19 for each of the 1-foot strips

and these values can be averaged to obtain the representative value for the channel.

The same sections of the channel can be used to measure the average longitudinal spacing, λ_p. The number of roughness crests divided into the total length of the sections sampled will give the value of λ_p. Some judgment must be used in counting the roughness crests: crests too small or too low to contribute materially to the flow resistance should not be counted.

Next, the regime of flow should be determined. For two-dimensional flows, the Reynolds number can be calculated from known values of unit discharge and viscosity. Thus:

$$\frac{q}{\nu}=\frac{Vd}{\nu}=Re$$

For Reynolds numbers greater than 500, the turbulent flow equations (equations 16 and 32) should

be used. For Reynolds numbers less than 500, the laminar flow equations (equations 26 or 27) are applicable.

If flows are in the laminar regime and it is assumed that boundary roughness is great enough to affect flow resistance $(\sigma \geq 2.58d/\sqrt{Re})$, normal depth can be calculated from equations 26 or 27. Then:

$$f = \frac{6.0 \times 10^4 S^{0.5} \left(\frac{\sigma}{\lambda_p}\right)}{Re} \qquad (26)$$

and

$$d = \sqrt[3]{\frac{7.5 \times 10^3 q \nu}{g\sqrt{S}} \left(\frac{\sigma}{\lambda_p}\right)} \qquad (27)$$

With this estimate of d, the criterion for boundary roughness, defined by equation 25, can be checked:

$$\sigma \geq \frac{2.58d}{\sqrt{Re}} \text{ for a rough boundary;}$$

$$\sigma < \frac{2.85d}{\sqrt{Re}} \text{ for a smooth boundary.} \qquad (25)$$

If the criterion does indicate the channel to be rough, the assumption is vindicated and the estimate of d may be assumed to be correct. In the event that the boundary is not rough, the flow depth may be calculated from equation 1, the theoretical equation for laminar flow in a wide, smooth, rectangular channel, rewritten in the following form:

$$d = \sqrt[3]{\frac{3q\nu}{gS}} \qquad (1)$$

The following sample calculation illustrates in detail an analysis of flow in the laminar regime, where it is assumed that the irrigation border is hydraulically rough, that is, where σ, the roughness height, is great enough to cause head losses greater than the theoretical for laminar flow $(\sigma \geq 2.58d/\sqrt{Re})$.

Given:

$q = 0.005$ c.f.s./ft.
$S = 0.001$
$\sigma = 0.010$ ft.
$\lambda_p = 0.20$ ft.
$T = 70°$ F.

Solution:

Compute the Reynolds number:

$$Re = \frac{Vd}{\nu} = \frac{q}{\nu} = \frac{0.005}{1.06 \times 10^{-5}} = 472$$

Since $Re < 500$, the flow is laminar. Assuming that the boundary is rough enough to affect flow, calculate depth using equation 27:

$$d = \left[\frac{7.5 \times 10^3 q \nu}{g\sqrt{S}} \left(\frac{\sigma}{\lambda_p}\right)\right]^{1/3}$$

$$= \left[\frac{7.5 \times 10^3 (0.005)(1.06 \times 10^{-5})}{32.2(0.0316)} \left(\frac{0.010}{0.20}\right)\right]^{1/3}$$

$$= 0.027 \text{ ft.}$$

To check the roughness assumption use criterion 25.

$$\frac{2.58d}{\sqrt{Re}} = \frac{2.58(0.027)}{\sqrt{472}} = 0.0032$$

$$\sigma > \frac{2.58d}{\sqrt{Re}}$$

Therefore, the boundary is hydraulically rough, as assumed, and the calculated value of d is correct.

If the Reynolds number is greater than 500, turbulent flow can be assumed to exist. For irrigation borders or very wide channels, equation 16 can be written in the form:

$$\frac{q}{\sqrt{gS}d^{3/2}} = 6.06 \log d - 6.06 \log \chi$$

where:

$$\chi = 12.9\sigma^{1.66} \qquad (32)$$

From equations 16 and 32, d can be found by trial and error, if q, S and σ are known. To assure that equation 16 is valid for the case being considered, the computed value of d can be inserted in criterion 31, where $\sqrt{gdS}$ is substituted for V_*:

$$\frac{\sqrt{gdS}\sigma}{\nu} > 6.0, \text{ for a rough boundary;}$$

$$\frac{\sqrt{gdS}\sigma}{\nu} < 6.0, \text{ for a smooth boundary.}$$

The following sample calculation illustrates in detail an analysis of flow in the turbulent regime, where it is assumed that the irrigation border boundary is hydraulically rough.

Given:

$q = 0.040$ c.f.s./ft.
$S = 0.001$
$\sigma = 0.010$ ft.
$T = 70°$ F.

Solution:

Compute the Reynolds number:

$$Re=\frac{q}{\nu}=\frac{0.040}{1.06\times10^{-5}}=3{,}780$$

Since $Re>500$, turbulent flow exists. Assuming that the boundary is hydraulically rough, compute χ using equation 32:

$$\chi=12.9\sigma^{1.66}$$
$$=12.9(0.010)^{1.66}$$
$$=0.00618$$

Compute depth by trial and error, using equation 16, which can be written as follows:

$$\frac{q}{\sqrt{gS}d^{3/2}}-6.06\log d=-6.06\log\chi$$

or:

$$\frac{q}{\sqrt{gS}}=d^{3/2}[6.06\log d-6.06\log\chi]$$

For the left-hand side of the equation:

$$\frac{q}{\sqrt{gS}}=\frac{0.040}{\sqrt{32.2}\sqrt{0.001}}=0.224$$

For the right-hand side:

Assume $d=0.10$ ft.

$$d^{3/2}[6.06\log d-6.06\log\chi]$$
$$=(0.10)^{3/2}[6.06\log(0.10)-6.06$$
$$\log(0.00618)]=0.234$$

Assume $d=0.090$ ft.

$$d^{3/2}[6.06\log d-6.06\log\chi]=0.190$$

Assume $d=0.098$ ft.

$$d^{3/2}[6.06\log d-6.06\log\chi]=0.224$$

Therefore, $d=0.098$ ft.

Check criterion 31, the criterion for distinguishing between rough and wavy boundaries.

$$\frac{V_*\sigma}{\nu}=\frac{\sqrt{gdS}\sigma}{\nu}=\frac{\sqrt{32.2(0.098)(0.001)}(0.010)}{1.06\times10^{-5}}=52.9$$

Since $\frac{V_*\sigma}{\nu}>6$, the boundary is hydraulically rough, as assumed.

Calculation of the flow variables for irrigation furrows is slightly more difficult. Equation 16 can be written:

$$\frac{V}{\sqrt{gRS}}=6.06\log R-6.06\log\chi$$

The relationship between flow area and hydraulic radius must be known either in graphical or equation form, for the channel being considered. Then for a given Q, S, and χ, a value of R is assumed, V is calculated, and the value of A determined. If these values satisfy $Q=AV$, the assumption for R was correct. During the laboratory testing of channel resistance, no runs were made on parabolic channels with wavy or transitional boundaries. However, it is assumed that criterion 31 is valid for these channels as well as for the rectangular channels.

SUMMARY AND CONCLUSIONS

The factors affecting flow resistance in irrigation borders and furrows are difficult to evaluate, owing largely to the nonuniformity of the roughness characteristics and to the wide ranges in rate of water discharge and size of roughness elements that occur. A review of literature revealed that past research has not provided sufficient information on hydraulic resistance of these channels to allow for rational design of surface irrigation systems. Therefore, a study of the hydraulics of simulated irrigation borders and furrows was conducted in the laboratory.

Small channels having boundaries formed of soil and chemically stabilized to prevent alteration of the roughness, were formed in a laboratory flume. Rectangular channels with smooth sidewalls and parabolic channels represented irrigation borders and furrows, respectively. Observations were made of dimensions of the boundary roughness elements, channel shapes, flow regime over a wide range of flow rates, and the flow parameters necessary for calculating flow resistance coefficients. Flow resistance coefficients then were empirically related to dimensions of the boundary roughness elements. Analysis of the experimental results leads to the following conclusions.

1. Both laminar and turbulent flows can occur when flow rates and flow boundaries are similar to those of surface irrigation systems.

2. Critical Reynolds numbers for the transition from laminar to turbulent flow are 500 for rough boundaries and 700 for smoother boundaries. A critical Reynolds number of 500 will probably be applicable to all wide irrigation channels.

3. The following criterion can be used to determine the height of roughness such that flow

resistance will be greater than the theoretical smooth boundary equation for laminar flow:

$$\sigma \geq \frac{2.58d}{\sqrt{Re}} \quad (25)$$

4. The resistance coefficient for rough, laminar flow can be predicted by the following equation:

$$f = \frac{6.0\times10^4 S^{0.5}\left(\frac{\sigma}{\lambda_p}\right)}{Re} \quad (26)$$

where σ and λ_p are measures of the roughness height and longitudinal spacing, respectively.

5. The transition from wavy to rough boundary conditions for turbulent flows occurs when

$$\frac{V_*\sigma}{\nu} = 6$$

All surface irrigation channels would be expected to be hydraulically rough when flow is turbulent.

6. The resistance coefficient for turbulent, hydraulically rough flows can be predicted for both wide rectangular and parabolic channels by the following equations:

$$\frac{C}{\sqrt{g}} = 6.06 \log\frac{R}{\chi} \quad (16)$$

and

$$\chi = 12.9\sigma^{1.66} \quad (32)$$

7. The variation in flow resistance caused by a range of parabolic cross sections is negligible compared to the effects of boundary roughness.

8. The magnitude of error involved in predicting resistance to flow using equations 16, 26, and 32 is small enough to allow practical application of the equations. Larger errors would result from the currently used procedure of estimating a single value of Manning's n to represent a channel for all discharges.

LITERATURE CITED

(1) ALLEN, J.
1934. STREAMLINE AND TURBULENT FLOW IN OPEN CHANNELS. Phil. Mag. and Jour. Sci. 116: 1081–1112.
(2) BAZIN, M.
1865. RECHERCHES EXPERIMENTALES SUR L'ECOULEMENT DE L'EAU DANS LES CANAUX DECOUVERTS. [Paris] Acad. des Sci. Math. et Phys. 19.
(3) CORNISH, R. J.
1928. FLOW IN A PIPE OF RECTANGULAR CROSS SECTION. Roy. Soc. London, Proc. series A, 120: 691–700.
(4) DAVIS, JOHN R.
1961. ESTIMATING RATE OF ADVANCE FOR IRRIGATION FURROWS. Amer. Soc. Agr. Engin. Trans. 4: 52–54, 57.
(5) GOLDSTEIN, S.
1938. MODERN DEVELOPMENTS IN FLUID DYNAMICS. v. 1, 330 pp. Oxford.
(6) HALL, W. A.
1956. ESTIMATING IRRIGATION BORDER FLOW. Agr. Engin. 37: 263–265.
(7) HOPF, L.
1925. TURBULENZ BEI EINEM FLUSSE [TURBULENCE IN A FLOW]. Ann. der Phys. 32: 777–808.
(8) HORTON, R. E., LEACH, H. R., and VAN VLIET, R.
1934. THEORY OF LAMINAR SHEET FLOW. Amer. Geophys. Union Trans. 15: 393–404.
(9) JEFFREYS, H.
1925. FLOW OF WATER IN AN INCLINED CHANNEL OF RECTANGULAR SECTION. Phil. Mag. and Jour. Sci. 49: 793–807.
(10) KEULEGAN, G. H.
1938. LAWS OF TURBULENT FLOW IN OPEN CHANNELS. [U.S.] Natl. Bur. Standards Jour. Res. 21: 707–741.
(11) NIKURADSE, J.
1930. TURBULENTE STROMUNG IN NICHT KREISFORMIGEN ROHREN. Ingen.-Archiv v. 1, 306 pp.
(12) ——
1932. GESETZMASSIGKEITEN DER TURBULENTEN STROMUNG IN GLATTEN ROHREN. Ver. Deut. Ingen., Forshungsheft 356: 301–315.

(13) ——
1933. STROMUNGSGESETZE IN RAUHEN ROHREN. Verein Deut. Ingen. Forshungsheft 361, 22 pp.
(14) OWEN, W. M.
1954. LAMINAR TO TURBULENT FLOW IN A WIDE OPEN CHANNEL. Amer. Soc. Civ. Engin. Trans. 119: 1157–1164.
(15) PARSONS, D. A.
1949. DEPTHS OF OVERLAND FLOW. U.S. Soil Conserv. Serv. Tech. Pub. 82, 33 pp.
(16) POWELL, R. W.
1949. RESISTANCE TO FLOW IN SMOOTH CHANNELS. Amer. Geophys. Union. Trans. 30: 875–878.
(17) SAYRE, W. W., and ALBERTSON, M. L.
1961. ROUGHNESS SPACING IN RIGID OPEN CHANNELS. Amer. Soc. Civ. Engin. Proc. 87 (HY 3): 121–150.
(18) SCHLICHTING, H.
1936. EXPERIMENTELLE UNTERSUCHUNGEN ZUM RAUHIGKEITSPROBLEM. Ingen.-Archiv 3: 1.
(19) SHULL, HOLLIS.
1960. FURROW HYDRAULICS STUDY AT THE SOUTHWESTERN IRRIGATION FIELD STATION. In Proceedings of the ARS-SCS Workshop on Hydraulics of Surface Irrigation. U.S. Dept. Agr. ARS 41–43: 56–62.
(20) STRAUB, L. G., SILBERMAN, E., and NELSON, H. C.
1956. SOME OBSERVATIONS ON OPEN CHANNEL FLOW AT SMALL REYNOLDS NUMBERS. Amer. Soc. Civ. Engin. Proc. 82 (EM3): 1–23.
(21) TINNEY, E. R., and BASSETT, D. L.
1961. TERMINAL SHAPE OF A SHALLOW LIQUID FRONT. Amer. Soc. Civ. Engin. Proc. 85 (HY5): 117–133.
(22) VANONI, V. A., and BROOKS, N. H.
1957. LABORATORY STUDIES OF THE ROUGHNESS AND SUSPENDED LOAD OF ALLUVIAL STREAMS. Calif. Inst. Technol. Sedimentation Lab. Rpt. E-68, 121 pp.
(23) WOO, D., and BRATER, E. F.
1961. LAMINAR FLOW IN ROUGH RECTANGULAR CHANNELS. Jour. Geophys. Res. 66: 4207–4217.

SYMBOLS

Symbol	Dimensions	Description
a	L^{-1}	Coefficient in equation for parabolas.
a	L	Constant in boundary regression equation.
a_w	----------	Hydraulic characteristic for wavy boundaries.
a_r	----------	Hydraulic characteristic for rough boundaries.
a_s	----------	Hydraulic characteristic for smooth boundaries.
A	----------	Constant, defined where used.
A	L^2	Cross-sectional area.
b	----------	Constant.
B	----------	Constant.
c	L	Depth correction.
C	$L^{1/2}T^{-1}$	Resistance coefficient from Chezy formula.
d	L	Normal flow depth.
f	----------	Resistance coefficient from Darcy-Weisbach formula.
g	LT^{-2}	Gravitational acceleration.
k	L	Roughness height.
k_s	L	Diameter of equivalent sand grain roughness.
n	----------	Resistance coefficient from Manning's equation.
n	----------	Number of measurements or observations.
q	L^2T^{-1}	Unit discharge.
Q	L^3T^{-1}	Total discharge.
r	L	Radius of circular pipe.
R	L	Hydraulic radius.
Re	----------	Reynolds number, VR/ν.
Re_k	----------	Tip Reynolds number.
Re_{kc}	----------	Value of tip Reynolds number at which separation occurs at the tops of the roughness elements (the critical value).
S	----------	Slope.
v	LT^{-1}	Velocity of flow at distance y from the boundary.
V	LT^{-1}	Mean flow velocity.

Symbol	Dimensions	Description
V_*	LT^{-1}	Shear velocity, $\sqrt{gRS}$.
V_k	LT^{-1}	Velocity at a level corresponding to the tops of the roughness elements.
x	L	Horizontal coordinate for measuring cross section of parabolic channels.
x_i	L	Distance from some datum at which elevation y_i is measured.
y	L	Depth of flow at center of parabolic channels.
y	L	Distance from boundary.
y	L	Channel elevation at distance x from center line of parabolic channels.
y_i	L	Individual bed elevation measurement.
β	----------	Channel shape factor.
γ	FL^{-3}	Unit weight of water.
δ'	L	Thickness of laminar sublayer.
ϵ	L	Height of roughness necessary for separation to occur in flow through pipes.
$\bar{\epsilon}$	----------	Channel shape factor.
κ	----------	von Karman universal turbulence constant.
λ_σ	L	Average longitudinal spacing of roughness elements projecting more than 1σ above mean bed elevation.
λ_p	L	Average longitudinal spacing of all roughness-element crests.
μ	FTL^{-2}	Absolute viscosity.
ν	L^2T^{-1}	Kinematic viscosity.
σ	L	Standard deviation of boundary elevation measurements about the mean elevation; a description of roughness height.
χ	L	Resistance parameter from Sayre-Albertson equation; a parameter representing effects of both roughness and channel shape.

APPENDIX

Figures 25 to 35 show the rectangular channels (simulated borders) constructed for this study. (The roughness preparation for channel B, not shown, was similar to that of channel D.) Figures 36 to 42 show the parabolic channels (simulated furrows) constructed.

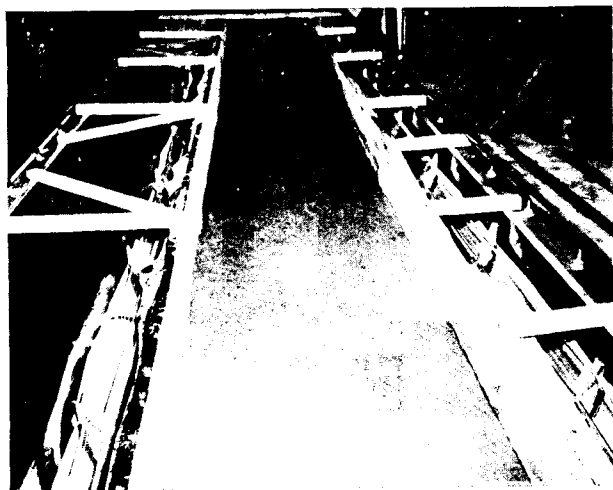Tables 8 to 11 summarize the experimental data obtained.

FIGURE 25.—Rectangular channel C. The boundary was troweled to produce the smoothest surface possible.
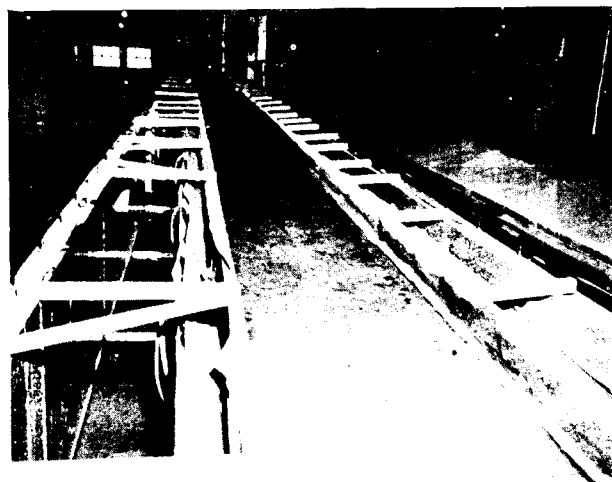

FIGURE 27.—Rectangular channel E. The boundary was roughened. A stream of water then formed small, widely spaced ripples.
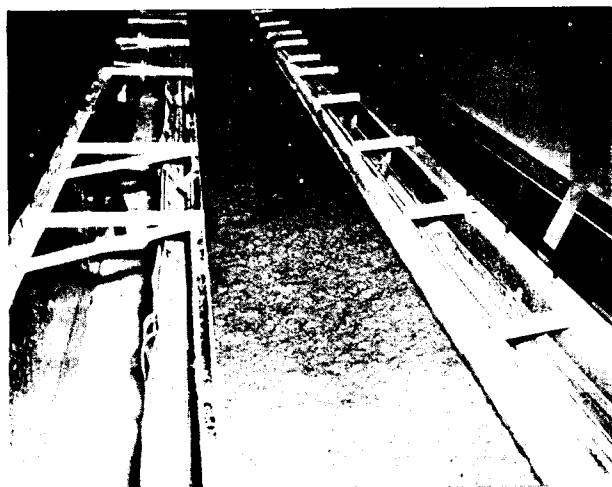
FIGURE 26.—Rectangular channel D. The boundary was roughened, then flooded with a nonerosive stream of water before stabilization.
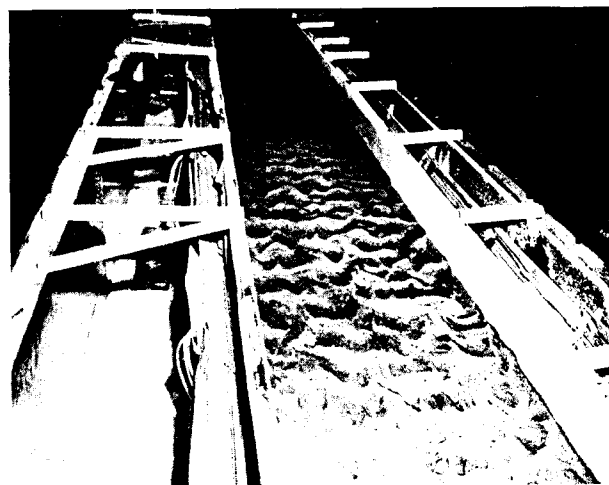
FIGURE 28.—Rectangular channel F. A large, erosive stream of water was used to form relatively large ripples.
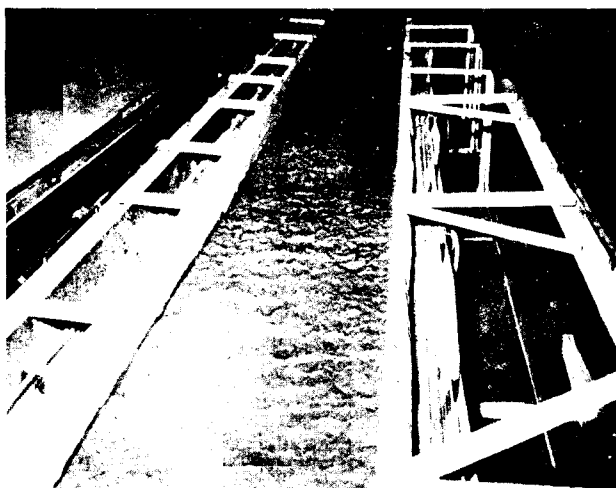
FIGURE 29.—Rectangular channel G. The ripples are smaller than those in channel F.
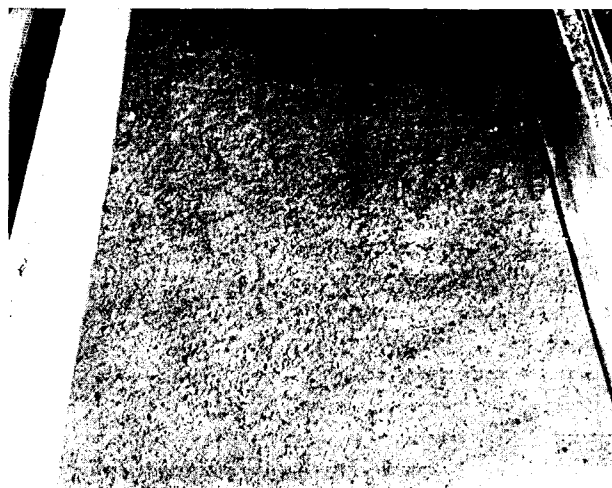
FIGURE 31.—Rectangular channel I. Small particles of soil were sieved onto the screeded boundary surface to form small, loosely spaced, very irregular roughness elements.
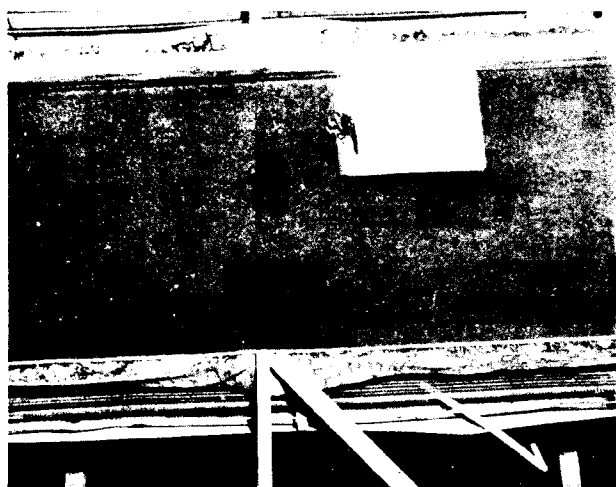
FIGURE 30.—Rectangular channel H. This boundary was stabilized in the condition existing after it was screeded. Small longitudinal grooves were formed by particles catching on the edge of the screed.
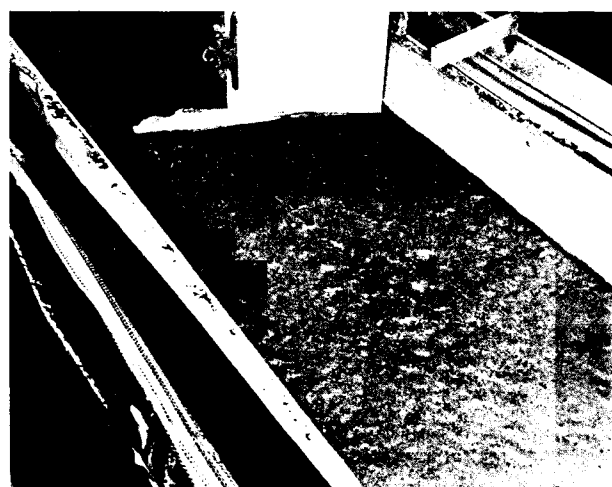
FIGURE 32.—Rectangular channel K. After being roughened, this boundary was modified by a very low flow of water.

FIGURE 33.—Rectangular channel L. This boundary was troweled. It is very similar to rectangular channel C.
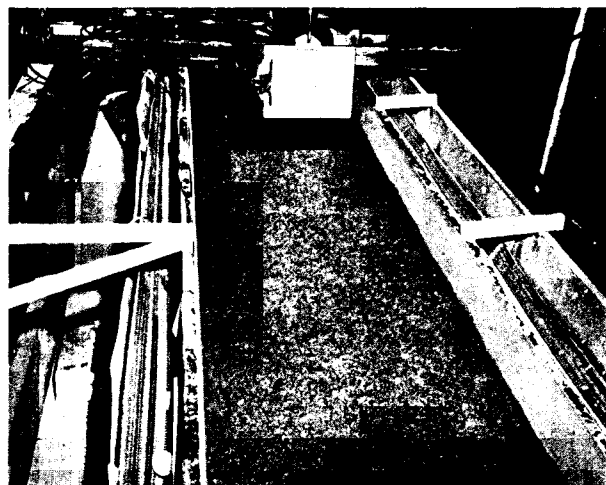
FIGURE 35.—Rectangular channel N. After being roughened, this boundary was sprayed lightly and uniformly with a garden hose.
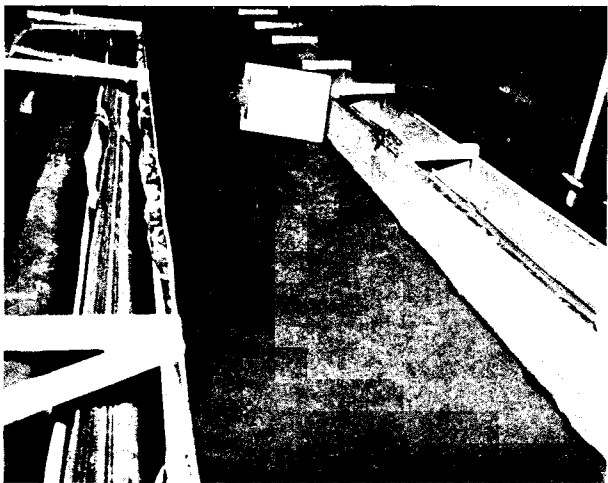
FIGURE 34.—Rectangular channel M. This boundary was roughened in a regular pattern by making indentations with the end of a trowel. A low flow of water was used to smooth the indentations.

FIGURE 36.—Parabolic channel A. This channel was formed with a furrowing shovel. It should be very similar to a newly formed furrow in the field.
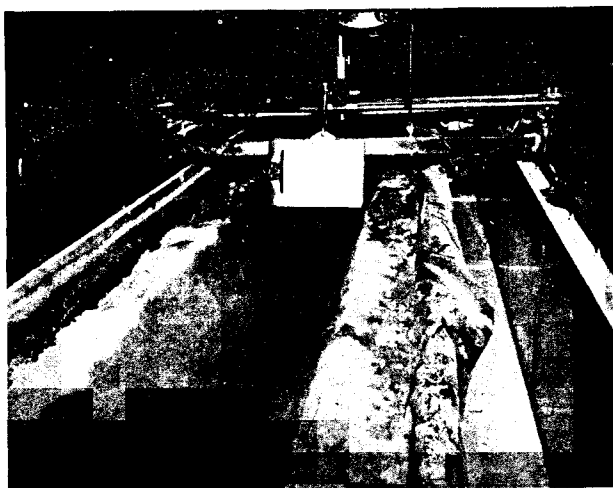
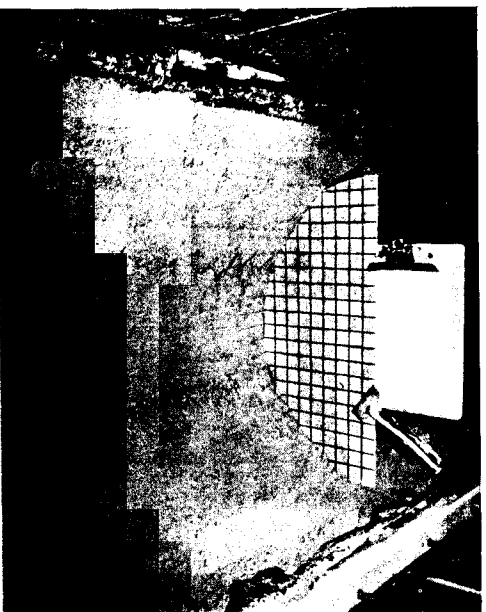FIGURE 37.—Parabolic channel B. This channel was screeded to the desired shape and left with a small degree of roughness.
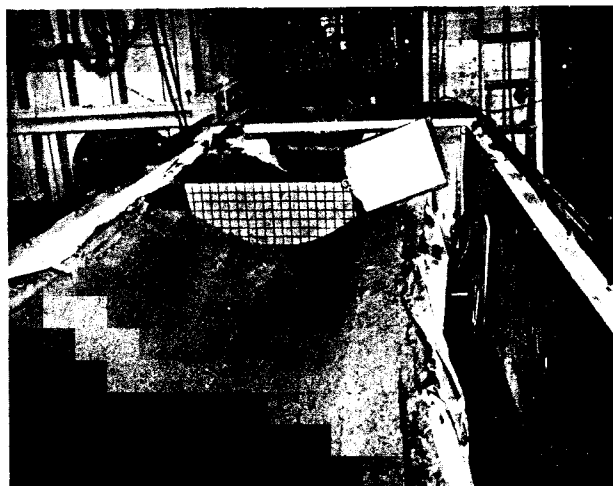
FIGURE 39.—Parabolic channel D. Preparation of this channel was similar to that of channel B.
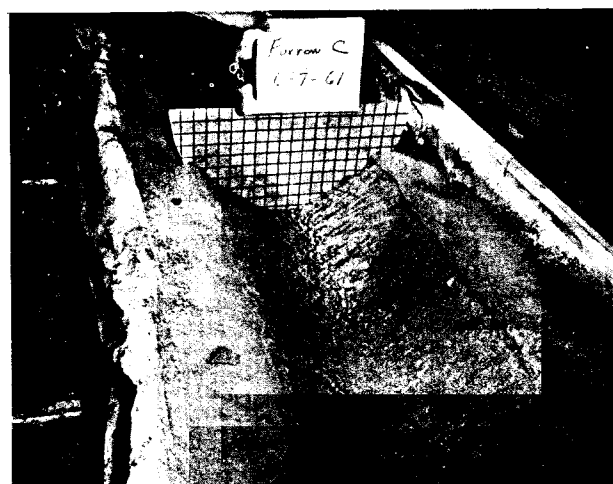
FIGURE 38.—Parabolic channel C. After being screeded this channel was roughened and then modified with a low flow of water. Channels B and C were the narrowest and deepest of the channels studied.
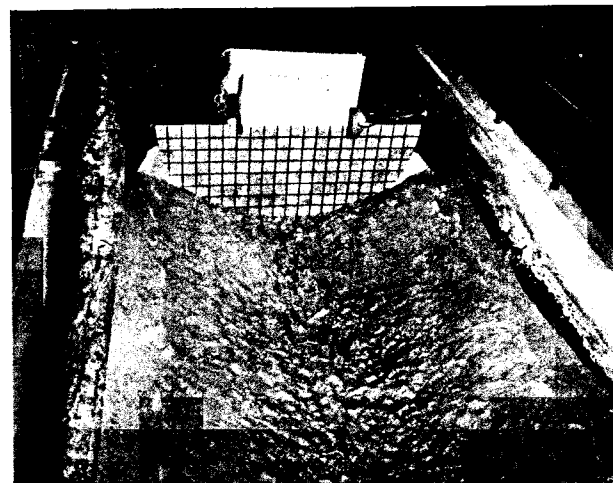
FIGURE 40.—Parabolic channel E. Preparation of this channel was similar to that of channel C. Channels D and E were the widest and shallowest of the channels studied.

FIGURE 41.—Parabolic channel F. Preparation of this channel was similar to that of channel B.
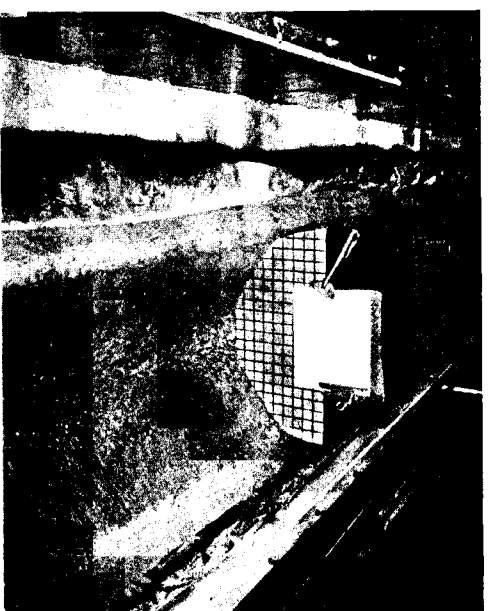
FIGURE 42.—Parabolic channel G. Preparation of this channel was similar to that of channel C.

TABLE 8.—*Summary of measured data—rectangular channels*

Channel and run	S	q	d	v	T	v×10⁵
		Ft.³/Sec./Ft.	Ft.	Ft./Sec.	°F.	Ft.²/Sec.
Channel B:						
1-B¹	0.001	0.0106	0.0702	0.151	52	1.37
2-B	.001	.0225	.0935	.240	48	1.46
3-B	.001	.0478	.1320	.360	48	1.46
4-B	.001	.0959	.1850	.517	47	1.49
5-B	.001	.1430	.2240	.636	48	1.46
6-B¹	.001	.2770	.3310	.834	47	1.49
7-B	.005	.0213	.0640	.332	50	1.41
8-B	.005	.0456	.0878	.519	50	1.41
9-B	.005	.0943	.1220	.774	52	1.37
10-B	.005	.1660	.1610	1.030	53	1.35
11-B	.005	.2770	.2050	1.330	50	1.41
Channel C:						
2-C	.005	.0160	.0237	.684	46	1.51
3-C	.005	.0331	.0343	.966	45	1.54
4-C	.005	.0725	.0532	1.360	42	1.60
7-C	.001	.0113	.0328	.345	47	1.49
9-C	.001	.0292	.0538	.541	45	1.54
10-C	.001	.0560	.0768	.725	46	1.50
11-C	.001	.1030	.1120	.915	45	1.54
12-C	.001	.1410	.1350	1.040	45	1.54
13-C	.001	.2670	.1980	1.340	47	1.49
16-C	.0005	.0117	.0396	.294	54	1.33
18-C	.0005	.0111	.0380	.291	49	1.44
19-C	.0005	.0169	.0482	.350	48	1.46
20-C	.0005	.0250	.0626	.399	47	1.49
21-C¹	.0005	.0655	.1160	.564	46	1.51
22-C¹	.0005	.1230	.1540	.795	45	1.54
23-C¹	.0005	.2580	.2520	1.020	45	1.54
24-C	.0005	.4440	.3660	1.210	45	1.54

See footnote at end of table, p. 49.

TABLE 8.—*Summary of measured data—rectangular channels*—Continued

Channel and run	S	q	d	v	T	v×10⁵
		Ft.³/Sec./Ft.	Ft.	Ft./Sec.	°F.	Ft.²/Sec.
Channel D:						
9-D	.0005	.2600	.3430	.756	46	1.51
10-D	.0005	.1650	.2630	.626	46	1.51
11-D	.0005	.0895	.1860	.480	48	1.46
12-D	.0005	.0490	.1350	.361	52	1.37
13-D	.0005	.0240	.0848	.283	45	1.54
14-D	.0005	.0128	.0690	.186	46	1.51
15-D¹	.0005	.0948	.252	.376	45	1.54
16-D	.0005	.0069	.0518	.133	46	1.51
17-D	.001	.00119	.025	.0475	53	1.35
18-D	.001	.00252	.032	.0789	51	1.39
19-D	.001	.00408	.039	.105	45	1.54
20-D	.001	.00778	.0500	.155	44	1.57
21-D	.001	.0160	.0666	.239	46	1.51
22-D	.001	.0308	.0904	.340	47	1.49
23-D¹	.001	.0607	.127	.476	49	1.44
24-D¹	.001	.122	.186	.654	50	1.41
25-D¹	.001	.284	.293	.967	47	1.49
26-D	.001	.514	.414	1.24	48	1.46
27-D	.00474	.00450	.029	.156	57	1.27
28-D	.00474	.00949	.0380	.251	56	1.29
29-D	.00474	.0186	.0508	.367	51	1.39
30-D	.00474	.0363	.0664	.547	50	1.41
31-D	.00474	.0704	.0908	.774	50	1.41
32-D	.00474	.137	.131	1.05	50	1.41
33-D	.00474	.290	.192	1.51	50	1.41
34-D	.00474	.472	.258	1.83	52	1.37
Channel E:						
1-E	.005	.00624	.0182	.345	60	1.21
2-E	.005	.0123	.0260	.473	57	1.27
3-E¹	.005	.0238	.0355	.678	55	1.31

TABLE 8.—*Summary of measured data—rectangular channels*—Continued

Channel and run	S	q	d	V	T	vx10⁵
		Ft.³/ Sec./Ft.	Ft.	Ft./ Sec.	°F.	Ft.³/ Sec.
Channel E:						
4-E	.005	.0506	.0540	.943	55	1.31
5-E [1]	.005	.102	.0780	1.31	55	1.31
6-E	.005	.202	.118	1.71	56	1.29
7-E [1]	.005	.380	.179	2.13	57	1.27
8-E [1]	.005	.596	.235	2.54	56	1.29
9-E	.001	.00236	.020	.118	58	1.25
10-E	.001	.00530	.026	.204	58	1.25
11-E [1]	.001	.0114	.0388	.296	57	1.27
12-E	.001	.0299	.0664	.452	56	1.29
13-E	.001	.0650	.101	.644	56	1.29
14-E [1]	.001	.140	.172	.809	57	1.27
15-E [1]	.001	.292	.254	1.15	57	1.27
16-E	.001	.538	.387	1.39	57	1.27
17-E	.0005	.00294	.025	.118	58	1.25
18-E	.0005	.00530	.031	.171	59	1.23
19-E	.0005	.0110	.0478	.231	58	1.25
20-E	.0005	.0233	.0710	.328	58	1.25
21-E	.0005	.0482	.106	.456	58	1.25
22-E	.0005	.0640	.126	.508	57	1.27
23-E	.0005	.127	.190	.671	57	1.27
24-E	.0005	.256	.290	.884	58	1.25
25-E [1]	.0005	.505	.458	1.10	58	1.25
26-E	.0005	.00162	.020	.081	63	1.15
Channel F:						
1-F [1]	.0005	.0179	.0949	.191	59	1.23
2-F [1]	.0005	.0105	.0765	.139	59	1.23
3-F	.0005	.0430	.140	.310	57	1.27
4-F	.0005	.146	.260	.561	57	1.27
5-F	.0005	.0835	.196	.428	57	1.27
6-F	.0005	.294	.391	.753	58	1.25
7-F [1]	.001	.0165	.0780	.214	59	1.23
8-F	.001	.0320	.102	.315	59	1.23
9-F	.001	.129	.204	.633	57	1.27
10-F	.001	.254	.290	.877	57	1.27
11-F	.001	.0675	.146	.466	57	1.27
Channel G:						
1-G	.0005	0.00750	0.0519	0.146	62	1.17
2-G	.0005	.0158	.0760	.208	62	1.17
3-G [1]	.0005	.0340	.102	.334	60	1.21
4-G	.0005	.0686	.149	.462	60	1.21
5-G [1]	.0005	.146	.237	.618	60	1.21
6-G [1]	.0005	.292	.349	.839	60	1.21
7-G [1]	.0005	.463	.468	.992	60	1.21
8-G	.001	.00777	.0441	.178	60	1.21
9-G [1]	.001	.0167	.0605	.277	60	1.21
10-G [1]	.001	.0331	.0829	.402	60	1.21
11-G	.001	.0686	.123	.560	60	1.21
12-G	.001	.142	.186	.768	59	1.23
13-G [1]	.001	.270	.270	1.00	59	1.23
14-G	.001	.565	.427	1.32	59	1.23
15-G	.005	.0101	.0355	.288	60	1.21
16-G	.005	.0224	.0495	.458	60	1.21
17-G	.005	.0435	.0664	.659	60	1.21
18-G	.005	.0930	.0960	.973	60	1.21
19-G	.005	.187	.137	1.37	60	1.21
20-G	.005	.368	.198	1.87	60	1.21
21-G [1]	.005	.570	.262	2.18	60	1.22
Channel H:						
1-H [1]	.005	.0107	.0245	.438	61	1.19
2-H	.005	.0214	.0342	.629	60	1.21

TABLE 8.—*Summary of measured data—rectangular channels*—Continued

Channel and run	S	q	d	V	T	vx10⁵
		Ft.³/ Sec./Ft.	Ft.	Ft./ Sec.	°F.	Ft.³/ Sec.
Channel H:						
3-H	.005	.0430	.0499	.862	60	1.21
4-H [1]	.005	.122	.0856	1.43	60	1.21
6-H	.001	.0105	.0312	.339	62	1.17
7-H	.001	.0181	.0444	.409	61	1.19
8-H	.001	.0390	.0680	.573	61	1.19
9-H	.001	.0776	.101	.769	60	1.21
11-H	.001	.304	.236	1.30	61	1.19
12-H [1]	.001	.520	.349	1.50	61	1.19
14-H	.0005	.0112	.0408	.276	64	1.15
15-H	.0005	.0221	.0622	.356	63	1.16
16-H	.0005	.0439	.0905	.485	63	1.16
17-H	.0005	.0878	.142	.622	62	1.17
18-H	.0005	.172	.214	.807	62	1.17
19-H	.0005	.360	.332	1.09	63	1.16
20-H	.0005	.543	.436	1.25	63	1.16
Channel I:						
1-I	.0005	.00146	.023	.0634	68	1.09
2-I	.0005	.00269	.032	.0842	68	1.09
3-I	.0005	.00735	.0496	.148	68	1.09
4-I	.0005	.0151	.0701	.215	68	1.09
5-I	.0005	.0276	.0970	.285	68	1.09
6-I	.0005	.0585	.153	.383	68	1.09
7-I	.0005	.121	.225	.537	67	1.10
8-I	.0005	.277	.354	.783	67	1.10
9-I	.0005	.451	.465	.972	67	1.10
10-I	.0005	.00092	.022	.0418	70	1.06
11-I	.0005	.00301	.031	.0971	70	1.06
12-I	.0005	.00767	.0494	.155	70	1.06
13-I	.0005	.145	.245	.595	68	1.09
21-I [1]	.0001	.0158	.150	.105	69	1.07
22-I	.0001	.00124	.037	.0334	70	1.06
23-I	.0001	.00043	.022	.0194	68	1.09
24-I	.0001	.00314	.048	.0654	70	1.06
25-I [1]	.0001	.00596	.0610	.0979	70	1.06
26-I [1]	.0001	.00702	.0760	.0927	69	1.07
27-I	.0001	.0308	.181	.170	68	1.09
28-I	.0001	.0554	.249	.223	68	1.09
29-I	.0001	.104	.342	.305	68	1.09
30-I	.0001	.187	.466	.401	68	1.09
31-I	.001	.00301	.028	.1074	69	1.07
32-I	.001	.00618	.0379	.164	69	1.07
33-I	.001	.0147	.0571	.258	69	1.07
34-I	.001	.0336	.0864	.389	69	1.07
35-I	.001	.0640	.127	.504	68	1.09
36-I	.001	.128	.187	.685	68	1.09
37-I	.001	.260	.277	.939	68	1.09
38-I [1]	.001	.520	.421	1.24	68	1.09
39-I [1]	.005	.00606	.0269	.227	69	1.07
40-I [1]	.005	.0120	.0363	.333	69	1.07
41-I [1]	.005	.0236	.0493	.480	69	1.07
42-I	.005	.0500	.0706	.708	69	1.07
43-I	.005	.0970	.0980	.990	68	1.09
44-I	.005	.187	.141	1.33	68	1.09
Channel K:						
1-K	.0001	.00068	.019	.0356	60	1.21
2-K	.0001	.00197	.031	.0636	60	1.21
3-K	.0001	.00311	.032	.0972	59	1.23
4-K	.0001	.00820	.062	.132	59	1.23
5-K	.0001	.00451	.045	.1003	59	1.23
6-K	.0001	.00676	.055	.123	59	1.23

See footnote at end of table, page 49.

TABLE 8.—*Summary of measured date—rectangular channels*—Continued

Channel and run	S	q	d	V	T	νx10⁵
		Ft.³/Sec./Ft.	Ft.	Ft./Sec.	°F.	Ft.²/Sec.
Channel K:						
7-K	.0001	.0143	.083	.172	58	1.25
8-K	.0001	.0246	.110	.223	56	1.29
9-K	.0001	.0470	.154	.305	57	1.27
10-K	.0001	.100	.241	.416	57	1.27
11-K [1]	.0001	.191	.365	.523	56	1.29
12-K [1]	.0001	.315	.481	.656	56	1.29
13-K [1]	.0005	.0178	.054	.328	57	1.27
14-K [1]	.0005	.0289	.072	.402	56	1.29
15-K [1]	.0005	.0500	.099	.505	57	1.27
16-K [1]	.0005	.101	.155	.649	58	1.25
17-K [1]	.0005	.174	.216	.806	58	1.25
18-K [1]	.0005	.437	.396	1.10	58	1.25
19-K	.0005	.00145	.019	.0765	58	1.25
20-K	.0005	.00083	.016	.052	58	1.25
21-K	.0005	.00252	.023	.1097	58	1.25
22-K	.0005	.00345	.025	.1379	58	1.25
23-K	.0005	.00449	.028	.1605	58	1.25
24-K	.0005	.00616	.032	.1930	58	1.25
25-K	.0003	.00064	.017	.0376	57	1.27
26-K	.0003	.00196	.023	.0852	57	1.27
27-K	.0003	.00219	.024	.0911	58	1.25
28-K	.0003	.00154	.022	.0702	58	1.25
29-K	.0003	.00114	.020	.0572	58	1.25
30-K	.0003	.00580	.036	.1612	58	1.25
31-K	.0003	.00693	.039	.1781	56	1.29
32-K	.0003	.00372	.029	.1281	56	1.29
Channel L:						
1-L	.0001	.00178	.0360	.0496	56	1.29
2-L	.0001	.00229	.0315	.0727	56	1.29
3-L	.0001	.00637	.0400	.1591	55	1.31
4-L	.0001	.00036	.0185	.0199	56	1.29
5-L	.0001	.00707	.0225	.0312	56	1.29
6-L	.0001	.00463	.0430	.1075	56	1.29
7-L	.0001	.00173	.0280	.0620	54	1.33
8-L	.0001	.00924	.0545	.1697	54	1.33
9-L	.0001	.00688	.0465	.1482	54	1.33
10-L	.0001	.00556	.0400	.1388	54	1.33
11-L	.0003	.00131	.0185	.0709	54	1.33
12-L	.0003	.00087	.0145	.0599	54	1.33
13-L	.0003	.00276	.0225	.1225	52	1.37
14-L	.0003	.00436	.0275	.1589	52	1.37
15-L	.0003	.00617	.0310	.1993	51	1.39
16-L	.0003	.00720	.0320	.2253	51	1.39
17-L	.0003	.00330	.0255	.1296	56	1.29
18-L	.0003	.00746	.0335	.2230	51	1.39
19-L	.0003	.01066	.0390	.2730	51	1.39
20-L	.0003	.00978	.0365	.2685	52	1.37
21-L	.0005	.00091	.0120	.0764	52	1.37
22-L	.0005	.00063	.0105	.0599	54	1.33
23-L	.0005	.00479	.0240	.2000	52	1.37
24-L	.0005	.00325	.0205	.159	52	1.37
25-L	.0005	.00522	.0240	.2173	52	1.37
26-L	.0005	.00680	.0270	.2523	52	1.37
27-L	.0005	.00735	.0280	.2626	52	1.37
28-L	.001	.00062	.0085	.0725	54	1.33
29-L	.001	.00208	.0130	.1607	54	1.33
30-L	.001	.00096	.0100	.0963	54	1.33
31-L	.001	.00394	.0170	.2323	54	1.33
32-L	.001	.00293	.0150	.1961	54	1.33
33-L	.001	.00503	.0185	.2723	54	1.33

Channel and run	S	q	d	V	T	νx10⁵
		Ft.³/Sec./Ft.	Ft.	Ft./Sec.	°F.	Ft.²/Sec.
Channel L:						
34-L	.001	.00595	.0200	.2976	53	1.35
35-L	.001	.00608	.0195	.3126	54	1.33
36-L	.001	.00681	.0210	.3251	53	1.35
37-L	.001	.00818	.0220	.3729	52	1.37
Channel M:						
3-M	.001	.00702	.0315	.2230	53	1.35
4-M	.001	.00474	.0260	.1826	54	1.33
5-M	.001	.00576	.0290	.1985	54	1.33
6-M	.001	.00106	.0160	.0663	56	1.29
7-M	.001	.00095	.0160	.0593	56	1.29
8-M	.001	.00083	.0150	.0553	56	1.29
9-M	.001	.00122	.0165	.0742	56	1.29
10-M	.001	.00347	.0220	.1579	56	1.29
11-M	.001	.00243	.0200	.1215	56	1.29
12-M	.0005	.00198	.0235	.0844	50	1.41
13-M	.0005	.00124	.0200	.0622	50	1.41
14-M	.0005	.00267	.0255	.1048	50	1.41
15-M	.0005	.00347	.0275	.1266	50	1.41
16-M	.0005	.00590	.0330	.1789	50	1.41
17-M	.0005	.00428	.0285	.1578	52	1.37
18-M	.0005	.00659	.0345	.1914	51	1.39
19-M	.0005	.00816	.0395	.2069	51	1.39
20-M	.0003	.00045	.0155	.0292	53	1.35
21-M	.0003	.00265	.0270	.0984	53	1.35
22-M	.0003	.00104	.0215	.0483	53	1.35
23-M	.0003	.00151	.0230	.0655	53	1.35
24-M	.0003	.00441	.0320	.1378	45	1.54
25-M	.0003	.00582	.0360	.1618	50	1.41
26-M	.0003	.00735	.0400	.1839	50	1.41
27-M	.0003	.01020	.0485	.2105	50	1.41
Channel N:						
3-N [1]	.0003	.00715	.0663	.107	54	1.33
4-N	.0003	.0108	.0758	.142	54	1.33
5-N	.0003	.0199	.104	.190	51	1.39
6-N [1]	.0003	.111	.258	.432	50	1.41
7-N	.0003	.146	.280	.520	49	1.44
8-N [1]	.0003	.280	.425	.657	51	1.39
9-N [1]	.005	.0114	.0443	.256	53	1.35
10-N	.005	.0244	.0593	.410	53	1.35
11-N	.005	.0576	.0882	.655	52	1.37
12-N	.005	.0779	.102	.766	51	1.39
13-N	.005	.109	.120	.908	51	1.39
14-N	.005	.205	.166	1.23	51	1.39
15-N	.005	.353	.223	1.58	48	1.46
16-N	.005	.00950	.0372	0.255	50	1.41
20-N	.001	.00842	.0510	.165	52	1.37
21-N	.001	.0189	.0733	.257	52	1.37
22-N	.001	.0305	.0925	.330	50	1.41
23-N	.001	.0671	.143	.469	49	1.44
24-N	.001	.115	.190	.606	49	1.44
25-N [1]	.001	.219	.266	.820	50	1.41
27-N	.0005	.00810	.0588	.137	52	1.37
28-N	.0005	.0162	.0798	.203	52	1.37
29-N	.0005	.0292	.111	.262	50	1.41
30-N	.0005	.0661	.161	.411	50	1.41
31-N [1]	.0005	.135	.258	.525	50	1.41
32-N [2]	.0005	.267	.373	.714	50	1.41
33-N	.0005	.00720	.0538	.133	52	1.37

[1] Data of questionable value, see page 10.

TABLE 9.—Resistance coefficients and calculated parameters—rectangular channels

Channel and run	n	$C/\sqrt{g}$	f	Re	σ/d
Channel B:					
1-B	0.0518	3.19	0.785	774	0.266
2-B	.0399	4.38	.416	1,540	.200
3-B	.0335	5.54	.260	3,260	.142
4-B	.0293	6.71	.177	6,410	.101
5-B	.0272	7.50	.142	9,760	.0834
6-B[1]	.0269	8.10	.122	18,500	.0565
7-B	.0499	3.25	.758	1,500	.292
8-B	.0397	4.36	.422	3,220	.213
9-B	.0328	5.52	.260	6,890	.153
10-B	.0300	6.40	.196	12,300	.116
11-B[1]	.0269	7.34	.148	19,300	.0912
Channel C:					
2-C	.0130	11.0	.0695	1,070	.0506
3-C	.0115	13.0	.0480	2,150	.0350
4-C	.0110	14.7	.0376	4,520	.0226
7-C[1]	.0131	10.6	.0640	760	.0366
9-C	.0124	13.0	.0475	890	.0223
10-C	.0117	14.6	.0378	3,710	.0156
11-C	.0120	15.3	.0344	6,650	.0107
12-C	.0119	15.8	.0322	9,140	.00890
13-C	.0119	16.8	.0282	17,800	.00605
16-C	.0130	11.6	.0598	875	.0303
18-C	.0130	11.7	.0586	769	.0316
19-C	.0127	12.5	.0516	1,160	.0249
20-C	.0132	12.6	.0510	1,680	.0191
21-C[1]	.0140	13.0	.0468	4,330	.0104
22-C[1]	.0121	16.0	.0315	7,950	.00779
23-C	.0130	16.0	.0312	16,700	.00476
24-C	.0141	15.8	.0322	28,800	.00328
Channel D:					
9-D	.0215	10.2	.0763	17,200	.0344
10-D	.0218	9.60	.0868	10,900	.0499
11-D	.0225	8.77	.104	6,120	.0635
12-D			.717	248	.0929
13-D[1]	.0347	4.62	.372	503	.2280
14-D	.0242	7.74	.134	3,160	.0874
15-D[1]	.0275	6.45	.193	1,550	.124
16-D	.0302	5.59	.255	850	.171
17-D			2.85	88	
18-D			1.32	182	
19-D	.0232	8.48	.112	7,900	.0635
20-D	.0249	7.48	.143	3,850	.0929
21-D	.0278	6.31	.200	2,030	.131
22-D[1]	.0323	5.17	.300	1,070	.177
23-D	.0412	3.86	.532	538	.236
24-D			.913	290	
25-D	.0210	10.8	.0688	34,500	.0285
26-D	.0215	10.0	.0800	19,400	.0403
27-D			1.54	355	
28-D[1]	.0465	3.30	.730	740	.310
29-D[1]	.0387	4.17	.401	1,340	.232
30-D	.0306	5.41	.272	2,580	.178
31-D[1]	.0267	6.55	.186	4,990	.130
32-D	.0252	7.40	.146	9,760	.0900
33-D	.0225	8.84	.102	20,600	.0615
34-D	.0226	9.25	.0938	34,500	.0457
Channel E:					
1-E	.0214	6.38	.206	520	.495
2-E[1]	.0198	7.31	.152	970	.346
3-E[1]	.0170	9.00	.103	1,840	.253
4-E	.0160	10.1	.0829	3,880	.167

TABLE 9.—Resistance coefficients and calculated parameters—rectangular channels—Continued

Channel and run	n	$C/\sqrt{g}$	f	Re	σ/d
Channel E:					
5-E	.0148	11.7	.0595	7,800	.115
6-E	.0148	12.4	.0522	15,600	.0763
7-E[1]	.0157	12.5	.0514	30,000	.0503
8-E[1]	.0158	13.1	.0474	46,300	.0383
9-E			.370	189	
10-E			.161	425	
11-E[1]	.0184	8.39	.118	904	.232
12-E	.0170	9.79	.0843	2,320	.136
13-E	.0158	11.3	.0630	5,040	.0891
14-E[1]	.0180	10.9	.0675	11,000	.0523
15-E[1]	.0164	12.7	.0499	23,000	.0354
16-E	.0180	12.5	.0517	42,400	.0232
17-E			.232	236	
18-E			.137	432	
19-E	.0190	9.17	.156	884	.188
20-E	.0173	9.70	.0855	1,860	.127
21-E	.0164	11.0	.0660	3,870	.0849
22-E	.0164	11.2	.0630	5,040	.0714
23-E	.0163	12.1	.0542	10,000	.0473
24-E	.0164	12.9	.0477	20,500	.0310
25-E[1]	.0164	12.8	.0483	40,300	.0196
26-E	.0178	12.8	.393	141	
Channel F:					
1-F[1]	.0367	4.88	.349	1,470	.149
2-F[1]	.0437	3.96	.539	865	.184
3-F	.0290	6.54	.190	3,420	.101
4-F	.0241	8.66	.107	11,500	.0542
5-F	.0262	7.63	.139	6,600	.0720
6-F	.0236	9.49	.0888	23,600	.0361
7-F[1]	.0407	4.29	.462	1,360	.181
8-F	.0331	5.51	.273	2,610	.138
9-F	.0257	7.83	.111	10,200	.0690
10-F	.0234	9.09	.0875	20,000	.0486
11-F	.0280	6.82	.175	5,360	.0966
Channel G:					
1-G	.0323	5.03	.329	648	.226
2-G	.0288	5.92	.230	1,350	.154
3-G[1]	.0218	8.25	.120	2,820	.115
4-G	.0203	9.44	.106	5,690	.0785
5-G[1]	.0207	10.0	.0803	12,100	.0493
6-G[1]	.0196	11.2	.0639	24,200	.0335
7-G[1]	.0202	11.4	.0614	38,400	.0250
8-G	.0336	4.74	.380	650	.265
9-G[1]	.0264	6.30	.208	1,380	.193
10-G[1]	.0224	7.79	.136	2,750	.141
11-G	.0208	8.94	.102	5,700	.122
12-G	.0199	9.95	.0814	11,600	.0950
13-G[1]	.0196	10.7	.0695	15,500	.0629
14-G	.0201	11.3	.0630	45,800	.0274
15-G	.0402	3.82	.590	845	.329
16-G	.0314	5.15	.318	1,870	.236
17-G	.0263	6.39	.203	3,610	.176
18-G	.0227	7.85	.132	7,730	.122
19-G	.0205	9.25	.0960	15,500	.0855
19-G	.0205	9.25	.0960	15,500	.0855
20-G[1]	.0192	10.5	.0740	30,600	.0590
21-G[1]	.0199	10.6	.0726	47,200	.0446
Channel H:					
1-H[1]	.0204	7.00	.166	903	.0992
2-H	.0175	8.46	.112	1,780	.0710
3-H	.0166	9.66	.0867	3,550	.0487

See footnote at end of table, page 52.

TABLE 9.—*Resistance coefficients and calculated parameters—rectangular channels*—Continued

Channel and run	n	C/√g	f	Re	σ/d
Channel H:					
4-H [1]	.0143	12.2	.0546	10,100	.0284
6-H	.0139	10.8	.0706	905	.0779
7-H	.0145	10.9	.0685	1,520	.0548
8-H	.0136	12.3	.0535	3,270	.0358
9-H	.0133	13.5	.0440	6,410	.0241
11-H	.0138	14.9	.0364	25,800	.0103
12-H [1]	.0155	14.2	.0403	44,000	.00696
14-H	.0143	10.7	.0691	980	.0596
15-H	.0146	11.3	.0635	1,910	.0391
16-H	.0138	12.7	.0495	3,780	.0269
17-H	.0145	13.0	.0473	7,550	.0171
18-H	.0147	13.8	.0423	14,800	.0114
19-H	.0147	14.9	.0362	31,200	.00732
20-H	.0153	14.9	.0362	47,000	.00557
Channel I:					
1-I	-------	-------	.737	134	------
2-I	-------	-------	.581	247	------
3-I	.0302	5.75	.240	674	.129
4-I	.0262	6.38	.196	1,380	.0910
5-I	.0245	7.22	.153	2,530	.0658
6-I	.0248	7.70	.134	5,370	.0417
7-I	.0229	8.92	.100	11,000	.0284
8-I	.0213	10.7	.0694	25,200	.0180
9-I	.0205	11.2	.0638	41,100	.0137
10-I	-------	-------	1.62	87	------
11-I	-------	-------	.423	283	------
12-I	.0288	5.50	.264	721	.129
13-I	.0219	9.46	.0890	13,400	.0260
21-I [1]	.0400	4.79	.346	1,470	.0426
22-I	-------	-------	.851	116	------
23-I	-------	-------	1.51	39	------
24-I	-------	-------	.289	296	------
25-I [1]	.0234	6.99	.163	563	.105
26-I [1]	.0288	5.94	.227	659	.0840
27-I	.0278	7.05	.160	2,820	.0353
28-I	.0264	7.88	.128	5,100	.0256
29-I	.0239	9.19	.0942	9,570	.0187
30-I	.0222	10.4	.0737	17,200	.0137
31-I	-------	-------	.625	281	------
32-I	.0326	4.72	.359	580	.168
33-I	.0270	6.03	.218	1,380	.112
34-I	.0236	7.39	.146	3,140	.0740
35-I	.0235	7.90	.128	5,870	.0502
36-I	.0224	8.87	.101	11,700	.0341
37-I	.0212	9.96	.0800	23,800	.0230
38-I [1]	.0214	10.7	.0692	48,000	.0152
39-I [1]	.0419	3.45	.671	571	.237
40-I [1]	.0347	4.37	.416	1,130	.176
41-I [1]	.0294	5.40	.271	2,210	.130
42-I	.0255	6.61	.183	4,670	.0905
43-I	.0225	7.86	.129	8,900	.0652
44-I	.0214	8.80	.103	17,200	.0453
Channel K:					
1-K	-------	-------	.385	56	------
2-K	-------	-------	.198	163	------
3-K	-------	-------	.087	253	------
5-K	-------	-------	.115	367	------
9-K	.0138	13.7	.0428	3,700	.0348
10-K	.0424	15.0	.0370	7,900	.0222
11-K [1]	.0145	15.2	.0344	14,800	.0147
12-K [1]	.0140	16.7	.0290	24,500	.0111

Channel and run	n	C/√g	f	Re	σ/d
Channel K:					
13-K [1]	.0143	11.1	.0610	1,390	.0990
14-K [1]	.0144	11.8	.0534	2,240	.0743
15-K [1]	.0141	12.6	.0454	3,940	.0540
16-K	.0147	13.0	.0406	8,050	.0346
17-K [1]	.0153	13.6	.0347	13,900	.0248
18-K [1]	.0163	13.7	.0298	34,800	.0135
19-K			.418	116	
20-K			.763	64	
21-K			.247	201	
22-K			.168	276	
23-K			.140	360	
24-K			.111	494	
25-K			.929	50	
26-K			.245	154	
27-K			.223	175	
28-K			.345	124	
29-K			.473	92	
30-K			.107	464	
31-K			.095	538	
32-K			.137	288	
33-K	.0143	11.3	.0626	1,190	.0940
Channel L:					
1-L			.377	138	
2-L			.153	178	
3-L			.041	487	
4-L			1.20	28	
5-L			.598	55	
6-L			.096	359	
7-L			.188	131	
8-L			.049	695	
9-L			.054	518	
10-L			.054	417	
11-L			.284	99	
12-L			.312	65	
13-L			.116	201	
14-L			.084	319	
15-L			.060	444	
16-L			.049	519	
17-L			.117	256	
18-L			.052	537	
19-L			.041	766	
20-L			.039	715	
21-L			.265	67	
22-L			.377	47	
23-L			.077	350	
24-L			.104	238	
25-L			.065	381	
26-L			.055	497	
27-L			.052	537	
28-L			.416	46	
29-L			.130	157	
30-L			.278	72	
31-L			.081	297	
32-L			.100	221	
33-L			.064	379	
34-L			.058	441	
35-L			.051	458	
36-L			.051	506	
37-L			.041	599	
Channel M:					
3-M			.163	515	
4-M			.201	350	

See footnote at end of table, page 52.

TABLE 9.—*Resistance coefficients and calculated parameters—rectangular channels*—Continued

Channel and run	n	$C/\sqrt{g}$	f	Re	σ/d
Channel H:					
4-H[1]	.0143	12.2	.0546	10,100	.0284
6-H	.0139	10.8	.0706	905	.0779
7-H	.0145	10.9	.0685	1,520	.0548
8-H	.0136	12.3	.0535	3,270	.0358
9-H	.0133	13.5	.0440	6,410	.0241
11-H[1]	.0138	14.9	.0364	25,800	.0103
12-H[1]	.0155	14.2	.0403	44,000	.00696
14-H	.0143	10.7	.0691	980	.0596
15-H	.0146	11.3	.0635	1,910	.0391
16-H	.0138	12.7	.0495	3,780	.0269
17-H	.0145	13.0	.0473	7,550	.0171
18-H	.0147	13.8	.0423	14,800	.0114
19-H	.0147	14.9	.0362	31,200	.00732
20-H	.0153	14.9	.0362	47,000	.00557
Channel I:					
1-I			.737	134	
2-I			.581	247	
3-I	.0302	5.75	.240	674	.129
4-I	.0262	6.38	.196	1,380	.0910
5-I	.0245	7.22	.153	2,530	.0658
6-I	.0248	7.70	.134	5,370	.0417
7-I	.0229	8.92	.100	11,000	.0284
8-I	.0213	10.7	.0694	25,200	.0180
9-I	.0205	11.2	.0638	41,100	.0137
10-I			1.62	87	
11-I	.0288	5.50	.423	283	.129
12-I	.0219	9.46	.264	721	.0260
13-I			.0890	13,400	
21-I	.0400	4.79	.346	1,470	.0426
22-I			.851	116	
23-I			1.51	39	
24-I	.0234	6.99	.289	296	.105
25-I	.0288	5.94	.163	563	.0840
26-I	.0278	7.05	.227	659	.0353
27-I	.0264	7.88	.160	2,820	.0256
28-I	.0239	9.19	.128	5,100	.0187
29-I	.0222	10.4	.0942	9,570	.0137
30-I			.0737	17,200	
31-I	.0326	4.72	.625	281	.168
32-I	.0270	6.03	.359	580	.112
33-I	.0236	7.39	.218	1,380	.0740
34-I	.0235	7.90	.146	3,140	.0502
35-I	.0224	8.87	.128	5,870	.0341
36-I	.0212	9.96	.101	11,700	.0230
37-I	.0214	10.7	.0800	23,800	.0152
38-I			.0692	48,000	
39-I[1]	.0419	3.45	.671	571	.237
40-I[1]	.0347	4.37	.416	1,130	.176
41-I[1]	.0294	5.40	.271	2,210	.130
42-I	.0255	6.61	.183	4,670	.0905
43-I	.0225	7.86	.129	8,900	.0652
44-I	.0214	8.80	.103	17,200	.0453
Channel K:					
1-K			.385	56	
2-K			.198	163	
3-K			.087	253	
5-K			.115	367	
9-K	.0138	13.7	.0428	3,900	.0348
10-K	.0424	15.0	.0370	7,900	.0222
11-K[1]	.0145	15.2	.0344	14,800	.0147
12-K[1]	.0140	16.7	.0290	24,500	.0111

TABLE 9.—*Resistance coefficients and calculated parameters—rectangular channels*—Continued

Channel and run	n	$C/\sqrt{g}$	f	Re	σ/d
Channel K:					
13-K[1]	.0143	11.1	.0610	1,390	.0990
14-K[1]	.0144	11.8	.0534	2,240	.0743
15-K[1]	.0141	12.6	.0454	3,940	.0540
16-K	.0147	13.0	.0406	8,050	.0346
17-K[1]	.0153	13.6	.0347	13,900	.0248
18-K[1]	.0163	13.7	.0298	34,800	.0135
19-K			.418	116	
20-K			.763	64	
21-K			.247	201	
22-K			.168	276	
23-K			.140	360	
24-K			.111	494	
25-K			.929	50	
26-K			.245	154	
27-K			.223	175	
28-K			.345	124	
29-K			.473	92	
30-K			.107	464	
31-K			.095	538	
32-K			.137	288	
33-K	.0143	11.3	.0626	1,190	.0940
Channel L:					
1-L			.377	138	
2-L			.153	178	
3-L			.041	487	
4-L			1.20	28	
5-L			.598	55	
6-L			.096	359	
7-L			.188	131	
8-L			.049	695	
9-L			.054	518	
10-L			.054	417	
11-L			.284	99	
12-L			.312	65	
13-L			.116	201	
14-L			.084	319	
15-L			.060	444	
16-L			.049	519	
17-L			.117	256	
18-L			.052	537	
19-L			.041	766	
20-L			.039	715	
21-L			.265	67	
22-L			.377	47	
23-L			.077	350	
24-L			.104	238	
25-L			.065	381	
26-L			.055	497	
27-L			.052	537	
28-L			.416	46	
29-L			.130	157	
30-L			.278	72	
31-L			.081	207	
32-L			.100	221	
33-L			.064	370	
34-L			.058	441	
35-L			.051	468	
36-L			.051	500	
37-L			.041	500	
Channel M:					
3-M			.163	515	
4-M			.201	350	

See footnote at end of table, page 52.

TABLE 9.—*Resistance coefficients and calculated parameters—rectangular channels*—Continued

Channel and run	n	C/√g	f	Re	σ/d
Channel M:					
5-M			.190	430	
6-M			.937	82	
7-M			1.17	73	
8-M			1.26	64	
9-M				95	
10-M			.773	266	
11-M			.228	187	
12-M			.348	137	
13-M			.425	86	
14-M			.666	184	
15-M			.299	240	
16-M			.184	405	
17-M			.221	318	
18-M			.133	459	
19-M			.147	564	
20-M			1.41	33	
21-M			.216	191	
22-M			.713	75	
23-M			.414	109	
24-M			.130	276	
25-M			.106	398	
26-M			.091	501	
27-M			.085	688	
Channel N:					
3-N [1]	.0392	4.23	.445	533	.299
4-N	.0344	5.25	.290	809	.261
5-N	.0322	6.01	.221	1,420	.190

TABLE 9.—*Resistance coefficients and calculated parameters—rectangular channels*—Continued

Channel and run	n	C/√g	f	Re	σ/d
Channel N:					
6-N [1]	.0241	8.67	.107	7,910	.0767
7-N [1]	.0211	10.0	.0798	10,100	.0707
8-N [1]	.0120	10.2	.0760	20,100	.0466
Channel N:					
9-N [1]	.0513	3.04	.0870	840	.447
10-N	.0392	4.20	.455	1,800	.334
11-N	.0318	5.50	.265	4,220	.224
12-N	.0298	5.98	.224	5,630	.194
13-N	.0282	6.53	.187	7,830	.165
14-N	-.0258	7.55	.141	14,700	.119
15-N	.0244	8.35	.114	24,100	.0888
16-N	.0459	3.30	.0740	673	.0532
17-N	.0393	4.08	.485	614	.388
18-N	.0318	5.30	.286	1,380	.270
19-N	.0310	6.07	.218	2,160	.214
20-N	.0274	6.92	.168	4,650	.138
21-N	.0255	7.80	.133	8,000	.104
22-N	.0237	8.90	.102	15,500	.0745
23-N	.0366	4.46	.403	588	.337
24-N	.0304	5.67	.250	1,180	.248
25-N	.0293	6.20	.208	2,060	.178
26-N	.0239	8.10	.122	4,700	.123
27-N	.0256	8.15	.121	9,600	.0767
28-N [1]	.0241	9.21	.0941	18,900	.0530
29-N [1]	.0354	4.50	.780	522	.368

[1] Data of questionable value: see page 10.

TABLE 10.—*Summary of measured data—parabolic channels*

Channel and run	s	Q (Ft.³/Sec.)	y (Ft.)	R (Ft.)	A (Ft.²)	v (Ft./Sec.)	T (°F.)	ν×10⁵ (Ft.²/Sec.)
Channel A:								
1-A	0.0005	0.00583	0.0855	0.0520	0.0344	0.176	56	1.29
2-A	.0005	.0221	.145	.0856	.0722	.310	56	1.29
3-A	.0005	.0389	.192	.116	.116	.334	54	1.33
4-A	.0005	.0716	.242	.142	.164	.438	54	1.33
5-A	.0005	.1619	.361	.202	.298	.544	52	1.37
6-A [1]	.0005	.1153	.298	.172	.224	.513	52	1.37
7-A [1]	.0003	.00692	.1005	.0628	.0435	.159	54	1.33
8-A	.0003	.0166	.1435	.0870	.0750	.222	56	1.29
9-A	.0003	.0366	.198	.1195	.122	.300	54	1.33
10-A	.0003	.0564	.240	.144	.161	.351	52	1.37
11-A	.0003	.0760	.271	.157	.194	.391	52	1.37
12-A	.001	.00972	.094	.0591	.040	.247	57	1.27
13-A	.001	.0199	.124	.0776	.0605	.329	56	1.29
14-A	.001	.0754	.212	.126	.134	.561	54	1.33
15-A	.001	.0353	.154	.0944	.0825	.428	54	1.33
16-A	.001	.1038	.243	.141	.163	.638	53	1.35
17-A	.005	.00688	.064	.041	.0225	.314	59	1.23
18-A	.005	.0190	.091	.056	.0370	.514	58	1.25
19-A	.005	.0347	.114	.071	.0525	.662	56	1.29
20-A	.005	.0582	.140	.086	.0715	.815	54	1.33
21-A	.005	.0824	.162	.099	.0900	.916	54	1.33
22-A	.005	.1093	.180	.106	.106	1.032	53	1.35
23-A	.005	.1685	.213	.135	.135	1.250	53	1.35

TABLE 10.—*Summary of measured data—parabolic channels*—Continued

Channel and run	S	Q	y	R	A	V	T	$\nu \times 10^5$
		Ft.³/Sec.	Ft.	Ft.	Ft.²	Ft./Sec.	°F.	Ft.³/Sec.
Channel B:								
1-B	.0003	.00585	.061	.0402	.0220	.266	60	1.21
2-B	.0003	.02037	.116	.0730	.0565	.361	56	1.29
3-B	.0003	.0403	.154	.0960	.0870	.464	56	1.29
4-B	.0003	.0647	.196	.118	.124	.522	56	1.29
5-B	.0003	.0899	.234	.139	.161	.558	56	1.29
6-B	.0003	.134	.279	.164	.210	.644	55	1.31
7-B	.0003	.176	.314	.181	.251	.700	55	1.31
8-B	.0005	.00727	.062	.0400	.0220	.330	60	1.21
9-B	.0005	.0240	.108	.0676	.0500	.480	58	1.25
10-B	.0005	.0563	.161	.0969	.0900	.626	57	1.27
11-B	.0005	.0916	.202	.121	.129	.710	56	1.29
12-B	.0005	.149	.258	.151	.185	.803	56	1.29
13-B	.0005	.226	.318	.182	.254	.891	56	1.29
14-B	.001	.00673	.053	.0343	.0174	.387	60	1.21
15-B	.001	.01697	.078	.0499	.0310	.548	58	1.25
16-B	.001	.0301	.102	.0640	.0460	.654	56	1.29
17-B	.001	.0728	.154	.0947	.0860	.847	56	1.29
18-B	.001	.132	.206	.123	.132	.996	56	1.29
19-B	.001	.228	.265	.156	.194	1.178	56	1.29
20-B	.001	.276	.295	.171	.228	1.211	55	1.31
21-B	.005	.00721	.039	.0256	.0111	.653	59	1.23
22-B	.005	.0197	.060	.0389	.0210	.940	59	1.23
23-B	.005	.0658	.103	.0659	.0475	1.386	57	1.27
24-B	.005	.1259	.139	.0850	1.22	1.718	56	1.29
25-B	.005	.231	.184	.112	1.28	2.063	56	1.29
26-B	.005	.354	.224	.126	1.34	2.353	56	1.29
Channel C:								
1-C	.0003	.0076	.079	.0492	.0314	.248	62	1.17
2-C	.0003	.0174	.118	.0739	.0574	.302	61	1.19
3-C	.0003	.0331	.160	.0979	.0910	.364	60	1.21
4-C	.0003	.0590	.213	.128	.140	.423	59	1.23
5-C	.0003	.0816	.250	.147	.177	.460	58	1.25
6-C	.0003	.1388	.299	.172	.232	.600	58	1.25
7-C	.0003	.229	.396	.221	.355	.646	58	1.25
8-C	.0005	.00692	.070	.0447	.0260	.266	60	1.21
9-C	.0005	.0296	.133	.0829	.0688	.429	60	1.21
10-C	.0005	.0583	.181	.110	.109	.534	59	1.23
11-C	.0005	.0924	.225	.134	.151	.612	59	1.23
12-C	.0005	.152	.277	.161	.207	.734	58	1.25
13-C	.0005	.234	.338	.192	.279	.839	58	1.25
14-C	.001	.0204	.096	.0608	.0422	.483	59	1.23
15-C	.001	.0517	.149	.0917	.0816	.632	59	1.23
16-C	.001	.0928	.197	.119	.124	.748	58	1.25
17-C	.001	.158	.249	.148	.176	.897	58	1.25
18-C	.001	.290	.327	.187	.266	1.091	58	1.25
19-C	.001	.409	.378	.211	.329	1.243	58	1.25
20-C	.005	.0189	.066	.0423	.0240	.790	60	1.21
21-C	.005	.0571	.115	.0720	.0552	1.034	59	1.23
22-C	.005	.100	.142	.0863	.0755	1.428	59	1.23
23-C	.005	.235	.207	.124	.134	1.761	58	1.25
24-C	.005	.391	.262	.153	.190	2.061	58	1.25
Channel D:								
1-D	.001	.00359	.037	.0245	.0151	.238	62	1.17
2-D	.001	.00744	.047	.0312	.0219	.340	62	1.17
3-D	.001	.0135	.061	.0402	.0320	.422	60	1.21
4-D	.001	.0374	.097	.0630	.0638	.586	60	1.25
5-D	.001	.0775	.137	.0884	.108	.721	58	1.25
6-D	.001	.161	.188	.120	.172	.936	58	1.25
7-D	.001	.226	.226	.143	.227	.995	59	1.23
8-D	.001	.3275	.262	.164	.284	1.153	58	1.25

See footnote at end of table, page 54.

TABLE 10.—*Summary of measured data—parabolic channels*—Continued

Channel and run	S	Q	v	R	A	V	T	$\nu \times 10^5$
Channel D:		*Ft.³/Sec.*	*Ft.*	*Ft.*	*Ft.²*	*Ft./Sec.*	*°F.*	*Ft.²/Sec.*
9-D	.0005	.00650	.052	.0344	.0253	.257	64	1.15
10-D	.0005	.0146	.078	.0540	.0462	.316	60	1.21
11-D	.0005	.0328	.106	.0690	.0734	.446	60	1.21
12-D	.0005	.0700	.148	.0953	.121	.578	60	1.21
13-D	.0005	.1415	.222	.140	.222	.639	60	1.21
14-D	.0005	.234	.259	.162	.280	.836	60	1.21
15-D	.0005	.383	.337	.208	.415	.926	60	1.21
Channel E:								
1-E	.0005	.00353	.076	.0497	.0432	.0818	68	1.09
2-E	.0005	.00566	.092	.0601	.0577	.0980	68	1.09
3-E	.0005	.0164	.126	.0813	.0926	.177	68	1.09
4-E	.0005	.0312	.154	.0984	.125	.250	62	1.17
5-E	.0005	.0746	.208	.132	.197	.380	61	1.19
6-E	.0005	.150	.282	.176	.310	.484	61	1.19
7-E [1]	.0005	.412	.338	.207	.406	1.014	61	1.19
9-E	.001	.00431	.071	.0475	.0394	.110	66	1.12
10-E	.001	.0127	.096	.0619	.0610	.209	66	1.12
11-E	.001	.0264	.124	.0800	.0900	.292	66	1.12
12-E	.001	.0692	.178	.113	.155	.447	62	1.17
13-E	.001	.1462	.239	.150	.241	.607	62	1.17
14-E	.001	.238	.294	.181	.330	.721	62	1.17
Channel F:								
1-F	.001	.00598	(2)	(2)				
2-F	.001	.0168	(2)	(2)				
3-F	.001	.0448	.118	.0751	.0675	.660	65	1.13
4-F	.001	.1089	.171	.106	.116	.937	64	1.15
5-F	.001	.197	.225	.138	.177	1.116	64	1.15
6-F	.001	.394	.319	.189	.298	1.321	65	1.13
7-F	.001	.580	.398	.231	.417	1.544	65	1.13
8-F	.00043	.00765	.065	.0421	.0273	.280	68	1.09
9-F	.00043	.01955	.092	.0624	.0463	.422	66	1.12
10-F	.00043	.0420	.136	.0859	.0830	.506	65	1.13
11-F	.00043	.0926	.195	.121	.143	.648	64	1.15
12-F	.00043	.1852	.273	.164	.236	.784	64	1.15
13-F	.00043	.593	.479	.271	.550	1.077	65	1.13
Channel G:								
1-G	.00043	.00428	(2)	(2)				
2-G	.00043	.00855	(2)	(2)				
3-G	.00043	.021	(2)	(2)				
4-G	.00043	.0431	.158	.0991	.106	.408	67	1.10
5-G	.00043	.0856	.214	.131	.166	.516	65	1.13
6-G	.00043	.167	.303	.180	.278	.600	65	1.13
7-G	.00043	.234	.350	.206	.346	.676	65	1.13
8-G	.00043	.374	.449	.256	.503	.744	66	1.12
9-G	.001	.00503	(2)	(2)				
10-G	.001	.0127	(2)	(2)				
11-G	.001	--------	(2)	(2)				
12-G	.001	.0694	.182	.113	.130	.534	66	1.12
13-G	.001	.1426	.233	.142	.188	.760	66	1.12
14-G	.001	.238	.302	.180	.277	.860	66	1.12
15-G	.001	.480	.413	.238	.444	1.082	66	1.12

[1] Data of questionable value; see page 10.
[2] Nonuniform flow.

FLOW RESISTANCE IN SIMULATED IRRIGATION BORDERS AND FURROWS

TABLE 11.—*Resistance coefficients and calculated parameters—parabolic channels*

Channel and run	n	$C/\sqrt{g}$	f	Re	σ/R
Channel A:					
1-A [1]	0.0263	6.10	0.216	709	0.1608
2-A [1]	.0209	8.33	.116	2,057	.0976
3-A [1]	.0238	7.74	.136	2,913	.0721
4-A [1]	.0208	9.13	.0966	4,677	.0589
5-A [1]	.0211	9.57	.0881	8,021	.0414
6-A [1]	.0201	9.74	.0843	6,441	.0486
7-A	.0256	6.48	.1927	751	.1331
8-A	.0232	7.56	.1407	1,497	.0961
9-A	.0208	8.84	.103	2,695	.0700
10-A	.0202	9.39	.0909	3,689	.0580
11-A	.0192	10.1	.0799	4,481	.0532
12-A	.0289	5.66	.250	1,150	.1413
13-A	.0260	6.57	.185	1,979	.1078
14-A	.0210	8.81	.101	5,315	.0664
15-A	.0228	8.09	.134	3,038	.0886
16-A	.0199	9.46	.0897	6,664	.0593
17-A	.0409	3.93	.586	1,046	.2040
18-A	.0301	5.39	.276	2,302	.1492
19-A	.0273	6.20	.209	3,643	.1179
20-A	.0251	6.94	.168	5,270	.0972
21-A	.0245	7.35	.152	6,818	.0845
22-A	.0234	7.75	.133	8,409	.0760
23-A	.0212	8.78	.105	11,670	.0664
Channel B:					
1-B	.0114	13.5	.0440	884	.0316
2-B	.0124	13.6	.0434	2,041	.0174
3-B	.0116	15.2	.0361	3,399	.0132
4-B	.0120	15.4	.0336	4,780	.0108
5-B	.0124	15.2	.0344	6,001	.00914
6-B	.0120	16.1	.0310	8,060	.00775
7-B	.0118	16.7	.0285	9,680	.00702
8-B	.0118	13.0	.0483	1,090	.0318
9-B	.0114	14.6	.0378	2,593	.0188
10-B	.0115	15.8	.0319	4,780	.0132
11-B	.0115	16.1	.0310	6,660	.0105
12-B	.0118	15.8	.0319	9,500	.00841
13-B	.0120	16.5	.0295	12,580	.00698
14-B	.0128	11.6	.0590	1,328	.0370
15-B	.0116	13.7	.0430	2,181	.0254
16-B	.0115	14.4	.0385	3,260	.0198
17-B	.0115	15.2	.0340	6,210	.0134
18-B	.0116	15.8	.0319	9,500	.0103
19-B	.0116	16.6	.0288	14,220	.00815
20-B	.0120	16.3	.0298	15,800	.00743
21-B	.0139	10.2	.0775	1,670	.0496
22-B	.0128	11.9	.0572	2,975	.0326
23-B	.0124	13.5	.0442	7,190	.0193
24-B	.0118	14.7	.0372	11,310	.0150
25-B	.0118	15.4	.0338	17,920	.0113
26-B	.0112	16.5	.0293	29,600	.0101
Channel C:					
1-C	.0139	11.4	.0618	1,042	.0593
2-C	.0150	11.3	.0625	2,230	.0396
3-C	.0150	11.8	.0571	2,940	.0298
4-C	.0154	12.0	.0553	4,400	.0228
5-C	.0156	12.2	.0538	5,400	.0199
6-C	.0132	14.2	.0370	8,250	.0170
7-C	.0146	14.0	.0410	11,400	.0132

See footnote at end of table, page 56.

TABLE 11.—*Resistance coefficients and calculated parameters—parabolic channels*—Continued

Channel and run	n	$C/\sqrt{g}$	f	Re	σ/R
Channel C:					
8-C	.0158	9.9	.0814	1,190	.0653
9-C	.0147	11.7	.0580	2,940	.0352
10-C	.0143	12.7	.0498	5,860	.0266
11-C	.0142	13.2	.0460	8,200	.0218
12-C	.0134	14.4	.0386	9,440	.0181
13-C	.0132	15.1	.0352	12,900	.0152
14-C	.0150	10.9	.0672	2,380	.0480
15-C	.0151	11.5	.0591	4,710	.0318
16-C	.0152	12.1	.0546	7,110	.0246
17-C	.0147	13.0	.0476	10,610	.0197
18-C	.0141	14.0	.0404	16,300	.0156
19-C	.0134	15.0	.0352	21,000	.0138
20-C	.0162	9.6	.0860	2,760	.0691
21-C	.0176	9.6	.0864	6,050	.0406
22-C	.0155	11.3	.0636	10,000	.0338
23-C	.0148	12.5	.0513	17,500	.0236
24-C	.0146	13.1	.0465	25,220	.0191
Channel D:					
1-D	.0166	8.5	.112	498	.121
2-D	.0138	10.7	.0696	905	.0952
3-D	.0131	11.7	.0580	1,050	.0739
4-D	.0126	13.0	.0472	3,050	.0471
5-D	.0130	13.5	.0436	5,100	.0336
6-D	.0122	15.1	.0352	8,990	.0248
7-D	.0129	14.7	.0371	11,600	.0208
8-D	.0122	15.9	.0318	15,140	.0181
9-D	.0136	10.9	.0669	739	.0864
10-D	.0144	11.0	.0656	1,410	.0550
11-D	.0125	13.4	.0446	3,080	.0430
12-D	.0120	14.7	.0368	4,550	.0312
13-D	.0140	13.4	.0444	7,390	.0212
14-D	.0118	16.4	.0299	11,900	.0183
15-D	.0126	16.0	.0312	15,900	.0143
Channel E:					
1-E	.0549	2.9	.957	373	.185
2-E	.0518	3.1	.806	538	.153
3-E	.0352	4.9	.333	1,320	.113
4-E	.0283	6.3	.202	2,100	.0933
5-E	.0227	8.2	.118	4,110	.0695
6-E	.0215	9.1	.0968	7,150	.0521
7-E [1]	.0113	17.5	.0260	17,670	.0443
9-E	.0561	2.8	1.016	466	.193
10-E	.0353	4.7	.368	1,154	.148
11-E	.0299	5.0	.241	2,080	.115
12-E	.0245	7.4	.145	4,320	.0812
13-E	.0218	8.7	.105	7,790	.0612
14-E	.0208	9.4	.0896	11,150	.0507
Channel F:					
1-F	(2)	(2)			
2-F	(2)	(2)			
3-F	.0127	13.4	.0444	4,390	.0194
4-F	.0112	16.0	.0311	8,640	.0138
5-F	.0112	16.8	.0284	15,400	.0106
6-F	.0117	16.9	.0279	22,100	.00772
7-F	.0114	17.9	.0250	35,700	.00631
8-F	.0133	11.5	.0555	1,180	.0340
9-F	.0115	14.3	.0360	2,640	.0234
10-F	.0119	14.7	.0340	3,050	.0170
11-F	.0116	15.8	.0297	7,840	.0121
12-F	.0118	16.4	.0276	11,180	.00808
13-F	.0120	17.5	.0241	26,680	.00659

TABLE 11.—*Resistance coefficients and calculated parameters—parabolic channels*—Continued

Channel and run	n	$C/\sqrt{g}$	f	Re	σ/R
Channel G:					
1–G	$(^2)$	$(^2)$	-------	-------	------
2–G	$(^2)$	$(^2)$	-------	-------	------
3–G	$(^2)$	$(^2)$	-------	-------	------
4–G	.0161	11. 0	.0612	3, 680	.0440
5–G	.0155	12. 1	.0511	6, 000	.0333
6–G	.0164	12. 0	.0517	9, 550	.0242
7–G	.0159	12. 7	.0460	12, 330	.0212
8–G	.0167	12. 5	.0479	17, 000	.0170
9–G	$(^2)$	$(^2)$	-------	-------	------
10–G	$(^2)$	$(^2)$	-------	-------	------
11–G	$(^2)$	$(^2)$	-------	-------	------
12–G	.0206	8. 9	.102	5, 390	.0386
13–G	.0168	11. 2	.0632	9, 640	.0307
14–G	.0174	11. 3	.0626	13, 830	.0242
15–G	.0167	12. 4	.0524	23, 000	.0183

[1] Data of questionable value; see page 10.
[2] Nonuniform flow.